A Manganese-Handling Deficit in Huntington's Disease Selectively Impairs ATM-p53 Signaling

By

Andrew Martin Tidball

Dissertation

Submitted to the Faculty of the

Graduate School of Vanderbilt University

in partial fulfillment of the requirements

for the degree of

DOCTOR OF PHILOSOPHY

in

Neuroscience

December, 2014

Nashville, Tennessee

Approved:

Michael Aschner, Ph.D.

Aaron B. Bowman, Ph.D.

Kevin C. Ess, M.D., Ph.D.

Christopher V. Wright, D.Phil.

To my wife and best friend, Samantha, thank you for your love, truth-speaking, and support through all my highs and lows. I am glad you like roller coasters.

&

To my children, Desmond and Briley, may you learn patience and perseverance for those you love and for what you love to do.

ACKNOWLEDGEMENTS

During my graduate time, I have had the pleasure to work with many intelligent, hard-working, amiable people in the Bowman laboratory. I am indebted to the work of prior graduate students Blairanne Williams and Gunnar Kwakye as well as former post-doctoral fellow, Michal Wegrzynowicz. I thank them for their discoveries, which formed the basis of this work. I am grateful to Diana Neely, Asad Aboud, and Bryan Cawthon for their pivotal roles in establishing the induced pluripotent stem cell model system methodology along with Bingying Han who provided endless hours of cell line maintenance. I am grateful also to my fellow graduate students TerryJo Bichell and Kevin Kumar who have been my close companions for so long. TerryJo has also been a life mentor who has talked me through the many difficult spots in the last few years and been an endless source of knowledge of how to raise a family. I also thank our new graduate students, Kyle Horning and in particular Miles Bryan, who was the largest contributor to this work after myself. Many undergraduate and rotation students have also contributed to this work including: Michael Uhouse, Gary Li, Molly Overmyer, Megan Culbreth, Mihir Odak, and others. We have also had the support of many wonderful collaborators including Dr. Kevin Ess and Reed Chamberlin at Genetics Associates, Inc. Special thanks to my sister, Angela Tidball, for her illustrations that grace the introductory chapter.

My committee members have all played a significant role in my development as a scientist. I cannot be sufficiently grateful for the guidance and training of my mentor, Dr. Aaron Bowman. He has thoroughly displayed many of the ideals that I hope to emulate in my scientific career including an endless supply of perseverance, patience, and scientific curiosity. He has also embodied a balance between creative and rigorous scientific thought, a key to any successful scientific career. This work would not have been possible without the financial support of the Vanderbilt Brain Institute Scholar Award and NINDS F31 NRSA Pre-doctoral Fellowship Award.

I especially thank my wife, Samantha, and son, Desmond, who have been patient, supportive, and a constant joy to come home to throughout this long, frustrating process. You have given me so much to work hard for and always bring me back to the present. I would also like to thank my parents for their support throughout my life and always believing in me. I thank God for providing me with all that I have and all that I am. I pray that I am always aware that I am not self-sufficient or self-existent.

TABLE OF CONTENTS

LIST OF TABLES

LIST OF FIGURES

CHAPTER I

MANGANESE AND HUNTINGTON'S DISEASE

Huntington's disease (HD) is a neurodegenerative disorder with hyperkinetic symptoms due to loss of medium spiny neurons (MSNs) in the caudate and putamen of the striatum. HD is caused by a polyglutamine tract expansion with longer expansions leading to earlier age at onset. However, environmental modifiers have been shown to play a large role in age of onset variability. Decreased manganese levels in HD cell and mouse models as well as patient brains illustrate a potential role for manganese as an environmental modifier. Strikingly, many HD-related phenotypes involve manganese-dependent enzymes; thus, dysregulated manganese homeostasis could underlie key aspects on HD pathophysiology. Additionally, manganese and mutant Huntingtin affect similar cellular signaling events. Although the decreased manganese accumulation in the mouse models of HD was intriguing, we wanted to investigate these findings in a human neuronal system, which has only recently become possible. Induced pluripotent stem cells (iPSCs) can be generated from a patient's dermal cells and can be subsequently differentiated into neuronal cells. Medium spiny neurons, the cells selectively degenerated in HD, have been directly differentiated from human iPS and ES cells.

Huntington's disease

Huntington's disease (HD) is a devastating neurodegenerative disease presenting with impaired movement, psychological and behavioral disturbances, and cognitive decline. The most pronounced symptoms are motor impairments including chorea, motor impersistence, and deterioration of coordination and motor skills (Walker, 2007). Typically, chorea, a hyper-kinetic "dance-like" symptom, presents around diagnosis and was the chief characteristic used by George Huntingtin to first describe the disease in 1872 (Huntington, 2003). In late stage HD - or earlier in the juvenile onset form - these hyper-kinetic symptoms give way to hypo-kinesis and rigidity similar to patients with Parkinson's disease (Zuccato et al., 2010). HD typically results in death in the second decade after the time of clinical diagnosis, often from cardiovascular disease or complications such as falls,

difficulty swallowing, aspiration leading to pneumonia, and an increased suicide rate (Folstein, 1989).The motor symptoms are thought to primarily result from neuronal degeneration in the caudate and putamen regions of the basal ganglia. The GABAergic medium spiny neurons in these regions are the most susceptible to HD-related degeneration (Gutekunst et al., 2002); however, neurons in the substantia nigra, globus pallidus, thalamus, subthalamic nucleus, subregions of the hypothalamus, and cortical layers 3, 5, and 6 are also vulnerable to cell death in HD (Walker, 2007; Zuccato et al., 2010). More recent MRI studies have found varying degrees of degeneration in nearly all brain regions in early disease (H D Rosas et al., 2003). Currently, no treatments have been proven effective for HD patients, and the specific mechanism underlying the selective degeneration is undetermined.

Huntington's disease (HD) is a dominantly inherited genetic disorder and affects approximately 6 persons per 100,000 (P. Kumar et al., 2010). In 1993, the genetic cause of the disease was identified in the gene now known as *Huntingtin* (*HTT*). In Huntington's disease patients, a *CAG* repeat region (typically 20 repeats) in *HTT* expands within the coding region of the Huntingtin gene (*HTT*) (MacDonald et al., 1993). HD can occur in individuals with repeat lengths greater than 35 glutamine codons (*CAG*). Individuals with 36-39 repeats show incomplete penetrance and those with >70 repeats typically display HD symptoms in childhood (David C Rubinsztein et al., 1996). However, one study reported a patient with a post-mortem diagnosis of HD had a repeat length of 29 on the longer allele (Kenney et al., 2007).

Environmental influence in Huntington's disease

Genetic factors determine a large portion of the variability in HD onset and progression; however, environmental factors also play a substantial role in disease modification. HD age of onset (AO) can occur from 2 to >80 years of age. More than half of this variability is determined by the length of the CAG repeat with longer repeats resulting in earlier onset (Andrew et al., 1993; Langbehn et al., 2004). The remaining variability is determined by other genetic and environmental disease modifiers. The environment was found to play the most significant role in this non-repeat dependent disease variability in one landmark study (Wexler, 2004). This environmental modifier contribution to age of onset is thought to increase with shorter repeat lengths. In

fact, patients with a repeat length of 40 can have ages of onset spanning four decades (Wexler, 2004). Even monozygotic twins with HD have shown differences in symptomatic manifestations and age of onset (up to 7 years) (Anca et al., 2004; Friedman et al., 2005; Georgiou et al., 1999; Gomez-Esteban et al., 2006). Therefore, environmental exposures play a role in HD disease progression but few specific environmental modifiers have been identified (Hockly et al., 2002; Spires et al., 2004; van Dellen et al., 2000).

Thus far, non-genetic influences such as environmental enrichment, exercise, and diet interventions have been shown to delay disease progression (Andreassen, Dedeoglu, et al., 2001; Andreassen, Ferrante, Dedeoglu, & Beal, 2001; Wenzhen Duan et al., 2003; Ferrante et al., 2000; Hockly et al., 2002; Pang et al., 2006; Spires et al., 2004; van Dellen et al., 2000). Rodent environmental enrichment includes access to running wheel and novel object, and this exposure decreases disease severity in transgenic HD mouse models (Nithianantharajah & Hannan, 2006). Reduced production and trafficking of brain-derived neurotrophic factor (BDNF) is a major phenotype of HD, and enrichment has been linked to increases in BDNF expression (Glass et al., 2004; Zajac et al., 2010; Zuccato & Cattaneo, 2007). Dietary restriction has also been shown to increase mouse BDNF levels and thereby normalizes the BDNF levels of HD mice decreasing disease severity and increasing lifespan [30]. Essential fatty acid supplementation can also prevent some motor deficits in an HD mouse model (Clifford et al., 2002; W Duan et al., 2001). In addition to these protective effects of the environment, many environmental compounds can synergistically increase the progression of neurodegeneration. In some neurodegenerative diseases, such as Parkinson's disease (PD), environmental toxins are thought to be a primary causative agent (Turski et al., 1991). Other factors which may accelerate the pace of HD are those that cause oxidative stress and mitochondrial damage such as heavy metals and pollutants, which are known to cause degeneration of basal ganglia subregions (Betarbet et al., 2000; Bowman, Kwakye, Herrero Hern√°ndez, et al., 2011; Jomova et al., 2010). Although it has been more than twenty years since the Huntingtin gene was identified, it has been difficult to identify environmental disease modifiers because the function of the ubiquitous Huntingtin protein throughout development is still only partially understood.

Huntingtin has many diverse functions, and for this reason, the mutant form leads to many diverse cellular pathologies including calcium signaling abnormalities, mitochondrial dysfunction, neurotrophic factor reduction, excitotoxicity, transcriptional dysregulation, protein aggregate formation, and altered autophagy (Damiano et al., 2010; Martinez-Vicente et al., 2010; Zeron et al., 2002; H. Zhang et al., 2008; Zuccato & Cattaneo, 2007; Zuccato et al., 2010). Knockout of the *Huntingtin* gene is embryonically lethal in mouse models (Duyao et al., 1995; Nasir et al., 1995; Zeitlin et al., 1995). Additionally, partial knockdown of Huntingtin leads to neurodevelopmental abnormalities in both zebrafish and mice (Lumsden et al., 2007; White et al., 1997). Mutant Huntingtin is able to rescue both of these phenotypes, suggesting that neurodegeneration in HD results from a toxic gain of function rather than a of loss of wild-type Huntingtin function (White et al., 1997). Interestingly, Hungtingtin is understood to be expressed in all tissues of the body at all developmental time points, and considering the late onset of neurodegeneration (typically between 30 and 50 years of age) may indicate that mutant Huntingtin expression is not sufficient to cause pathology but requires normal age-related environmental stress (D C Rubinsztein et al., 1997; Stine et al., 1995; White et al., 1997; Woda et al., 2005). This potential environmental role in Huntington's disease opens up the possibility of delaying onset by avoiding potential toxic exposures or by enriching environments and increasing nutritional protection and thereby altering the impact of age-related environmental stress. Furthermore, the identification of specific pollutants or heavy metals, which may serve as environmental modifiers, could lead to potential targets for pharmaceutical intervention to delay the onset of Huntington's disease symptoms.

Huntington's disease and metal ions

Heavy metals are closely linked with both function and dysfunction in the basal ganglia, and are, therefore, likely candidates to be the environmental modifiers for age of onset in HD (Bowman, Kwakye, Herrero Hern√°ndez, et al., 2011). The high metabolic requirements of the brain as well as the need for tight regulation and detoxification of reactive oxygen species necessitates high concentrations of micronutritive heavy metal ions (i.e. Fe^{2+}, Mn^{2+}, Cu^{2+}, and Zn^{2+}) that are important cofactors for enzymes that regulate these processes. On the other hand, excessive metal ion concentrations result in increased oxidative stress, mitochondrial

dysfunction, protein aggregation, and apoptosis. For this reason, heavy metal toxicity and neurodegeneration have many shared mechanisms and symptomatic features (Gaeta & Hider, 2005; Jomova et al., 2010; Molina-Holgado et al., 2007). Excess accumulation of heavy metals in the brain either from exposure (e.g. manganism) or via genetic disturbance of metal ion homeostasis (e.g. Wilson's disease) can lead to degeneration of brain regions, particularly in the basal ganglia (Ala et al., 2007; Dobson et al., 2004). Abnormally low concentrations of micronutritive metals in the brain are also detrimental to brain development and function (Beard, 2003; Dipaolo et al., 1974; Erway et al., 1970; Keen et al., 1998; Walter et al., 1989; Zidenberg-Cherr et al., 1983). The similarities in pathobiology between neurodegeneration and metal toxicity or deficiency, warrants further investigation into shared mechanisms. Because manganism and Huntington's disease overlap in symptomology, a derangement in manganese exposure or handling may explain some of the variation in timing of disease onset, as well as some of the function of the Huntingtin protein in brain.

Manganese and HD

Few studies have measured the level of manganese in the brains of HD patients. Dexter et al (1991) did not find any differences in manganese levels, but a more recent study, Rosas et al (2012), found a significant decrease in manganese concentration in parts of HD cortex (Dexter et al., 1991; H Diana Rosas et al., 2012). Additionally, increased iron accumulation in the striatum and pallidum of HD patients has been seen in multiple studies (Bartzokis et al., 1999; Dexter et al., 1991; H Diana Rosas et al., 2012), and manganese has a strong inverse correlation to iron concentration in the basal ganglia (Erikson et al., 2004). Therefore, increased iron accumulation could result in a slight reduction in manganese levels in Huntington's disease striatum beyond the detection of the previous studies. Manganese is known to accumulate in the globus pallidus and caudate nucleus, two areas highly susceptible to HD neurodegeneration (Larsen et al., 1979; Prohaska, 1987). This accumulation may highlight a specific necessity of manganese for proper function, and may also make these brain areas more susceptible to fluctuations in manganese levels.

Recently, an immortalized striatal murine Huntington's disease model cell line (ST*Hdh*$^{Q7/Q7}$ *and* ST*Hdh*$^{Q111/Q111}$) showed differential toxicological sensitivity to manganese (Mn^{2+}) and cadmium (Cd^{2+}) but no other metal ions tested (Fe^{3+}, Cu^{2+}, Pb^{2+}, Co^{2+}, Zn^{2+}, Ni^{2+}) (Williams, Kwakye, et al., 2010). Mutant Huntingtin expression conferred a survival advantage under manganese exposure conditions in these cells due to a dramatic decrease in manganese uptake (Williams, Kwakye, et al., 2010). This differential manganese level was also observable under basal conditions despite the extremely low concentration of manganese in normal cell culture conditions.(Williams, Kwakye, et al., 2010) Expression of human mutant Huntingtin also caused a decrease in manganese levels in the brains of manganese-exposed mice (Williams, Kwakye, et al., 2010). Interestingly, this difference was seen only in the mouse striatum, the specific region that degenerates in the brains of Huntington's disease patients, and not the cerebellum, cortex, or hippocampus, which are largely spared early in disease progression. The proximal cause for this alteration in manganese homeostasis is currently under investigation; however, the possibility of a manganese-handling defect in Huntington's disease will be further explored in this chapter.

Glia make up 50% of total brain tissue and >75% of the cerebral cortex (Azevedo et al., 2009). These cells are reported to contain ~80% of total brain manganese, and gliosis is a known manifestation of HD (Filipov & Dodd, 2012; Tholey et al., 1988; F. Wedler & Denman, 1984). A more dramatic deficit in the amount of manganese in HD patient neurons could, therefore, exist despite relatively small differences in overall cortical manganese and no observable differences in manganese in the basal ganglia, when measured without regard to cell type (Dexter et al., 1991; H Diana Rosas et al., 2012). The *in vivo* striatal differences revealed in the HD mice were seen using a manganese over-exposure paradigm but not under basal conditions (Williams, Kwakye, et al., 2010). Therefore, the human HD caudate and putamen may have a cell-type specific manganese defect that would only become apparent with over exposure. To address a cell-type specific defect, *ex vivo* primary cell culture of both medium spiny neurons and astrocytes from the HD mouse striatum are warranted.

In addition to the differences in manganese accumulation, manganese exposure exacerbated abnormalities in dendritic complexity and arborization seen in the medium spiny neurons of YAC128 HD model

mice, which contain a mutant human HTT gene containing 128 CAG repeats (Madison et al., 2012). In this same *in vivo* model, curiously, the HD genotype suppressed the Mn-dependent decrease in striatal dopamine levels(Madison et al., 2012). Therefore, HD brains may have manganese deficits that can endanger processes requiring manganese as a cofactor, while also being more susceptible to some aspects of manganese toxicity. These studies into the interactions between manganese and HD have produced useful insights into the potential altered regulation of manganese homeostasis; however, the full range of potential reasons for the underlying disease-toxicant interaction has not yet been explored. The breadth of HD-related cellular phenotypes is diverse and multi-factorial (Ross et al., 2014; Zuccato et al., 2010). For this reason, a clear hypothesis connecting the similarities in manganese and HD pathology is needed. Section 3 of this chapter will outline numerous HD-related phenotypes that may have relevance to manganese biology. Within each section, HD-associated manganese-containing enzymes and similarities in manganese deficiency and/or toxicity to HD pathology will be highlighted because of the critical balance of this metal.

Iron and HD

In addition to abnormalities in manganese homeostasis, Huntington's disease has also been associated with abnormal iron homeostasis. HD patients have increased accumulation of iron in the caudate, putamen, and pallidum (Bartzokis et al., 1999; Dexter et al., 1991; H Diana Rosas et al., 2012). In the same studies, ferritin levels were unchanged between HD patients and control subjects in all of the brain regions examined; however, other authors have found increased ferritin levels in striatum and cortex of HD brains, with staining primarily in microglia (J. Chen et al., 1993; Simmons et al., 2007). Neuroferritinopathy, a condition caused by mutation in the ferritin light chain gene (FTL1), results in accumulation of iron and ferritin in the basal ganglia (Levi et al., 2005). Neuroferritinopathy is associated with low serum ferritin levels, accumulation of iron and ferritin in the basal ganglia, oxidative stress, and signs of mitochondrial dysfunction, which are all seen in HD (Bonilla et al., 1991; Curtis et al., 2001). Neuroferritinopathy results in neurodegeneration in the basal ganglia as well as other symptomology similar to HD, and patients are often misdiagnosed as having Huntington's disease (Chinnery et al., 2007; Curtis et al., 2001). Several studies have also linked wild-type Huntingtin

protein function directly to iron homeostasis. Partial knockdown of H*untingtin* in a zebrafish embryo model resulted in a lack of bioavailable iron for hemoglobin in red blood cells despite adequate levels of total iron in the cells. Therefore, Huntingtin may be needed for iron release from endocytic vesicles (Lumsden et al., 2007). Increasing the morpholino concentration to knock-down more Huntingtin in this fish model resulted in a dramatic effect on overall CNS development with reduced size of brain and eye, and brain necrosis, which may or may not be linked to iron availability (Lumsden et al., 2007).

This close link between iron homeostasis and Huntington's disease suggested that an iron trafficking defect could have caused the altered manganese concentration in striatal neurons seen in Williams et al 2010 (Williams, Kwakye, et al., 2010). A shared defect seems likely because many iron transport processes (e.g. transferrin, DMT1) also traffic manganese ions (Roth, 2006). Iron transporters were assessed in the cultured striatal lines, and the transferrin receptor was found to be significantly lower (less than 50%) in the mutant cells compared to wild type (Williams, Kwakye, et al., 2010). High concentrations of iron were then used to saturate iron-dependent transporters, which partially blocked manganese uptake. This paradigm diminished Mn-dependent cell death in both cell lines equally, suggesting that iron transporters, such as the transferrin receptor, do account for a portion of manganese uptake in the mouse striatal cells but do not account for altered manganese accumulation in HD cells. Accumulation of iron (Fe^{3+}) in the mutant cells was also lower in HD cells; however, the fold change was much less than that of manganese and seemed to correlate with the difference in transferrin receptor expression. Unlike manganese levels, iron levels were the same in both cell lines when they were not exposed to excess iron (Williams, Kwakye, et al., 2010).

In addition to the need for bioavailable iron for many key cellular processes, excess iron and/or copper can increase oxygen free radicals via Fenton chemistry. In this process, a metal ion cycles between redox state II and III by disproportionate cleavage of a hydrogen peroxide molecule resulting in the formation of water and a highly reactive free radical (either HO• or HOO•) (Wardman & Candeias, 1996). These reactive oxygen species (ROS) can then cause DNA damage and both protein and lipid peroxidation, processes that cause cellular dysfunction and activate necrotic and apoptotic events. Huntington's disease models demonstrate higher levels of (ROS) and increased sensitivity to ROS mediated damage (Browne et al., 1999). Derangement

of metal ion uptake and transport may partially contribute to the neurodegeneration seen in Huntington's disease through this iron-related formation of ROS, along with damage caused by imbalances in other metal ions such as manganese and copper.

Copper and HD

In addition to iron, copper was also found to be increased in the brains of HD patients in some studies but not others (Dexter et al., 1991; H Diana Rosas et al., 2012). Accumulations were seen in the striatum and cortex of R6/2 HD model mice (Fox et al., 2007). Expression of mutant exon1 of the *Huntingtin* gene in yeast led to increased expression of eight copper binding proteins including metallothionein 1 and 2 (MT1 and MT2) (Hands et al., 2010). These two genes also showed increased mRNA expression in HD patient brains (Hodges et al., 2006). Copper has been shown to facilitate mutant Huntingtin aggregation (Fox et al., 2007). Mutant Huntingtin is known to cause inclusions via aggregation in the nucleus and cytoplasm (Davies et al., 1997). These aggregates were thought to be important mediators of HD pathology; however, recent studies have shown a lack of direct connection between cell death and aggregates, indicating a potentially protective effect of aggregation (Bjokoy et al., 2005).

Despite this potentially positive role of copper in inducing mutant aggregation, reduction of copper via chelation or via genetically knocking-down copper transporters has mitigated HD pathology in both mouse and fly models of HD while simultaneously reducing aggregation (Nguyen et al., 2005; G. Xiao et al., 2013). Copper treatment also further decreased the lifespan of HD flies (G. Xiao et al., 2013). These models, however, express only exon1 of the mutant gene, and aggregation may be a necessary step in pathology with these imperfect model systems. Therefore, copper may play a different (or no) role in patients and animals expressing the full-length mutant *Huntingtin* gene. Alternatively, Boll et al 2008 showed decreased activity of Cu/Zn SOD in HD patients with a trend for increased free copper in the patient CSF (Boll et al., 2008). Since free copper is a Fenton reagent leading to increased ROS production, copper may add to HD pathology in this way. The alterations in iron, copper, and manganese seen in HD patients and in HD model organisms

suggests that metal-handling may be one of the functions of the Huntingtin protein affected by expansion of the pathogenic polyglutamine domain.

Manganese essentiality and toxicity in HD related phenotypes

As discussed above, HD patients and mouse *in vivo* and *in vitro* models exhibit decreased manganese levels either upon basal and/or elevated exposure to manganese (Section X.2.1). Manganese deficiency results in many dysfunctional manifestations similar to Huntington's disease including: urea cycle dysfunction, altered glutamate regulation, increased oxidative stress, and metabolic disturbances including altered IGF-AKT signaling. The following subsections will investigate the interrelationship between these manganese-dependent processes and HD-related pathological phenotypes highlighting enzymes in each process that use manganese as a cofactor.

Regulation of amines and nitric oxide

Nitrogen is one of the most important elements in biological systems. Amino acids, protein monomers, all contain one amine group containing nitrogen, and many contain an additional amine on their R-subunit (i.e. asparigine, arginine, glutamine, and lysine). During normal cellular biochemical processes, deamination releases ammonia into the cytoplasm and eventually the blood stream, but elevated ammonia levels are toxic and can lead to encephalopathy and death. To regulate ammonia levels, the liver produces urea to be excreted into urine to deplete the human body of excess amines. Arginine is an important precursor in the urea cycle as well as an additional process called the nitric oxide cycle. Nitric oxide (NO) is a compound produced from arginine via nitric oxide synthase (NOS). NO regulates many important functions and in the CNS it acts as a neurotransmitter and neuromodulator, particularly regulating glutamate release in the cortex, striatum, and hippocampus. Although its production is vital to many biological functions, excess NO can be neurotoxic via glutamate excitotoxicity and oxidative stress (Calabrese et al., 2007; Dawson et al., 1991). Increased arginine levels can activate NOS activity increasing NO signaling (Durante et al., 2007). Therefore, although the liver is

the primary producer of excreted urea, the brain also converts arginine to ornithine and urea to regulate the production of NO.

Arginase is a manganese-dependent enzyme that catalyzes the conversion of arginine to ornithine. Arginase contains a binuclear manganese cluster of six Mn ions that is vital for its function and cannot be substituted with magnesium like many other manganese containing enzymes (Kanyo et al., 1996). Dietary manganese deficiency decreases arginase activity and increases NOS activity (Brock et al., 1994; Ensunsa et al., 2004). Two genes (*ARG1* and *ARG2*) encode for the two isozymes, ARG1 and ARG2. These two enzymes have identical enzymatic function, but ARG1 is primarily in the cytoplasm whereas ARG2 is located in the mitochondria. ARG1 has been found at higher levels in the brain than ARG2 (Yu et al., 2001). ARG2 expression is especially high in particular areas of the brain affected by HD, including the putamen and ventral striatum (Braissant et al., 1999).

Evidence of altered arginase activity has been reported in both mouse models of HD and peripheral measures from HD patients. At least two different HD model mice (the "R6/2" and a Hdh knock-in model have shown increased ammonia and citrulline levels, both indicative of decreased arginase activity (Chiang et al., 2007; Pouladi et al., 2013). Similarly, HD patients were shown to have increased blood citrulline levels indicating increased NOS activity (Chiang et al., 2007). Arginase transcript levels were also found to be reduced in HD mouse liver (Chiang et al., 2009). Other groups using a non-neuronal cell model showed increase *ARG1* expression, NOS and arginase activity in HD mutant cells that correlated with an increase in arginine uptake (Colton et al., 2004). Dysregulation of arginase by altered manganese homeostasis/bioavailability could result in localized ammonia and NO-related toxic processes as well as altered production of glutamate and GABA which require the conversion of ornithine from arginine as a precursor for their production (Shank, 1983). These HD phenotypes could be the result of altered bioavailability of manganese as has been seen in manganese exposed mouse striatal cells and striatal tissues (Williams, Kwakye, et al., 2010).

Knockdown of neuronal NOS in the R6/1 mouse model of HD delayed disease symptoms and increased dietary arginine accelerated symptom onset by increasing NO synthesis (Deckel, 2001; Deckel et al.,

2002). This interaction between NO level and HD pathology may be due to the necessity of NO in a process called glutamate excitotoxicity, a well-studied HD pathological phenotype (Dawson et al., 1991). Excessive NO can also interact with superoxide radicals to form more reactive oxygen species (ROS) as well as toxic reactive nitrogen species (RNS) that can cause severe cellular dysfunction. Increased oxidative stress due to reactive oxygen and nitrogen species (ROS and RNS) has been reported for several HD model systems (Browne & Beal, 2006; Browne et al., 1999). Increased nitrates and nitrites, which are downstream products of NO signaling, are found in the cerebrospinal fluid of HD patients (Boll et al., 2008). Arginase 1 regulation of nitric oxide production has been shown to be a key to survival of trophic factor-deprived motor neurons (Estevez et al., 2006). Thus, altered arginase activity via altered manganese homeostasis in HD could potentially contribute to a wide range of HD-related phenotypes.

Arginase activity increases polyamine synthesis downstream of the arginase reaction causing beneficial effects. Reduced arginase activity seen in HD models could also lead to dysfunction by reduced production of these polyamines. The production of spermidine in particular has been found to be neuroprotective and actually promotes axonal regeneration (Deng et al., 2009). Spermidine is a scavenger of reactive oxygen species and may therefore be protective against HD pathological processes (Ha et al., 1998). Spermine can rescue HD-related memory deficits in a rodent model (Velloso et al., 2009). One study found that spermine increased the rate of aggregate formation in a poly-Q cell model with increased cell death;(Colton et al., 2004) however, as previously mentioned, aggregation is no longer thought to be a part of the disease process and may actually be protective against mutant Huntingtin pathogenesis (Bjokoy et al., 2005; Slow et al., 2005). In fact, this may be a part of the protective nature of spermine in Huntington's disease.

Glutamate excitotoxicity

Glutamate excitotoxicity is a well-supported pathophysiological process in Huntington's disease (Behrens et al., 2002; Zeron et al., 2002). This neurotoxic mechanism involves excessive glutamate-induced intracellular calcium release resulting in mitochondrial dysfunction. **Figure 1** illustrates potential steps of glutamate cycling and signaling, the first steps of excitotoxicity, which manganese may impinge. There is no consensus yet about

how mutant Huntingtin leads to elevated exictotoxicity. This section will outline several steps in the process from glutamate release to mitochondrial dysfunction and identify points in the process where either manganese and/or mutant Huntingtin may play a role in this pathophysiological process.

Glutamate is the primary excitatory neurotransmitter of the CNS. In the caudate and putamen, a large component of excitatory tone comes from glutamatergic cortical presynaptic axon terminals synapsing with dendrites of the medium spiny neurons. Glutamate then binds to AMPA and NMDA glutamate receptors to cause membrane depolarization. NMDA receptors are permeable to Ca^{2+} in addition to Na^{+} and K^{+}. This influx of calcium during depolarization is important for long-term potentiation and memory formation. Excessive glutamate released at the synapse can result in abnormal Ca^{2+} influx.

To maintain efficient neurotransmission glutamate must be efficiently cleared from the synapse after release. Astrocytes typically account for 80% of synaptic glutamate uptake (Fitsanakis et al., 2006). Manganese decreases astrocytic glutamate uptake and decreases GLAST (astrocytic glutamate transporter) expression (Erikson & Aschner, 2003; Normandin & Hazell, 2002). Manganese can also increase synaptic glutamate release and inhibit NMDA receptors conductance as a channel blocker (Crooks et al., 2007; Guilarte & Chen, 2007).

Huntington's disease models have shown reductions in protein and mRNA of another astrocytic glutamate transporter, GLT1, as well as reductions in astrocytic glutamate uptake (Behrens et al., 2002; Lievens et al., 2001). As already discussed, the manganese-dependent enzyme arginase can also play a role in glutamate release by regulating ornithine production, a precursor to glutamate. In addition to contributing to glutamate release and clearance, manganese also regulates glutamate levels through the process of converting of glutamate to glutamine.

Glutamate that is taken up by astrocytes is converted into glutamine by glutamine synthetase within the glial cell. Glutamine can then be exported from the astrocyte for reuptake by the presynaptic neuron for conversion back into glutamate to help maintain neurotransmitter levels. Glutamine synthetase is the most abundant manganese-containing enzyme in the brain and is primarily expressed in glia (F. C. Wedler et al.,

1982). Like arginase, glutamine synthetase has a high specificity for manganese over magnesium (F. C. Wedler & Ley, 1994).

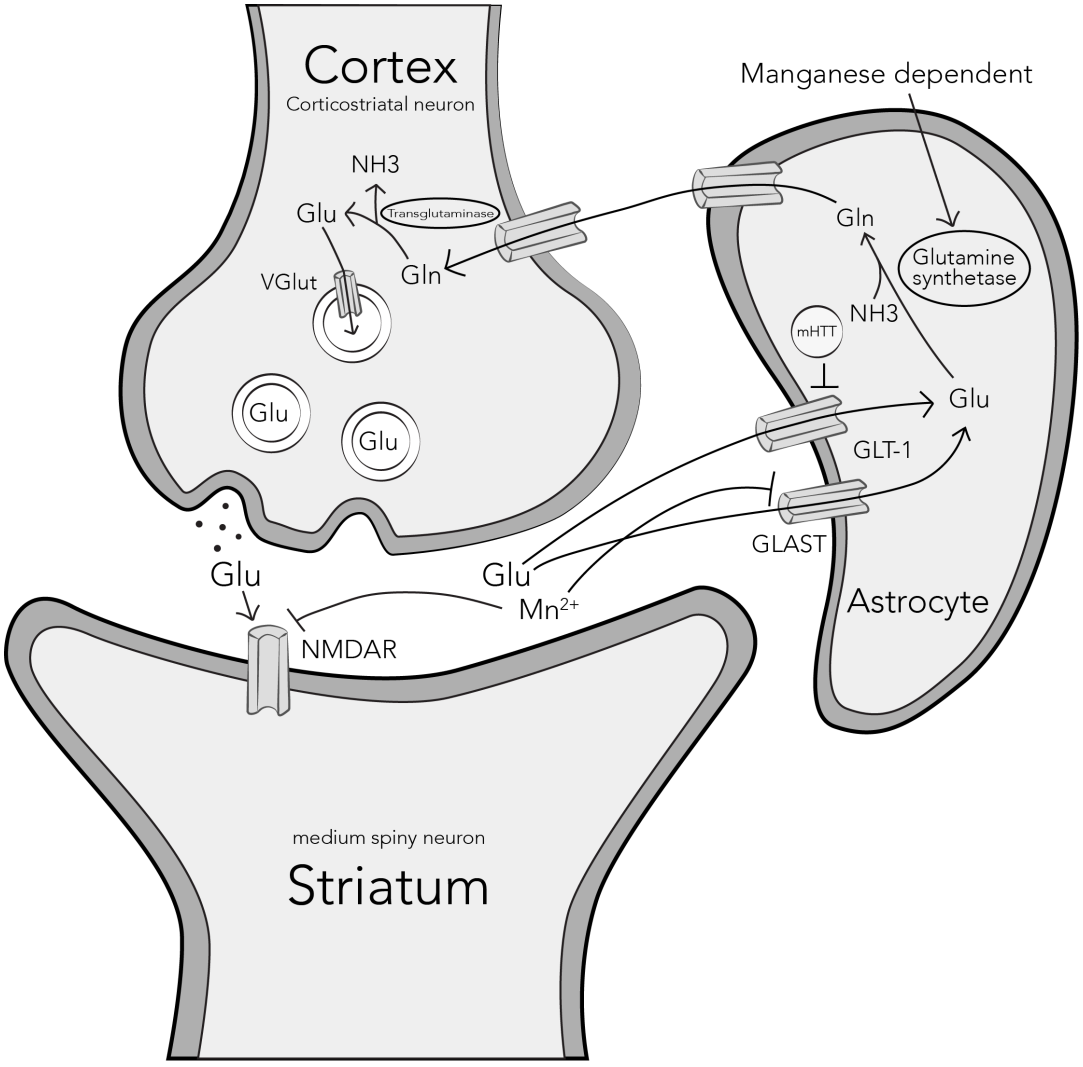

Figure 1. Effects of manganese and mutant Huntingtin on glutamate signaling and cycling at the corticostriatal synapse. A cortical projection neuron (presynaptic) is synaptically joined to the dendrite of a medium spiny neuron in the striatum (postsynaptic). Upon depolarization, glutamate is released from the presynaptic terminal where it interacts with glutamate receptors such as the NDMA receptor. This receptor is calcium permeable and is important for calcium signaling but excess glutamate can cause excess calcium influx leading to excitotoxicity. Manganese is a known inhibitor of the NMDA receptor. Glutamate is cleared from the synapse by supporting astrocytes through glutamate transporters, GLAST and GLT-1, whose expression is known to be inhibited by manganese and mutant Huntingtin (mHTT) respectively. Glutamate is converted to glutamine in the astrocyte by glutamine synthetase, a manganese-dependent enzyme. Glutamine is released from the astrocyte to be taken back up in the presynaptic terminal. It is then converted back into glutamate via transglutaminase releasing ammonia. The glutamate is then repackaged into vesicles by a VGlut transporter. Illustrated by Angela Tidball.

Loss of glutamine synthetase function by genetic mutation or inhibition of gene expression can lead to epileptic seizures (Thomas Eid et al., 2004; Häberle et al., 2005). These seizures are the result of glutamate-

glutamine cycle dysregulation leading to excess extracellular glutamate (Tore Eid et al., 2008). Elevated risk for seizures occurs in HD, and post mortem brains of HD patients show a significant decrease in glutamine synthetase activity in the caudate and putamen compared to matched controls (Butterworth, 1986; Carter, 1982). Mouse models have shown reductions in glutamine synthetase mRNA levels as well as activity (Behrens et al., 2002; Lievens et al., 2001). Additionally, patients with juvenile onset Huntington's disease have even further increased risk of seizures with ~25% of patients presenting (Gambardella et al., 2001; Nance & Myers, 2001). A manganese-handling defect in isolated brain regions could potentially be reflected in reduced glutamine synthetase activity in HD although this direct relationship has not yet been explored.

Manganese deficiencies alone are related to an increased seizure rate in both rats and humans (Dupont & Tanaka, 1985; Hurley et al., 1963; Papavasiliou et al., 1979). Since glutamate is the most abundant compound in the brain, cycling between glutamate and glutamine requires a high enzymatic output via glutamine synthetase and transglutaminase (Birken & Oldendorf, 1989). Manganese deficiency is proposed to decrease glutamine synthetase activity resulting in increased extracellular glutamate, which increases the propensity for seizures.

The production of glutamine from glutamate also uses a free ammonia molecule. Increased ammonia levels in hyperammonemia have been known to increase the rate of glutamine production potentially buffering the brain from toxic levels of ammonia (Cooper, 2001). Reductions in hepatic glutamine synthetase have also been associated with hyperammonemia (Tuchman et al., 1997). Therefore, altered action of glutamine synthetase in Huntington's disease and manganese deficiency could result in localized dysregulation of ammonia levels. Manganese is clearly a crucial player in neuronal energetics as well as intercellular detoxification processes.

Calcium dysregulation

Calcium is tightly regulated in neurons. As mentioned above, excess glutamate increases calcium influx through NMDA receptors. NMDA and voltage-gated calcium channels allow calcium into the post-synaptic neuron during glutamate mediated membrane depolarization. In addition, metabotropic glutamate receptors

can cause calcium release from the endoplasmic reticulum via the inositol 1,4,5-triphosphate (IP3) pathway. These processes are vital for long-term potentiation and memory formation but can cause damage in excess. Medium spiny neurons containing mutant Huntingtin have been found to have abnormally high calcium release when exposed to the same concentration of glutamate (Tang et al., 2005). In addition to alterations in glutamate processing in HD which may lead to excess Ca^{2+} influx, mutant Huntingtin has been found to cause calcium dysregulation by binding to the IP3 receptor (IP3R) resulting in constitutive release of calcium from the smooth endoplasmic reticulum (SER) (Tang et al., 2005). Mutant Huntingtin may also cause the ryanodine receptor to leak calcium from the SER (M. Suzuki et al., 2012). Cytoplasmic calcium is buffered by mitochondria; however, when calcium becomes excessively high, overwhelmed mitochondria can swell, depolarize, and open the mitochondrial membrane transition pore leading to apoptosis (Brustovetsky et al., 2002). Interestingly, along with excess calcium, excess manganese also accumulates in the mitochondria where it can lead to dysfunction and depolarization.

Many studies have used manganese as a calcium surrogate because it can easily be traced by MRI and radioactivity apart from the complexities of internally stored calcium (Koretsky & Silva, 2004). Manganese homeostasis is thought to rely heavily on calcium transporters. Huntington's disease alterations in calcium homeostasis may alter shared calcium/manganese transporters, and, thus, underlie the HD-dependent manganese accumulation phenotype.

Mitochondrial dysfunction: oxidative stress and energetics

Mitochondrial stress can be caused by both excess calcium as well as excess manganese **(Figure 2).** Manganese and calcium are taken up by the mitochondrial calcium uniporter, and manganese is released very slowly by the Na(+)-independent efflux process (Gavin et al., 1998). These slow release kinetics help to buffer the cytosol from potentially toxic effects of these divalent cations; however, when the mitochondria become overloaded with either manganese or calcium, the imbalance can lead to impaired adenosine triphosphate (ATP) synthesis, membrane depolarization, uncoupling of the electron transport chain, and production of reactive oxygen species (Peng & Greenamyre, 1998). Manganese toxicity is known to inhibit all four

mitochondrial complexes of the electron transport chain via oxidative stress (S. Zhang et al., 2004). In isolated mitochondria, significant complex inhibition was achieved by 50 μM manganese that was blocked by several antioxidants indicating that oxidative stress is a major pathway of manganese inhibition of mitochondrial complexes (S. Zhang et al., 2004). Additionally, manganese toxicity inhibits the release of calcium from the mitochondria leading to a potentially toxic buildup (Gavin et al., 1998). In addition to mitochondrial toxicity due to excess manganese, reduced manganese levels are also harmful, altering the activity of the protective manganese super oxide dismutase, which also leaves mitochondria vulnerable to damage (**Figure 2**). Striatal

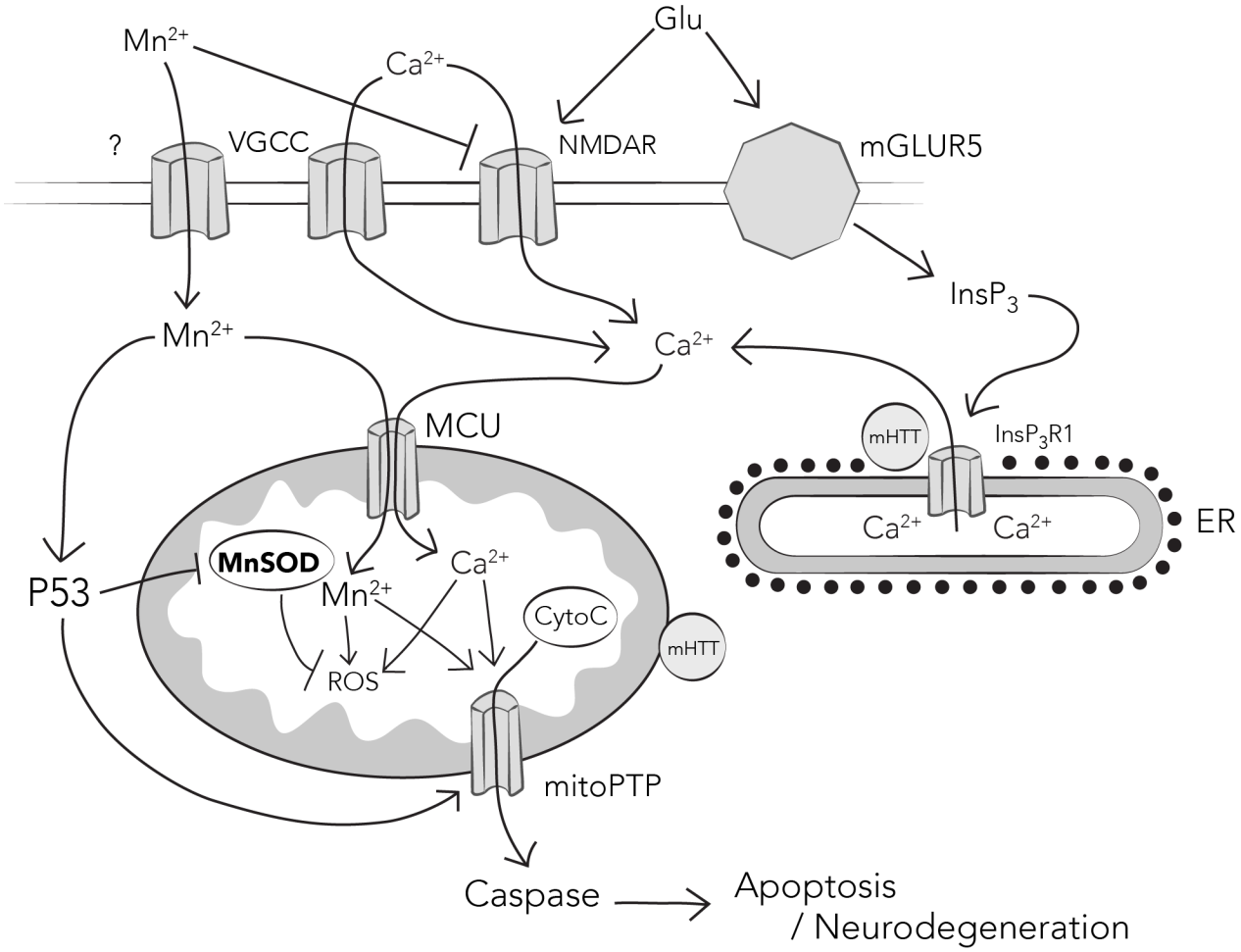

Figure 2. Effects of manganese and mutant Huntingtin on calcium signaling and mitochondrial function. Models of HD have excess glutamate release at the synapse that can cause excessive influx of calcium into the cell from NMDA receptors. Mutant huntingtin (mHTT) has also been shown to cause leaking of the $InsP_3$receptor causing dysregulated release of calcium from the endoplasmic reticulum. Excess calcium is buffered by the mitochondria where it is taken up by the mitochondrial calcium uniporter (MCU); however, in excess, calcium can cause mitochondrial swelling, depolarization, and opening of the mitochondrial permeability transition pore (mitoPTP) leading to apoptosis. In the same way, excess manganese is buffered in the mitochondria and can lead cell death in a similar mechanism. Additionally, manganese exposure has recently been shown to activate p53, which accelerates apoptosis by inhibiting manganese super oxide dismutase, a manganese-dependent free radical scavenger and by potentiating the opening of the mitoPTP. Illustrated by Angela Tidball.

neurons are particularly sensitive to glutamate-mediated excitotoxic cell death. This apoptotic event is dependent on elevated mitochondrial calcium levels (Schinder et al., 1996). Several groups have found that mitochondria are particularly susceptible to calcium-induced membrane depolarization in the presence of mutant Huntingtin (Fernandes et al., 2007).

In summary, this HD-related mitochondrial vulnerability could stem from increased cytosolic calcium levels due to altered glutamate release and clearance, from increased calcium release from the endoplasmic reticulum, from slower recovery kinetics of mitochondrial calcium buffering (Fernandes et al., 2007), or increased mitochondrial sensitivity. In any case, depolarization of the membrane results in opening of the mitochondrial membrane permeability transition pore (MPTP), which releases cytochrome c and initiates apoptotic caspase signaling (Brustovetsky et al., 2002). Striatal neurons have proven to be particularly susceptible to this process of cell death, which may explain the selective degeneration in HD (Brustovetsky et al., 2003). Blockade of the MPTP formation by either cyclosporine A or bongkrekic acid were able to block NMDA-induced and HD-related striatal apoptosis highlighting the importance of this process for HD pathology (Fernandes et al., 2007; Zeron et al., 2002).

Mitochondria may be especially dependent on proper manganese handling because manganese superoxide dismutase (MnSOD) is critical for detoxifying reactive oxygen species in the mitochondria, and manganese is a necessary cofactor for this activity. Manganese supplementation is known to increase MnSOD activity in lymphocytes, while iron supplementation decreases MnSOD activity presumably due to the inverse relationship between iron and manganese accumulation (Davis & Greger, 1992). Neuronal concentration of manganese is very low (< 10 μM); however, the demand for high mitochondrial activity in neurons may be the reason for increased MnSOD activity compared to that found in glia (M. Aschner & Aschner, 1991). Manganese deficiency results in decreased MnSOD activity and increased mitochondrial lipid peroxidation in rats (Zidenberg-Cherr et al., 1983), and HD patients have demonstrated increased lipid peroxidation in their CSF (Boll et al., 2008). Manganese deficiency also causes reduced oxygen uptake and dysmorphic elongation of mitochondria, likely due to lack of ROS detoxification (Hurley et al., 1970).

Partial loss of MnSOD in heterozygous knockout mice results in increased sensitivity to 3-nitroproprionic acid (Andreassen, Ferrante, Dedeoglu, Albers, et al., 2001). 3-nitroproprionic acid (3NPA) causes oxidative stress in neurons by inhibiting succinate dehydrogenase, complex II of the electron transport chain (Huang et al., 2006). This uncoupling of the electron transport chain results in increased production of superoxide, a potent reactive oxygen species that can result in mitochondrial dysfunction as well as oxidative damage of proteins and DNA. 3NPA is also known to cause a preferential lesion to the striatum and was commonly used to model HD in rodents and primates prior to the cloning of *HTT* (Beal et al., 1993). Furthermore, cells expressing mutant Huntingtin are more susceptible to this toxicant (Gines et al., 2003; Williams, Kwakye, et al., 2010). Together, these data argue for a mechanistic link between MnSOD and HD via mitochondrial biology. Clearance of the toxic byproducts of cellular respiration is clearly inefficient in neurons bearing the HD gene mutation, but other functions, such as cellular energetics, are also impacted by mutant HTT, the delicate balance of intracellular metal ions, and possibly by the interaction between the two.

Since mitochondria are the primary site of ATP production in the cell, mitochondrial function is tightly linked to ATP levels. Many disease models of HD demonstrate reduced ATP levels hinting at underlying mitochondrial dysfunction (Gines et al., 2003; Mochel et al., 2012; Seong et al., 2005; Weydt et al., 2006). Furthermore, a striking inverse relationship between ATP/ADP levels and CAG repeat lengths, both pathogenic and non-pathogenic, was observed in human lymphoblastoid lines(Seong et al., 2005). Defects in extra-mitochondrial energy metabolism have been observed in mouse striatal models of HD (J.-M. Lee et al., 2007). In addition to the potential mitochondrial dysfunction via decreased MnSOD discussed in the previous section, reductions in important metabolites necessary for the TCA cycle can also lead to reduced mitochondrial respiration and ATP production. One important enzyme that produces metabolites for the TCA cycle is pyruvate carboxylase.

Pyruvate carboxylase (PC) is a manganese-dependent enzyme that converts pyruvate to oxaloacetate, which is a metabolite for the TCA cycle (Scrutton et al., 1966). Deficiencies in PC can lead to increased lactate in the blood and lactic acidosis, a serious medical condition (Mochel et al., 2005). The activity of pyruvate carboxylase was found to be highly variable in post mortem brains of HD patients;(Butterworth, 1986) however,

many studies have found alterations that indicate reduced activity of this enzyme in HD patients. Lactate has reduced clearance in HD patients (Josefsen et al., 2010). Increased lactate was also seen in the frontal lobe, occipital lobe, and striata of HD patients (Harms et al., 1997; Jenkins et al., 1993). In addition to increasing lactate levels, reduced PC activity decreases the availability of metabolite precursors to the TCA cycle, which is the major source of ATP production. Reduced ATP levels have been seen in many disease models of HD (Gines et al., 2003; Mochel et al., 2012; Seong et al., 2005; Weydt et al., 2006).

Additionally, n-acetyl aspartate (NAA), for which oxaloacetate (OAA) is a precursor, is decreased in the same areas that see an increase in lactate in HD, and both of these potential biomarkers for HD correlate in a concentration dependent manner with duration of the illness (Harms et al., 1997; Jenkins et al., 1993). There is a high concentration of NAA in brain, and production of NAA from OAA is an alternate route for the removal of free cellular ammonia via the addition of an amine (Chiosa et al., 1965). In fact, NAA is the second most abundant molecule in the brain after glutamate (Birken & Oldendorf, 1989). The urea cycle alterations seen in HD may be interconnected with HD-related reduction in NAA. Additionally, the amino acid asparagine, for which NAA is a precursor, is found to be reduced in HD patient brains with high predictive ability (Gruber et al., 2013). Interestingly, creatine treatment can reduce the levels of lactic acid in patients with lactic acidosis (Rodriguez et al., 2007). Creatine has been shown in multiple HD mouse models to ameliorate many of the pathological phenotypes, including motor deficits, weight loss, hyperglycemia, and brain atrophy (Andreassen, Dedeoglu, et al., 2001; Ferrante et al., 2000). Although there may be other derangements of the TCA cycle stemming from the Huntington's disease gene mutation, some of alterations that lead to increased lactate may be explained by the reduced regional uptake of manganese which is necessary for crucial cofactors in this cycle.

In theory manganese deficiency, should lead to a reduction in pyruvate carboxylase activity; however, manganese deficient pups have elevated PC activity by postnatal day 3. Despite this finding, plasma glucose levels are reduced on postnatal days 1 and 2, suggesting glucose metabolism is compromised by manganese deficiency (Baly et al., 1985). PC expression may increase to compensate for diminished activity from a lack of available manganese, with this increase in PC production becoming evident once manganese is replaced in

the diet. Of note, gene expression profiling data from a striatal model of HD implicated several genes in glucose metabolism as being altered in HD, in particular expression of *PCX* (the gene which encodes PC) is elevated in an HD mutant line (J.-M. Lee et al., 2007). Thus, both HD models and manganese deficiency models in rodents result in increased PC expression or activity.

IGF/PI3K/AKT signaling in HD and Manganese exposure

Metabolic disturbances in HD may also be due to altered cell signaling via the insulin and IGF-1 pathways that regulate important rate limiting steps in energy production including glucose transport, glycogen synthesis, and production of precursors for the TCA cycle. As described in section X.1, HD is a neurodegenerative disorder, with select regions showing severe neuronal death, indicating a cell-type specific response to the pathogenic mutation of the Huntingtin protein. Growth factors such as IGF-1 and BDNF have been shown be essential for the survival of striatal neurons, and lack of these growth factor signals may contribute to HD (Zuccato et al., 2010). IGF signaling, and insulin to a lesser extent, lead to activation of the PI3K/AKT pathway, which is an important signaling cascade that promotes proliferation and cell survival. Insulin like growth factor 1 (IGF-1) can stimulate this pathway via the IGF-1 receptor (IGF-1R) and can also activate the insulin receptor as well.

Several studies have found reduced activation of the AKT pathway as measured by the ratio of phospho-AKT(S473) over total AKT in HD cells from patients and mice (Colin et al., 2005; Maglione et al., 2010; Williams, Kwakye, et al., 2010). The increased risk for developing diabetes and insulin resistance in Huntington's disease may result from the altered ability of IGF-1 and insulin to activate AKT and its downstream targets (Farrer, 1985; Podolsky et al., 1972). Blood glucose levels have also been shown to be increased in mice expressing mutant Huntingtin, and HD patients have decreased cerebral glucose consumption (Hurlbert et al., 1999; Mazziotta et al., 1987). Increased activation of the AKT pathway by IGF-1 supplementation has been shown to protect striatal neurons from mutant Huntingtin induced toxicity indicating that this phenomenon may be important in HD neurodegeneration (Humbert et al., 2002b). An alternative route to ameliorate HD-related AKT dysfunction has been administration of ganglioside GM1, which is reduced in HD mice and patient fibroblasts (Maglione et al., 2010).

Several groups have reported alterations in AKT signaling with manganese deficiency and exposure although not in the context of Huntington's disease. Manganese deficiency has been shown to decrease expression of both insulin and IGF-1 (Clegg et al., 1998). Alternatively, exposure to manganese has been shown to increase IGF-1 expression,(Hiney et al., 2011) increase AKT phosphorylation at serine473 in the striatum,(Cordova et al., 2012) and activate both AKT and iNOS activity in microglia (J.-H. Bae et al., 2006). These increases in AKT activity could be due to stimulation of IGF-1 and insulin production or via a more direct route resulting from an observed insulin-like mimetic activity of manganese (Baquer et al., 2003; Subasinghe et al., 1985).

In any case, changes in manganese levels, perhaps via effects on insulin and IGF-1, result in altered glucose regulation and metabolism. Manganese deficiency has been shown to decrease glucose metabolism, insulin secretion, and insulin-induced glucose uptake while manganese exposure can cause hypoglycemia (Baly et al., 1984; Hassanein et al., 1966). In fact, one reported case of "sweet urine disease" was effectively treated with a traditional folk remedy of alfalfa tea. The "sweet urine" was found to have both elevated glucose and manganese urinary output. The alfalfa tea was high in manganese and found to reduce the urinary glucose levels (Keen et al., 2000). Therefore, supplementation of manganese may be efficacious as a treatment in diabetes or to regulate blood glucose levels in HD patients where insulin-resistance and diabetes are common (Farrer, 1985; Hurlbert et al., 1999). AKT signaling, insulin secretion, and blood glucose regulation are all affected by both manganese and mutant Huntingtin, but other modifiers of the AKT pathway can also be altered through this gene-environment interaction.

Protein phosphatase 1 (PP1) is an important phosphatase in many cellular signaling pathways, including the AKT pathway. In fact, PP1 has been shown to directly dephosphorylate AKT at serine 473 and p53 at ser15 (to be discussed further in section 3.5) (D. W. Li et al., 2006; L. Xiao et al., 2010). Interestingly, both AKT and p53 phosphorylation have been shown to increase with manganese exposure; however, this would presumably increase the ability of PP1 to dephosphorylate at these sites as well (J.-H. Bae et al., 2006; Williams, Kwakye, et al., 2010).

One of the many functions of PP1 is to regulate the function of glycogen synthase by dephosphorylation and, thereby, increase its activity. The increased glucose levels noted in Huntington's disease model mice could indicate a deficiency in glycogen synthase activity. Glycogen synthase is also regulated by GSK3B, which phosphorylates and inhibits activity. Intriguingly, GSK3B inhibitors are protective in some HD models, possibly because of deficient ability of PP1 to dephosphorylate glycogen synthase (Carmichael et al., 2002). Further analysis is needed to elucidate the role of this manganese-dependent enzyme, PP1, in HD.

P53 pathway in HD and manganese

P53 is one of the most studied and interconnected cellular signaling molecules known. P53 is important for regulating nearly all cellular stress signals including: DNA damage, oxidative stress, and various other stressors by integrating cellular stress response pathways to elicit an appropriate pro-survival or apoptotic transcriptional response (Carvajal & Manfredi, 2013). P53 has been implicated as a player in mutant Huntingtin mediated neurodegenerative processes, and this pathway is activated under low manganese exposure conditions. Therefore, the p53 pathway may be another point of intersection between manganese homeostasis and Huntington's disease pathology.

HD patients have been shown to have brain accumulation of p53 that correlates with disease stage. Many cellular models of HD have also shown increased p53 activation by phosphorylation at serine15 (B.-I. Bae et al., 2005; J. L. Illuzzi et al., 2011). Mutant Huntingtin is thought to bind to p53 and alter its function (Steffan et al., 2000). Additionally, when HD model mice were crossed onto a p53 knock-out background, nearly all of the pathogenic and behavioral phenotypes in HD were ameliorated, suggesting that p53 may play an important role in the disease-associated neurodegeneration (B.-I. Bae et al., 2005). Additionally, the mitochondrial depolarization and fragmentation phenotypes seen in HD human and mouse cell models were also shown to be diminished by using a inhibitor of p53 transcriptional activity (B.-I. Bae et al., 2005; X. Guo et al., 2013). In fact, single-nucleotide polymorphism (SNP) variants of the P53 gene have also been found to strongly modify age at onset in HD. In fact, 12.6% of variability after taking CAG repeat length into account could be explained by p53 polymorphisms, further underscoring the importance of p53 in HD pathology

(Chattopadhyay et al., 2005). Finally, human induced pluripotent stem cells from HD patients also demonstrate increased activation of p53 as well as one of its upstream kinases, ATM (Jung-Il et al., 2012). ATM has also been implicated in abnormal activation and phosphorylation of p53 (Grison et al., 2011).

P53 has been shown to be a metal-binding protein that relies on a divalent metal ion, Zn^{2+}, to maintain its proper conformation (Meplan et al., 2000). The ability of Mn^{2+} to interact directly with p53 has not been explored. Cellular exposure to several other divalent metal ions (Cd^{2+}, Cu^{2+}, Zn^{2+}, Co^{2+}, Cr^{2+}) has been shown to cause the activation of p53 as monitored by phosphorylation at serine 15, but manganese had not been investigated in this context (Matsuoka & Igisu, 2001; Ostrakhovitch & Cherian, 2004; Stenger et al., 2011; S. Wang & Shi, 2001). However, primates exposed to manganese showed increases in p53 dependent transcripts,(Guilarte et al., 2008) .

In the context of DNA damage, ATM is the canonical kinase for p53, and its activity is increased in some HD models as evidenced by autophosphorylation at serine 1981 (Jung-Il et al., 2012). ATM is an important kinase in the double-stranded DNA break (DSB) repair process (Banin et al., 1998; Canman et al., 1998). In this process, breaks in genomic DNA are associated with a change in the inactive dimer form of ATM being converted into an active monomer that phosphorylates important downstream targets which regulate DNA repair (MRN, gamma-H2AX), cell cycle arrest (CHK2, p53), and apoptosis (p53). ATM has also been recently shown to be activated by oxidative stress through an alternative process of dimer conjugation via a cysteine disulfide bond formation (Z. Guo et al., 2010). Manganese has been shown to be necessary for the *in vitro* enzyme activity of ATM as demonstrated by phosphorylation of downstream targets such as p53 at ser15 (Chan et al., 2000; Z. Guo et al., 2010). While these studies roughly describe ATM as a manganese-dependent enzyme, the exact nature of the relationship between Mn and ATM activity is poorly defined. Manganese may be necessary for proper ATM function in the context of other stressors, or the manganese itself may elicit ATM activation via oxidative stress resulting in the dimerization pathway shown in Guo et al 2010. This seems possible given that very high concentrations of manganese (5 mM) used for activation of ATM and subsequent phosphorylation of p53. The nature of the activation of ATM and p53 via manganese exposure needs to be more clearly defined.

Due to the broad role of p53 in regulating metabolism, DNA repair, stress response, and apoptosis via both transcriptional and non-transcriptional means, p53 dysregulation is also closely related to several of the HD phenotypes explored in previous sections. For example, p53 regulates the IGF-1/AKT pathway by regulating the transcription of several AKT regulatory genes (e.g. IGFBP3, PTEN) (Feng et al., 2007; Feng & Levine, 2010; Levine et al., 2006). AKT also regulates p53 signaling by binding and phosphorylating HDM2, a major regulatory protein of p53 (Gottlieb et al., 2002).

There is also a role for p53 in the mitochondrial dysfunction seen in HD. The HD propensity for mitochondrial depolarization and fragmentation have been shown in cell culture to be blocked by a p53 inhibitor (pifithrin-α) and by knockdown of p53 expression, and p53 has been found to be integral to opening of the mitochondrial membrane transition pore and the release of cytochrome c (B.-I. Bae et al., 2005; X. Guo et al., 2013; Mihara et al., 2003; Vaseva et al., 2012). Interestingly, both the activity and transcription of MnSOD, which detoxifies mitochondrial ROS, are also negatively regulated by activated p53 (Drane et al., 2001; Pani et al., 2000). Therefore, increased mitochondrial susceptibility to glutamate/Ca^{2+} excitotoxic processes could be due to observed increases in p53 activity, leading to either increased propensity to open the MPTP or by diminishing MnSOD expression and activity and thereby increasing reactive oxygen species production and mitochondrial dysfunction.

Activation of p53 has also been shown to reduce glutamate uptake in astrocytes as well as increase the level of mitochondrial glutaminase, which generates glutamate and ammonia (W. Hu et al., 2010; Panickar et al., 2009; S. Suzuki et al., 2010). Thus, activation of p53 in HD or via manganese exposure could lead to increased glutamate production and decreased glutamate clearance from the synapse and increased ammonia levels all of which have been seen in HD models (see section X.3.2.1) (Chiang et al., 2007; Lievens et al., 2001). The far-reaching effects of p53 in regulating the cellular transcriptome as well as its intimate regulation of cell signaling, mitochondrial health, and apoptosis provide a potential unifying theory for the broad effects of manganese homeostasis alterations.

Summary

Metal toxicity and deficiencies can have many detrimental effects on the brain particularly the basal ganglia, which is also selectively susceptible in many neurodegenerative diseases such as HD and Parkinsonism. Iron, copper, and, more recently, manganese levels have been shown to be altered in patients and mouse models of HD. Interestingly, manganese seems to be regionally decreased in organisms containing the mutant Huntingtin protein. The underlying manganese homeostatic dysfunction may cause reduced activity of enzymes that depend on manganese as a cofactor. Reduced manganese levels can lead to many maladaptive phenotypes found in HD models including: urea cycle dysfunction, altered synaptic glutamate regulation, decreased energy production, increased oxidative stress, and altered cell signaling that regulates energy homeostasis and cellular stress. This close relationship between manganese levels and Huntington's disease indicates that deepening our understanding of the underlying defect could lead to therapeutics that rescue deficient manganese levels ameliorating dysfunctional HD processes.

Modeling HD with Human Induced Pluripotent Stem Cells

Previous HD models

Animal models have provided many important insights into HD disease mechanisms; however, a complementary human-based model would overcome several obstacles in HD research (Chamberlain et al., 2008). Model systems have including the original 3-nitroproprionic acid lesioned rodent model followed by transgenic mice, rats, fish, flies, and monkeys as well as immortalized murine striatal cell lines (Brouillet et al., 1999; Sipione & Cattaneo, 2001; Trettel et al., 2000). The divergent evolutionary time between rodents and humans has allowed for large genetic differences, and these interspecies genetic differences could alter disease mechanisms and gene-environment interactions. The most common HD model has been an exon1 transgenic mouse referred to as R6/2 (Mangiarini et al., 1996). Neurodegeneration occurs extremely early throughout the brain in this model with noticeable loss of brain volume at postnatal day 60 and neuronal loss at day 45 (Stack et al., 2005); however, the huge amount of Huntingtin protein missing in this model could result

in missing key aspects of human Huntington's disease. Furthermore, murine HD models with similar size polyQ repeats can have completely different phenotypes indicating the importance of genetics other than the CAG repeat region (Zuccato et al., 2010). Interestingly, the endogenous murine huntingtin only has a polyQ expansion of 7 *CAG* repeats while the human gene averages around 20*,* and the functional significance behind this difference could also alter disease mechanisms and environmental disease modification based on species (Zuccato et al., 2010).

Using human cells and tissues would circumvent these interspecies genetic differences. Post-mortem tissues have provided an important supply of human HD culture material; however, since HD patients lose the majority of their striatal volume during disease progression, these tissues are even more limited. Peripheral tissues such as dermal fibroblasts can be propagated in culture for a limited time period, but differences in expression pattern between CNS and dermal cells reduce their usefulness for modeling neurodegeneration.

Induced Pluripotent Stem Cells

Until recently, post-mortem and peripheral tissues were the only human models available for neurodegenerative studies, but with the advent of induced pluripotent stem cell (iPSC) technology, this paradigm is changing. In 2007, Shinya Yamanaka's lab first demonstrated the direct reprogramming the epigenetic status of human somatic cells into iPSCs, cells equivalent to embryonic stem cells (Takahashi et al., 2007; Takahashi & Yamanaka, 2006). In this landmark study, four transcription factors (OCT4, KLF4, SOX2, and c-MYC) were introduced using retroviral integration into cultured human dermal fibroblasts. Within 30 days, iPSC colonies appeared in culture (Takahashi et al., 2007). After establishing these colonies into stable cells lines, the endogenous pluripotency genes were found to be epigenetically active and the retroviral constructs were silenced. Further studies have validated that the expression pattern, telomerase activity, mitochondrial regulation, and pluripotency of hiPSCs is similar to that of human embryonic stem cells (hESCs) (Armstrong et al., 2010; Suhr et al., 2009; Takahashi et al., 2007).

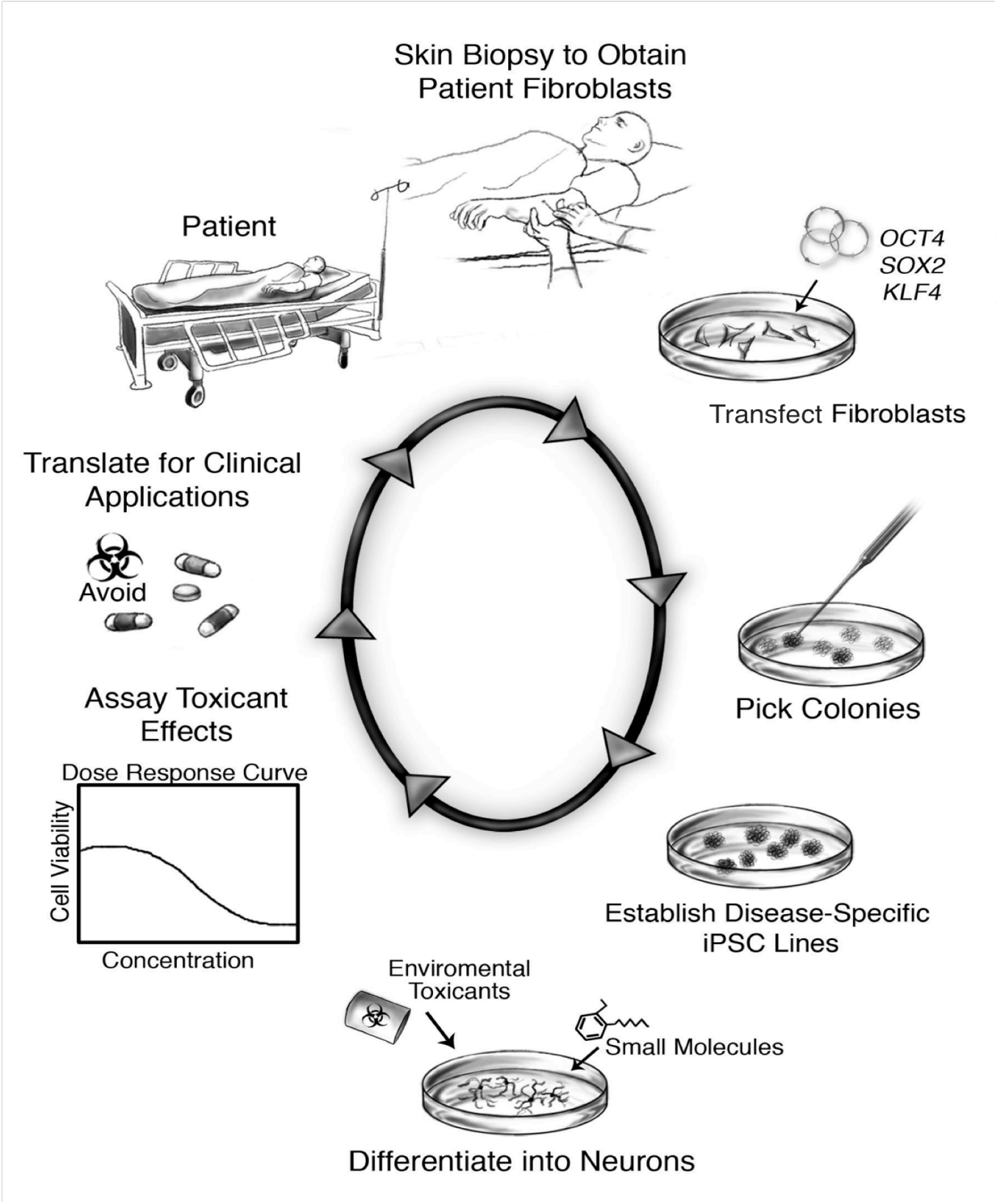

Figure 3. Scientific approach: from bedside to bench and back again. A schematic overview is given of the steps involved in deriving patient-specific neurons and how observations from experimentation with these neurons can potentially benefit patients. Fibroblasts harvested from a skin biopsy are transduced to become patient-specific human induced pluripotent stem cells (iPSCs). The human iPSCs are then differentiated into neurons that can be assessed for their response to the neurotoxicants of interest. The knowledge obtained from these experiments may directly benefit the patients or allow the testing of novel hypotheses related to disease pathogenesis.

Like human embryonic stem cells (hESCs), iPSCs can be differentiated into any cell type in the body. Patient-specific iPSCs have also been generated (e.g. HD, ALS, PD, Down syndrome, spinal muscular atrophy) providing researchers with patient-specific cell lines for *in vitro* disease modeling (**Figure 3**) (Dimos et al., 2008; Ebert et al., 2009; G. Lee et al., 2009; Park et al., 2008). Recent studies have also provided increased reprogramming efficiencies by small molecule incubation and integration-free iPSC induction techniques using cell permeable proteins and non-integrating DNA vectors(Jia et al., 2010; Lin et al., 2009; Zhou et al., 2009). One study has also shown induction of iPSCs from culturing T cells found in a single milliliter of blood (Seki et al., 2010).

These technical advancements will soon provide a simple, integration-free patient-specific generation method for HD iPSC lines that can be differentiated into relevant cell types. Indeed, the Yamanaka lab further improved their original technique by developing a episomal non-integrating plasmid method of expressing the reprogramming genes that has proved highly efficient(Okita et al., 2011). Huntington's disease was one of the first diseased iPSC lines ever generated (Park et al., 2008) and since that time a plethora of papers generating and using HD iPSC disease models have been published (An et al., 2012; Camnasio et al., 2012; Consortium, 2012; Jeon et al., 2012; Jung-Il et al., 2012; Juopperi et al., 2012; X. Zhang et al., 2010).

In vitro Differentiation to Medium Spiny Neurons

With the correct incubation of signaling molecules, HD iPSC lines can then be differentiated into striatal neurons. Neurodevelopment requires many spatial-temporal signaling events that are complicated by the multiple roles of signaling molecules. Unfortunately, the majority of neurodevelopmental research has been based on murine embryo brain development, and the timing and function of human homologs cannot be assumed from these data. Using human pluripotent stem cells *in vitro* allows for elucidation of both normal and disordered human neurodevelopment. Several laboratories have already used human recombinant signaling proteins and small molecules to exogenously direct differentiation of iPSC and ESC *in vitro* cell cultures to enriched populations of motor neurons, midbrain dopaminergic neurons, and forebrain GABAergic and glutamatergic neurons(Aubry et al., 2008; Chambers et al., 2009; Dimos et al., 2008; Ebert et al., 2009;

Gaspard et al., 2008; Kim et al., 2010; X.-J. Li et al., 2009). Neurons differentiated from HD and control iPSC could be used for *in vitro* studies of disease mechanisms, gene-environment interactions, drug-screening, and regenerative medicine.

The first stage of human stem cell differentiation is toward one of the three germ layers: neuroectoderm, mesoderm, and endoderm. Neuroectoderm has been found to be the default tissue fate of epiblast culture, and cultured hESCs have been shown to be in an epiblast stage(Buecker et al., 2010; Muñoz-Sanjuán & Brivanlou, 2002). Signaling by the TGF-β super family, including bone morphogenic proteins (BMPs), inhibits the formation of neuroectoderm (Vallier et al., 2004). *In vivo,* proteins like noggin bind to BMPs to block their signaling allowing default neural tissue to form. Initial neural induction studies used either the formation of embryoid bodies or co-culture with stromal cells. Unfortunately, embryoid bodies induce small numbers of neural cells, and stromal cells take several weeks to cause efficient neural induction followed by laborious mechanical picking of neural rosettes (Dhara & Stice, 2008). These difficulties were overcome when Chambers et al. induced ~80% PAX6-expressing cells, a neuroectodermal markers, in less than a week in monolayer hESC culture (Chambers et al., 2009; X. Zhang et al., 2010). This was achieved using noggin and a TGFβ small molecule inhibitor (Chambers et al., 2009). Noggin can also be replaced with dorsomorphin, a small molecule that blocks the downstream Alk-SMAD pathway of BMP signaling (Chambers et al., 2009; Kim et al., 2010). Unfortunately, iPSC lines have been found to be highly variable in their neural induction efficiencies (B.-Y. Hu et al., 2010). However, this variability may be attenuated with the production of iPSC lines screened by more strict validation methods. In any case, a large percentage of neural progenitors can be produced from iPSC lines.

Medium spiny neurons (MSNs), which are particularly vulnerable in HD, develop in the lateral ganglionic eminence of the ventral telencephalon. Gradients of signaling molecules give developing progenitors positional identity. LGE progenitors need to be patterned by signaling molecules that lead to an anterior, ventral, and finally lateral position during the neural patterning process. The anterior-posterior axis is set up by anterior expression of Wnt inhibitors, Cerberus (also a BMP inhibitor) and dikkopf-1 (DKK1), and BMP inhibitors inducing anterior fate (**Figure 4A**) (Rallu et al., 2002). Sonic hedgehog (SHH), is secreted from

the floorplate of the neural tube, setting up the dorso-ventral axis by inhibiting the dorsally expressed Gli3 repression of fibroblast growth factor (FGF) signaling (**Figure 4B**) (Hébert & Fishell, 2008). FGF is the major ventralizing signal of the CNS. FGF receptor knockouts lose most of the ventral region of the telenchepalon (Hébert & Fishell, 2008). However, incubation of chick lateral ganglionic eminence (LGE) explants, which normally develops into striatum, with FGF8 causes expression of medial ganglionic eminence (MGE) markers (Lupo et al., 2006). Therefore, FGF8 I is most likely dispensable for LGE induction. Several laboratories have incubated hESCs with exogenous DKK-1 and SHH to produce cells expressing ventral telencephalic markers(Aubry et al., 2008; X.-J. Li et al., 2009).

To specify LGE identity over MGE requires the signaling molecule retinoic acid (RA)(Lupo et al., 2006). RA expression in chick embryos causes expansion of the LGE at the expense of both MGE and dorsal regions (Marklund et al., 2004). Additional studies have found RA receptor antagonists block the formation of LGE(Lupo et al., 2006). Few studies have used RA for the specification of LGE-like progenitors despite its apparent necessity. The ventral telencephalon has been shown to endogenously produce RA, which could lead to LGE patterning *in vitro* (Guillemot, 2005; Waclaw et al., 2004). However, for a more robust directed differentiation protocol, RA may be necessary.

After patterning, neural progenitors must be induced to terminally differentiate into mature neurons. BDNF is a key molecule in striatal differentiation. It induces the expression of DARPP-32, and BDNF loss decreases striatal projection neuron markers and MSN dendritic arborization complexity (Bédard et al., 2006; Jain et al., 2001; Rauskolb et al., 2010). Additionally, exogenous expression of BDNF and noggin in the adult striatal ventricular zone has been found to reactivate nascent progenitors to become new MSNs (Chmielnicki et al., 2004). The first report of DARPP-32 positive MSN generation from human ES cells used a combination of BDNF with valproic acid and dibutryl-cyclic-AMP, two compounds known to increase striatal neurogenesis (Aubry et al., 2008; Bédard et al., 2006; Laeng et al., 2004). This paper from the Perrier lab showed that MSN-like differentiation is possible; however, the protocol was highly inefficient and took nearly two months to complete. The most refined protocol for MSN-like differentiation(Carri et al., 2013) combines the SHH and

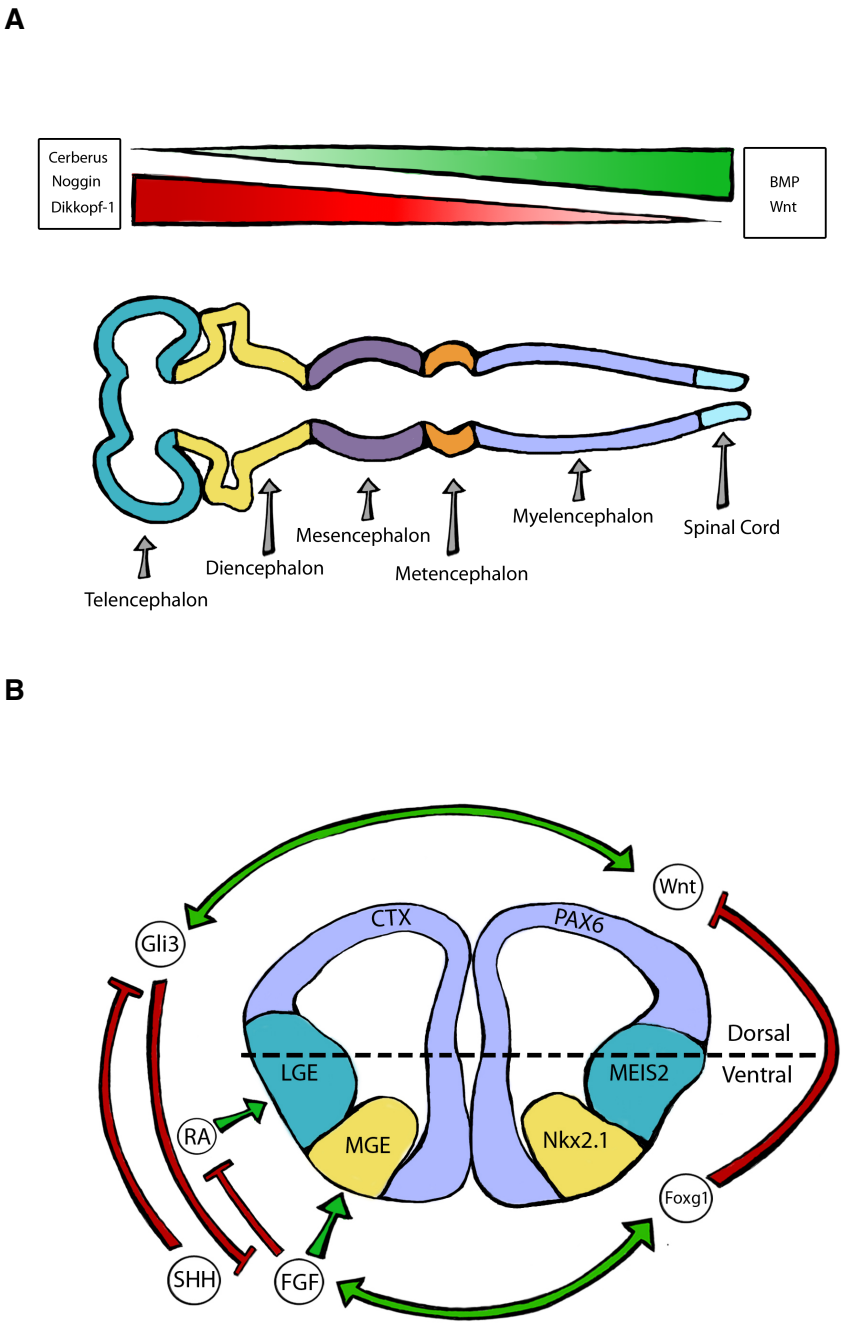

Figure 4. *In vivo* patterning of the telencephalon via endogenous signaling molecules. ***A*** Several important signaling molecules in anterior-posterior axis formation. Wnt and BMP promote posterior formation, and Cerberus, noggin, and dikkopf-1 inhibit the function of these posteriorizing molcules leading to anterior formation. ***B*** Major telencephalic signaling molecules. The three major regions are labeled on the left cortex (CTX), lateral ganglionic eminence (LGE), and medial ganglionic eminence (MGE). To the right are specific markers of these regions. Sonic hedgehog (SHH), fibroblast growth factors (FGF), retinoic acid (RA), Wnt, Foxg1, and Gli3 have both active and repressive roles in setting up the dorso-ventral and medio-lateral axes.

DKK1 (Aubry et al., 2008; X.-J. Li et al., 2009) after dual-SMAD inhibition (Chambers et al., 2009) followed by neurobasal medium with BDNF, N2, and B27 supplements. These cells were highly characterized as valid MSNs by immunostaining, microarrays, and electrophysiological recordings; however, the efficiency of DARPP-32 expressing cells was still 10%.

Modeling Huntington's disease with patient-specific iPSC derived neurons

Although medium spiny neurons (MSNs) are the first cells affected in typical disease progression, current differentiation protocols to MSNs from iPSCs are highly inefficient and time-consuming (Aubry et al., 2008). While these protocols are being developed, many labs have begun using neural stem cells or neuroprogenitors to model Huntington's disease allowing for more homogeneous cell populations for assay disease phenotypes (Camnasio et al., 2012; Consortium, 2012; N. Zhang et al., 2010). In fact, some publications have indicated a potential development role in Huntington's disease (Molero et al., 2009); therefore, assaying disease phenotypes throughout *in vitro* development may provide new insights into the disease. Although there is no indication that early neural progenitors are affected in HD, new studies indicate that the specificity to MSNs is due to a quantitative regional difference of the neurodegenerative process rather than a region-specific qualitative difference (Fossale et al., 2011). In fact, many brain regions in addition to the striatum degenerate in late stage HD presumably for this reason (Zuccato et al., 2010). Furthermore, in juvenile HD nearly all regions of the brain degenerate. Therefore, since neural progenitors have a similar expression pattern to mature cells and mutant Huntington is expressed in all cells, we expect at least some of the neurodegenerative disease process to be active in neuroprogenitors.

Given the great breadth of Huntington's disease related phenotypes in patients and both animal and cell models(Zuccato et al., 2010), initial experiments investigating genotype-phenotype relationships in HD iPSC models often rely upon the investigators prior experience. For this reason, nearly all of the HD iPSC papers published to date focus on different outcome measures. Thus far, HD related phenotypes shown in human iPS cell models have included increased caspase activity after growth factor withdrawal, increased lysosomal activity, reduced ATP levels, and accumulation of vacuoles(Camnasio et al., 2012; Consortium,

2012; Juopperi et al., 2012; N. Zhang et al., 2010). Many of these observations further validate disease differences shown in previous models systems(Castiglioni et al., 2012; Gines et al., 2003; Martinez-Vicente et al., 2010; Mochel et al., 2012; Nagata et al., 2004; Seong et al., 2005; Weydt et al., 2006). Recent advances in genome editing, such as the advent of CRISPR technology, provide the ability to create isogenic control lines to reduce the possibility of none genotype related phenotypes from other genetic differences between control and HD lines(Hou et al., 2013). One HD iPS cell study replaced a pathogenic 72 CAG repeat length in the mutant allele with a non-pathogenic length of 21 CAG repeats(An et al., 2012). This contraction of the repeat region eliminated elevations in apoptosis, caspase cleavage, reduced BDNF, TGF-β1, and N-Cadherin expression. With the rapid progression in efficiency and accessibility of CRISPR technology, these types of controls should soon become standard to iPS cell model research.

Conclusion

Induced pluripotent stem cells will provide an important model for the study of Huntington's disease. These cells can be generated from patients with well-documented genotypes and symptoms in much less time than generating a transgenic mouse. They can be propagated indefinitely and differentiated into medium spiny neurons. *In vitro* differentiation allows for better understanding of human neurodevelopment and how disease and toxicants affect developmental time points. Maintenance of the human genetic background allows for an adequate model to study gene-environment interactions, and these studies could lead to treatments that delay disease onset and progression for HD patients.

CHAPTER II

A MANGANESE-HANDLING DEFICIT IN HUNTINGTON'S DISEASE SELECTIVELY IMPAIRS ATM-p53 SIGNALING

The essential micronutrient manganese is enriched in brain, especially the basal ganglia. We sought to identify neuronal signaling pathways responsive to neurologically relevant manganese levels, as previous data suggested manganese alterations occur in Huntington's Disease (HD). We found that p53 phosphorylation is highly responsive to manganese levels in human and mouse striatal-like neuroprogenitors. The Ataxia Telangiectasia Mutated (ATM) kinase is responsible for this manganese-dependent phosphorylation of p53. Activation of ATM-p53 by manganese was severely blunted by pathogenic alleles of *Huntingtin*. HD neuroprogenitors exhibited a highly manganese selective deficit in ATM kinase activation, since DNA damage and oxidative injury, canonical activators of ATM, did not show similar deficits. Manganese was previously shown to activate ATM kinase in cell-free assays. We found that human HD neuroprogenitors have reduced intracellular manganese with neurologically relevant manganese exposures. Pharmacological manipulation to equalize manganese between HD and control neuroprogenitors rescued the ATM-p53 signaling deficit.

Introduction

Huntington's disease (HD) is a devastating neurological disorder characterized by motor, psychological, and cognitive impairments and premature death (Zuccato et al., 2010). Symptoms stem primarily from central nervous system (CNS) neurodegeneration - most notably death of medium spiny neurons (MSNs) in the caudate and putamen. HD is caused by an expansion of a CAG triplet-repeat region in exon 1 of the *Huntingtin* gene. Although HD is a monogenic, autosomal-dominant disease, environmental factors play a major role in modifying age of disease onset. CAG repeat length contributes to just over half of the variability in age of onset, and the majority of the remaining age of onset variability was attributed to unknown environmental factors in a landmark genetic study of a large Venezuelan kindred (Wexler, 2004). For example, among

patients with repeat lengths of ~40, ages of onset can span four decades or more (Wexler, 2004). Even monozygotic twins with HD have shown differences in both age of onset (differences up to 7 years) and symptomatic manifestation, despite identical repeat lengths (Anca et al., 2004; Friedman et al., 2005; Georgiou et al., 1999). These data strongly support a role for environmental modifiers in HD pathobiology, even though few specific environmental modifiers have been discovered. Aside from environmental enrichment in HD mouse models, metals (copper, iron, cadmium, and manganese) are important environmental modifiers of HD (Fox et al., 2007; Glass et al., 2004; Wild & Tabrizi, 2007; Williams, Li, et al., 2010; G. Xiao et al., 2013). We have previously shown differential toxicological sensitivity to manganese (Mn^{2+}) and cadmium (Cd^{2+}), but not other metal ions tested (Fe^{3+}, Cu^{2+}, Pb^{2+}, Co^{2+}, Zn^{2+}, Ni^{2+}) in an immortalized mouse striatal neuroprogenitor model of HD (ST*Hdh*$^{Q7/Q7}$ *and* ST*Hdh*$^{Q111/Q111}$) (Trettel et al., 2000; Williams, Li, et al., 2010). Expression of mutant *Huntingtin* conferred a survival advantage under cytotoxic manganese exposure conditions due to a substantial decrease in net manganese uptake, whereas mutant *Huntingtin* increased sensitive to cadmium cytotoxicity (Williams, Li, et al., 2010).

Manganese, an essential element, is required for several enzymatic processes (J. L. Aschner & Aschner, 2005), and several of the processes are altered in HD (e.g. oxidative stress, glutamate cycling, and the urea cycle) (Bowman, Kwakye, Herrero Hernández, et al., 2011). On the other hand, excess manganese causes cytotoxicity via increased oxidative stress in part from direct inhibition of mitochondrial respiration (S. Zhang et al., 2004). Thus, appropriate homeostatic regulation of manganese levels is needed to ensure biological function but avoid toxicity (Santamaria, 2008) . The globus pallidus, caudate nucleus, and other areas of the basal ganglia contain the highest level of manganese in the brain and are the areas most susceptible to HD degeneration (Larsen et al., 1979; Prohaska, 1987). Pre-symptomatic HD mice (Tg-YAC128Q) have elevated sensitivity to manganese exposure, with increased dendritic spine loss in MSNs (Madison et al., 2012). HD patients also have reduced manganese levels in cortical regions, and manganese exposed HD mouse models have reduced manganese accumulation in the striatum, the most vulnerable region in HD(H Diana Rosas et al., 2012; Williams, Li, et al., 2010). Collectively, these data suggested a potential alteration in brain manganese-handling in HD. In this study, we assessed whether biological

responses to manganese are altered by pathogenic CAG repeat expansions in *Huntingtin* using human induced pluripotent stem cell (iPSC)-derived early striatal-like (ventralized) forebrain lineage neuroprogenitors and mouse ST*Hdh* striatal neuroprogenitors (Carri et al., 2013; Chambers et al., 2009; Ma et al., 2012; Okita et al., 2011).

We postulated that manganese exposure and mutant *Huntingtin* may impinge upon common intracellular signaling pathways. Manganese exposure increases AKT and ERK phosphorylation in the rat striatum, and mouse striatal and microglial cultures (J.-H. Bae et al., 2006; Cordova et al., 2012; Williams, Li, et al., 2010). Manganese exposure in non-human primates elicited alterations in p53-dependent transcripts and increased p53 immunoreactivity in the frontal cortex (Guilarte et al., 2008). Additionally, in PC12 cells, manganese can increase p21 mRNA expression, an established transcriptional target of p53 (Zhao et al., 2012). Expression of mutant *Huntingtin* has also been shown to alter AKT (Colin et al., 2005; Cordova et al., 2012; Humbert et al., 2002a; Williams, Li, et al., 2010), p53 (B.-I. Bae et al., 2005; Steffan et al., 2000), ERK (Apostol et al., 2006; Fan et al., 2012), mTOR (Ravikumar et al., 2004), AMPK (Ju et al., 2011), and GSK3β (Carmichael et al., 2002) signaling. However, most of the manganese studies were performed at acutely cytotoxic levels of manganese. To test the hypothesis that expression of mutant *Huntingtin* would alter intracellular signaling in response to neurologically-relevant manganese levels, we assessed the response of several signaling pathways to sub-cytotoxic levels of manganese in human and mouse striatal-like neuroprogenitor models of HD.

Results

Generation and validation of human HD patient and control iPSC lines

We generated iPSC lines from dermal fibroblasts (Coriell Cell Repositories [GM21756 and GM09197]) of 2 juvenile-onset HD patients with large *Huntingtin* CAG repeat lengths (70 and 180). We also derived iPSC lines from fibroblasts of 2 control subjects with no history of neurological conditions (CE and CF) (see **Materials and methods**). Integration-free iPSC lines were generated by electroporating fibroblasts with episomal plasmid

vectors (Okita et al., 2011). The iPSC lines were validated for expression of protein markers of pluripotency such as OCT4 and Nanog (**Figure 5A**). HD genetic status was confirmed by assessing the CAG repeat length in exon 1 of *Huntingtin* in both the iPSC lines and the originating fibroblast lines (**Figure 5B**). We identified one clonal line, HD180 clone 6 (referred to as HD180-6), that demonstrated an expansion of the CAG repeat from 180 to >210 in the pathogenic allele. To our knowledge, this is the first reported expansion of the *Huntingtin* gene CAG repeat region in an iPSC line; however, iPSC lines from patients with Friedrich's ataxia often demonstrate expansion of the GAA triplet repeat due to high expression of *MSH2*, which is known to mediate somatic triplet expansion in the *Huntingtin* gene (Ku et al., 2010; Manley et al., 1999). To validate the quality of our iPSC lines, we performed PCR for DNA isolated from each clonal iPSC line to ensure the absence of plasmid integration. The episomal vectors are typically lost over successive cell cycles; however, they can integrate into the genome at a low frequency (Okita et al., 2011). Primers were targeted to the WHP Posttranscriptional Regulatory Element (WPRE) region of the plasmid that would constitute a novel sequence in the human genome. Lines maintaining the WPRE region were excluded from our studies. A normal euploid karyotype was confirmed for all validated lines. Lastly, we performed an mRNA microarray and performed the PluriTest bioinformatics assay to test for conformity to pluripotency (**Figure 5C**). All iPSC lines used in this study were confirmed by this test with very little variance between lines and high similarity to a previously published teratoma-validated control line (Neely et al., 2012).

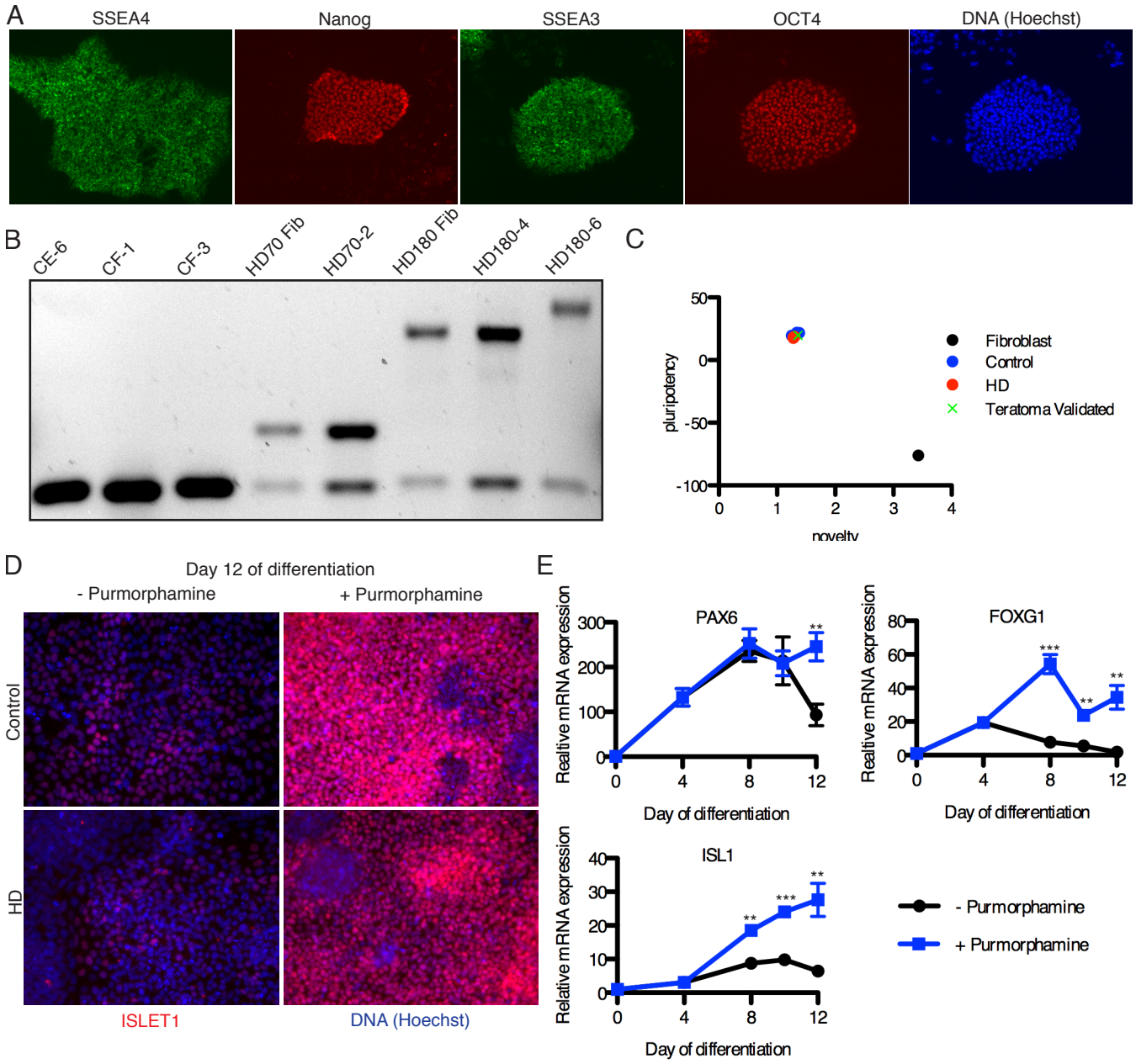

Figure 5. Differentiation of iPSCs into early striatal-like neuroprogenitors. (**A**) Immunofluorescent staining of HD iPSC line HD70-2 for markers of pluripotency. (**B**) PCR for the *Huntingtin* gene including the CAG repeat region. The lower bands are the non-pathogenic alleles, and the larger bands are pathogenic. All iPSC lines show similar sizes to the fibroblast lines from which the iPSCs were generated except HD180-6, which shows an expanded CAG repeat size. (**C**) The PluriTest analysis was used to validate the mRNA microarray profile from our iPSC lines, and all lines had a similar pluripotency profile, including a teratoma-validated iPSC line. (**D**) Control (CA-24) and HD (HD180-2) iPSCs were differentiated to early forebrain neuroprogenitors by the dual SMAD small molecule technique with and without purmorphamine (SHH agonist) and were immunostained for ISL1 (*red*), a marker of striatal progenitors, with nuclei labeled with Hoechst dye (*blue*). (**E**) Expression of markers of neurodevelopment was measured by qRT-PCR from the CF-3 control cells differentiated with and without purmorphamine. ** for $p < 0.01$, *** $p < 0.001$ by t-test. N = 4. Mean ± SEM.

Differentiation to neuroprogenitors expressing early striatal markers

We used the established "dual-SMAD inhibition" method of neuralization via SB431542 and DMH1 to generate telencephalic neural progenitors from our iPSC cultures (Chambers et al., 2009; Ma et al., 2012; Neely et al., 2012). These early neuroprogenitors expressed the neuroectodermal marker, PAX6, and the telencephalic marker, FOXG1 (**Figure 5E**)(X. Zhang et al., 2010). Addition of sonic hedgehog (SHH) or a SHH agonist, purmorphamine, has been shown to ventralize these neuroprogenitors to express markers of the lateral ganglionic eminence (LGE) from which striatal MSNs develop (Ma et al., 2012). Addition of purmorphamine to the neuroprogenitor cultures from day 4 of differentiation onward resulted in a significant increase in expression of Islet1 (ISL1) protein and mRNA over time (**Figure 5D, E**). In the developing telencephalon, *ISL1* is expressed specifically in the earliest post-mitotic cells of the striatum (H.-F. Wang & Liu, 2001). A recently published method for generating fully validated MSNs uses an analogous technique in the first stage (Carri et al., 2013). Our *ISL1+* neuroprogenitors provided a nearly homogenous cell population (~90% ISL1+ cells by immunofluorescence microscopy) regardless of the genotype (HD or control) to begin assessing the effects of manganese. Furthermore, quantitative reverse-transcriptase PCR (qPCR) for *ISL1* demonstrated statistically identical expression levels between control and HD neuroprogenitors (**Figure 6**). These human striatal-like neuroprogenitors are at a homologous developmental time point as the ST*Hdh*$^{Q7/Q7}$ and ST*Hdh*$^{Q111/Q111}$ cells, which were isolated from the mouse striatum on embryonic day 14 (E14), a developmental time point wherein *ISL1* expression defines the developing striatum (López-Bendito et al., 2006; Trettel et al., 2000). Thus, allowing for more valid comparisons between these two model systems.

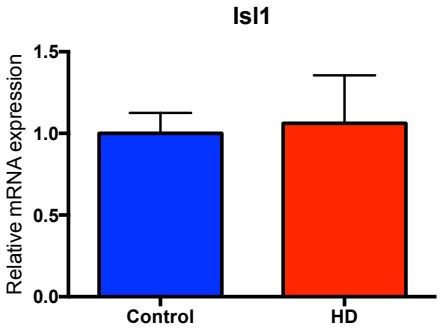

Figure 6. *ISL1* mRNA expression is the same in control and HD human neuroprogenitors. On day 12 of differentiation, mRNA samples were obtained from control and HD cells. Quantitative RT-PCR was performed on 10 ng of cDNA, and the values were normalized to actin and ribosomal RNA expression. N = 4 for control (2 each for CE-6 and CF-1) and HD (2 each for HD70-2 and HD180-4). Bars, mean + SEM.

Manganese exposure evokes strong p53 response in human and mouse striatal neuroprogenitors

To elucidate the effect of sub-toxic manganese exposure on intracellular signaling pathways in both the human and mouse cell models, we performed the PathScan ELISA-based signaling pathway array (PathScan, Cell Signaling Technology, Danvers, MA). The sub-toxic manganese exposure (24-hour) concentrations in the human and mouse neuroprogenitors were determined via the CellTiterBlue cell viability assay (Promega, Madison, WI) (**Figure 7**). In human *ISL1*+ neuroprogenitors, no difference in manganese cytotoxicity was observed between HD and control (**Figure 7A**). This finding is in contrast to the decreased sensitivity of mouse HD ST*Hdh*$^{Q111/Q111}$ cells to manganese cytotoxicity relative to control shown here (**Figure 7B)** and previously published (Williams, Li, et al., 2010). We selected 200 μM manganese exposure for the human *ISL1+* neuroprogenitors, and 50 μM manganese for the mouse striatal ST*Hdh* cells because these concentrations caused similar, but minimal (< 15%), loss of viability across the two model systems (**Figure 7C**). These concentrations are at, or just above, the threshold associated with brain toxicity *in vivo* (Bowman & Aschner, 2014). Furthermore, these manganese levels are within the range we previously found to elicit a strong HD/manganese interaction in the mouse ST*Hdh* model (Williams, Kwakye, et al., 2010; Williams, Li, et al., 2010).

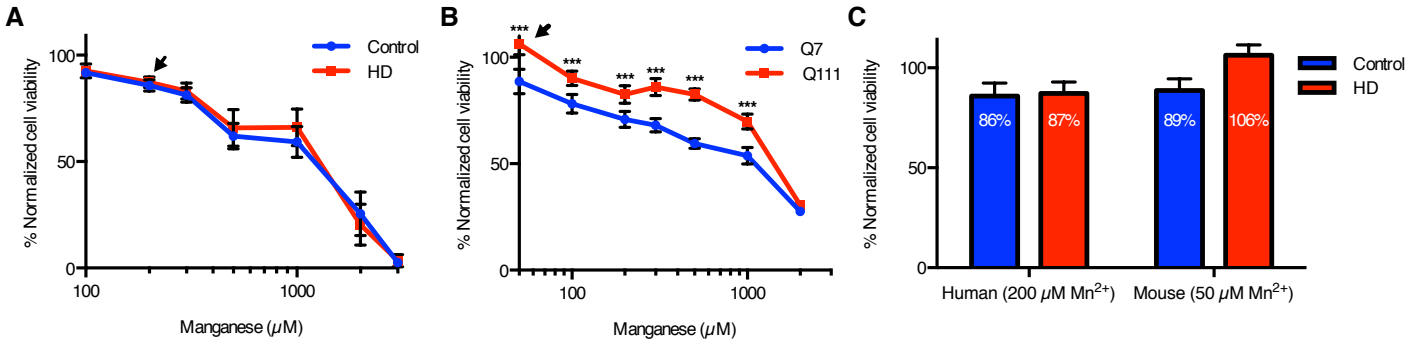

Figure 7. Manganese-induced loss of viability in human neuroprogenitors is unaffected by mutant *Huntingtin.* The cell viability assay, CellTiterBlue, was performed on human (**A**) and mouse (**B**) neuroprogenitors. The signals were normalized by defining the vehicle treated cells as 100% viability. The data for 200 μM manganese exposure in humans and 50 μM in the mouse ST*Hdh* cells (Q7 and Q111), labeled here with arrowheads in **A** and **B**, were replotted for further comparison (**C**). N = 6 for control and 5 for HD in human neuroprogenitors, and N = 6 wells in mouse striatal cells. For genotype comparisons * for $p < 0.05$, ** $p < 0.01$, *** $p < 0.001$ by t-test. Bars, mean + SEM (**A**) and SD (**B,C**).

The PathScan array was used to assess manganese-induction of 18 unique signaling events (phosphorylation or proteolytic cleavage) in control and HD neuroprogenitors (**Figure 8**). Phosphorylation of several signaling proteins displayed a manganese-dependent increase in control cells (Human: p53 and AKT; mouse: p53, GSK3β, and AKT). Phosphorylation of p53 at serine-15, p53(S15), and phosphorylation of AKT at threonine-308 were significantly changed in both model systems, with phosphorylation of p53(S15) showing the most robust change in both human and mouse models (**Figure 8A,B**). Interestingly, manganese-induced phosphorylation of p53(S15) was severely diminished in HD neuroprogenitors in both human (223% in control vs. 113% in HD; $p < 0.01$) and mouse striatal-like neuroprogenitors (384% in control vs. 163% in HD; $p < 0.05$). As expected from our cytotoxicity assays, proteolytic activation of Caspase-3 and PARP-1, enzymes activated during apoptotic cell death, showed no change between vehicle and manganese exposures, indicating minimal apoptotic cell death in our PathScan array experiments (**Figure 8C,D**). We suspect the slight decrease in detected viability by the CellTiterBlue assay at these manganese exposure levels (**Figure 7A**) is due to decreased cell proliferation over the 24-hour exposure period, rather than cell death.

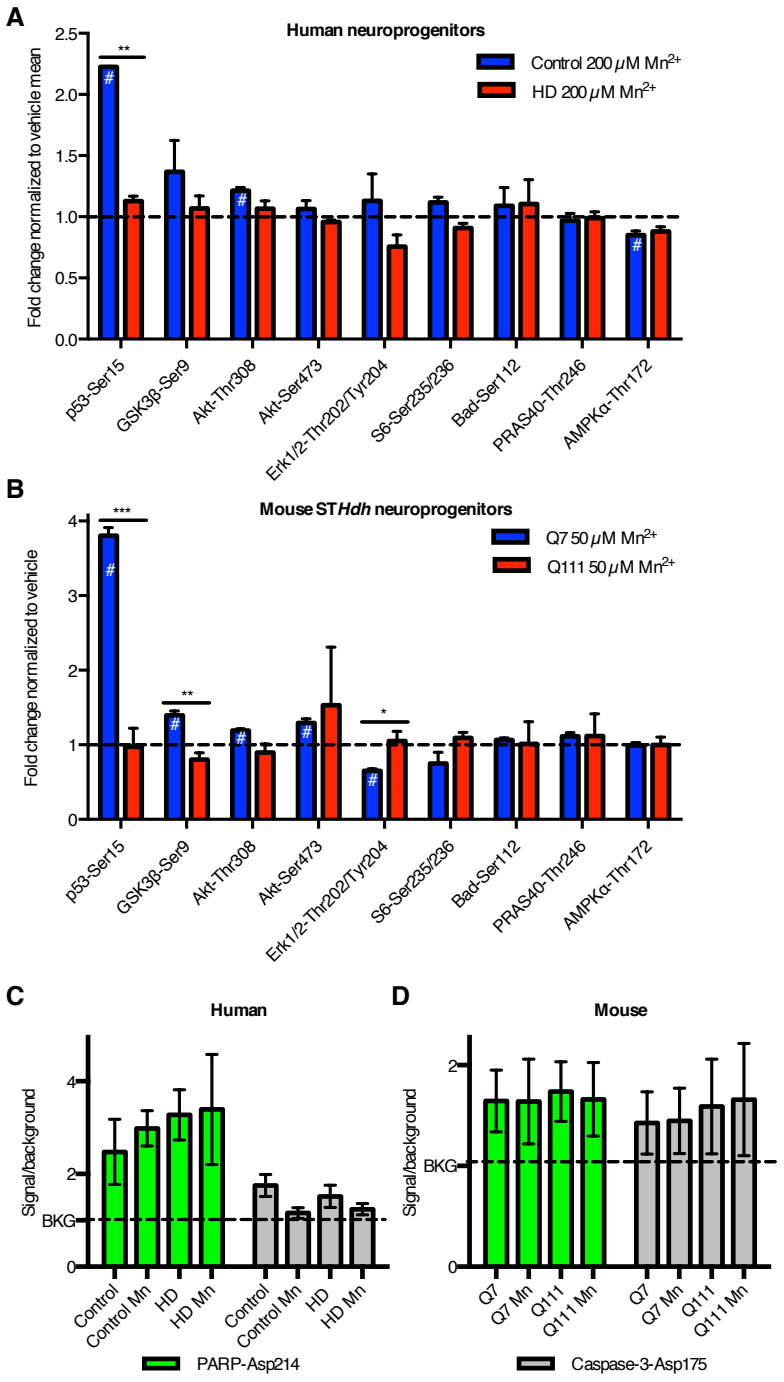

Figure 8. PathScan ELISA array shows manganese-induced phospho-p53(S15) at sub-cytotoxic manganese concentrations. (**A**) Human cells were exposed for 24 hours to 200 μM Mn^{2+}. N = 2 for control (CE-6 and CF-1, once each) and HD (HD70-2 and HD180-6, once each). (**B**) Mouse ST*Hdh* neuroprogenitors (Q7 and Q111) cells were exposed for 24 hours to 50 μM Mn^{2+}. (**A,B**) Phosphorylation and cleavage events were measured by the Fluorescent PathScan Intracellular Signaling Array sandwich ELISA. Background from no protein sample was subtracted, and signals were divided by the mean of the untreated samples by genotype. The array was imaged and quantified using an Odyssey IR imager. Antibodies whose signal was less than 4 times the background were not plotted. For both human and ST*Hdh* cells this included phosphorylation at Stat1-Tyr701, HSP27-Ser78, p38-Thr180/Tyr182, PARP-1 cleavage, and caspase-3 cleavage. For human cells (**A**) phosphorylation at Stat3-Tyr70 was below detection, and phosphorylation of mTOR-Ser2448, p70 S6 Kinase-Thr389, and SAPK/JNK-Thr183/Tyr185 were below detection for the mouse striatal cells (**B**). (**C,D**) The PathScan values for caspase-3 and PARP-1 cleavage are plotted relative to background fluorescence with N=2 for human cells (**C**) and N=3 for mouse (**D**). # for $p < 0.05$ compared to vehicle-treated by t-test. For genotype comparisons * for $p < 0.05$, ** $p < 0.01$ by t-test. Bars, mean + SEM for **A,B** and + SD for **C,D**.

Phosphorylation of p53 by manganese is dose-dependent and deficient in HD mutant cells

Western blot analysis was used to further assess the manganese and HD/manganese interaction effects on p53(S15) phosphorylation. Manganese-induced phosphorylation of p53(S15) was concentration-dependent (**Figure 9A,B**). The control lines (CE-6 and CF-1) had substantially greater phosphorylation with manganese treatment (at 100 and 250 μM) than the HD mutant lines (HD70-2 and HD180-6) (e.g. 418% in control vs. 169% in HD at the 250 μM manganese exposure, $p < 0.01$) (**Figure 9A,B**). Human and mouse HD neuroprogenitors showed a small, but significant, manganese-induced p53(S15) phosphorylation, that was significantly blunted compared to control cells. Levels of total p53 were also significantly increased by manganese exposure in the control cells ($p < 0.01$), but not enough to account for the differences in phosphorylation (2.1 fold increase in total p53 vs. 4.2 fold increase in phosphorylated p53[S15]) (**Figure 9C**). The mouse striatal neuroprogenitor model showed a similar dose-dependent phosphorylation of p53(S15) with a strong deficit in HD cells (**Figure 9F,G**). Control mouse neuroprogenitors also showed a manganese-dependent increase in the p53 transcriptional target p21 (*CDKN1A*) mRNA expression (6.87 fold increase above vehicle, $p < 0.001$), while the HD mutant cells did not (with only a non-significant 1.82 fold increase above vehicle)(**Figure 10**). Elevated expression of this canonical p53 transcriptional target is highly consistent with manganese exposure increasing p53 transcriptional activity. To determine if the HD/manganese interaction effect occurred with other manganese-responsive phosphorylation events, the same blots were probed for phosphorylation of AKT at serine-473 (S473), a known manganese-responsive signaling event (Cordova et al., 2012; Williams, Li, et al., 2010). Manganese exposure was associated with a dose-dependent increase in phosphorylation of AKT(S473), as expected, but unlike p53(S15), the HD cells had a similar degree of phosphorylation as the controls (**Figure 9D**).

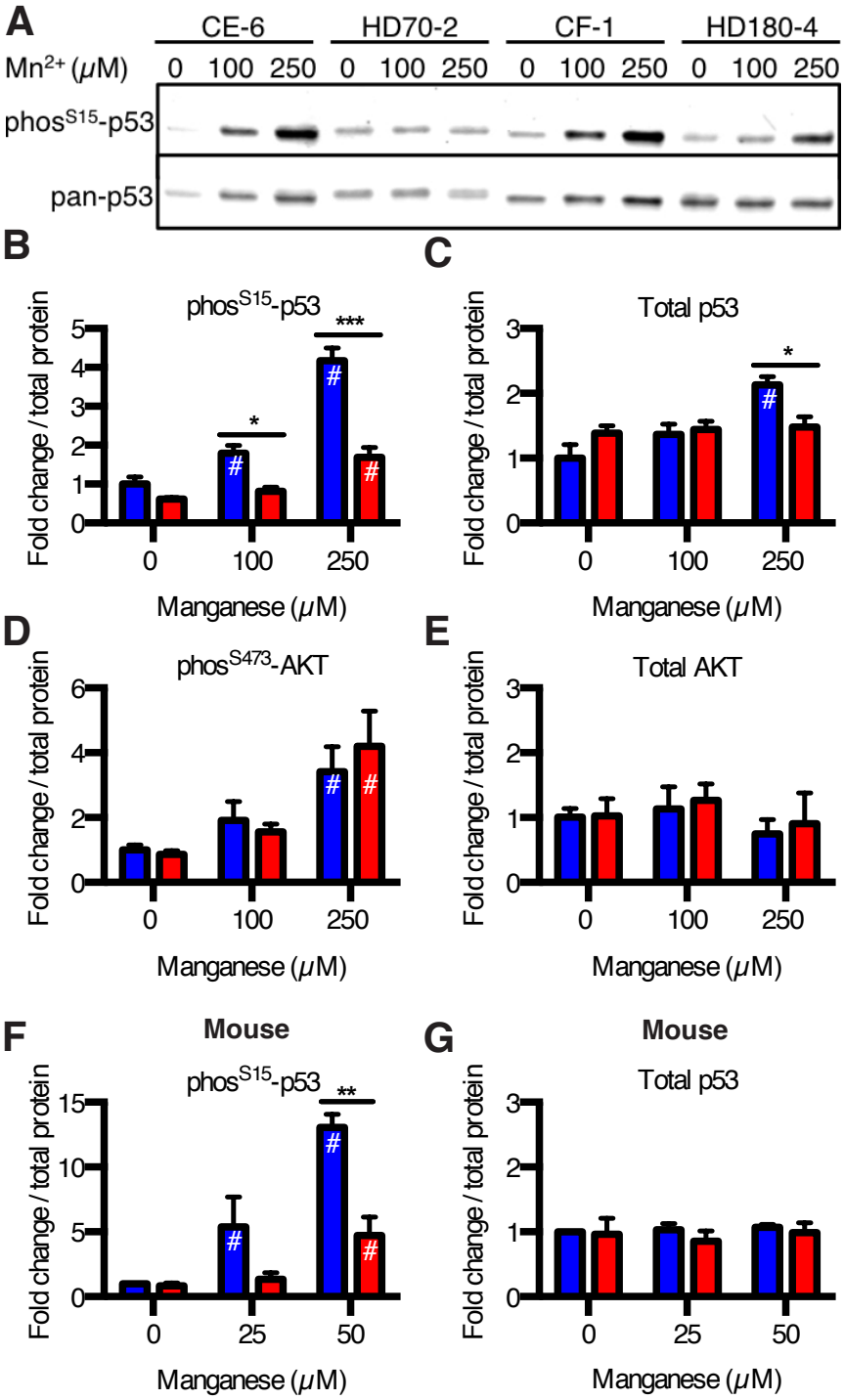

Figure 9. HD striatal progenitors show reduced manganese-dependent p53(S15) phosphorylation. (**A**) Human cells exposed to manganese were probed by western blot for phospho-p53(S15) and total p53. (**B,C**) Western blot data was quantified and demonstrates significant differences in p53 phosphorylation between genotypes. N = 4 for control (CE-6 and CF-1, twice each) and HD (HD70-2 and HD180-4, twice each). (**D,E**) Quantification of western blot data for phospho-AKT(S473) and total AKT. N = 4 for control (CE-6 and CF-1, twice each) and HD (HD70-2 and HD180-4, twice each). (**F,G**) Mouse control and HD ST*Hdh* cells were exposed to manganese for 24 hours followed by western blot analysis for phos-p53(S15) and total p53. # for $p < 0.05$ compared to vehicle-treated by t-test. * $p < 0.05$, ** $p < 0.01$, *** $p < 0.001$ by t-test. N=3. Bars, mean + SEM.

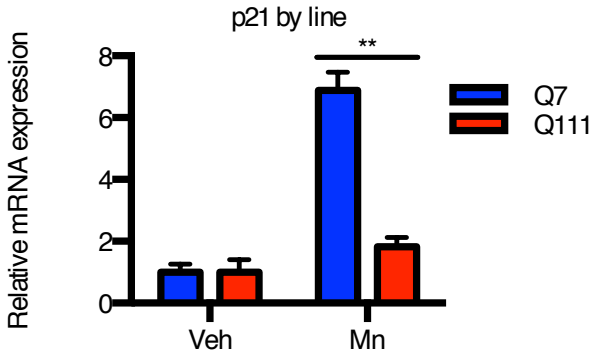

Figure 10. Manganese induces p21 (*CDKN1A*) mRNA expression but not in HD cells. Mouse ST*Hdh* neuroprogenitors (Q7 and Q111) were exposed to 50 μM manganese or vehicle. Quantitative RT-PCR was performed on 10 ng of cDNA, and the values were normalized to actin expression. N = 3 for each. ** < 0.01 by t-test. Bars, mean + SEM.

To further validate our western blot findings, we performed immunostaining for phos^{S15}-p53 and total p53 in the mouse striatal cells exposed to vehicle or 50 μM manganese (**Figure 11**). The manganese-dependent increase in nuclear localized phosphorylated (S15) p53 can be seen in Q7 but not Q111 cells.

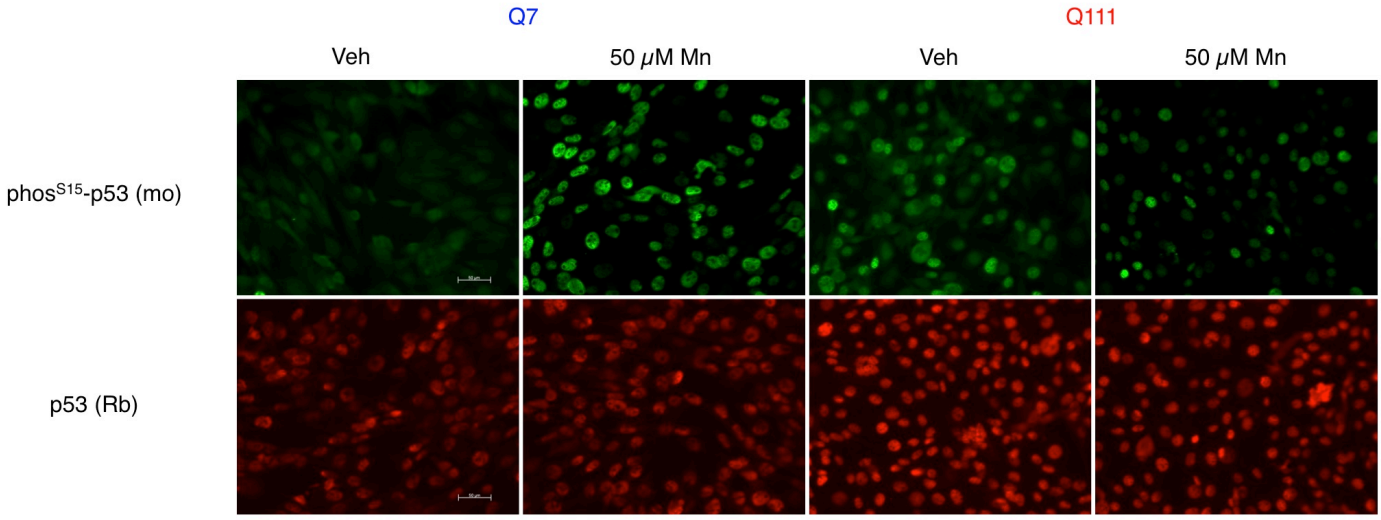

Figure 11. Immunostaining confirms manganese dependent increase in p53 phosphorylation with deficit in HD cells. Cells were immunostained for phospho^{S15}-p53 and total p53 after 24 hours of treatment in either vehicle or 50 μM manganese supplemented medium.

ATM activity is required for manganese-dependent p53 activation

ATM, AMPK, ERK1/2, and p38 are known to phosphorylate p53(S15) (Banin et al., 1998; Canman et al., 1998; Jones et al., 2005; She et al., 2000). We did not see a manganese-dependent increase in phosphorylation of AMPK-α (threonine-172), ERK1/2 (threonine-202/tyrosine-204), or p38 (threonine-180/tyrosine-182) by the PathScan array, but ATM kinase was not on the array. High concentrations of manganese (5 mM) have been reported to activate ATM (ataxia telangiectasia mutated) to induce phosphorylation of p53(S15) in cell-free kinase assays (Banin et al., 1998; Canman et al., 1998; Chan et al., 2000; Z. Guo et al., 2010).

First, we measured ATM autophosphorylation at serine 1981, an indicator of activated ATM kinase, in the *Hdh* mouse striatal cells (**Figure 12**). We found a similar pattern of phosphorylation as phosphorylation of p53 at serine 15 (**Figure 9F**) with a deficit in manganese-dependent phosphorylation in the mutant huntingtin expressing Q111 cells. Next, we tested the hypothesis that blocking ATM kinase activity during manganese exposure would inhibit p53(S15) phosphorylation. We observed by both an In-Cell Western assay (**Figure 13A**) and ELISA Array (**Figure 13G**) that the selective ATM inhibitor, KU-55933, completely blocked the manganese-dependent phosphorylation of p53 in the human neuroprogenitors (Hickson et al., 2004).

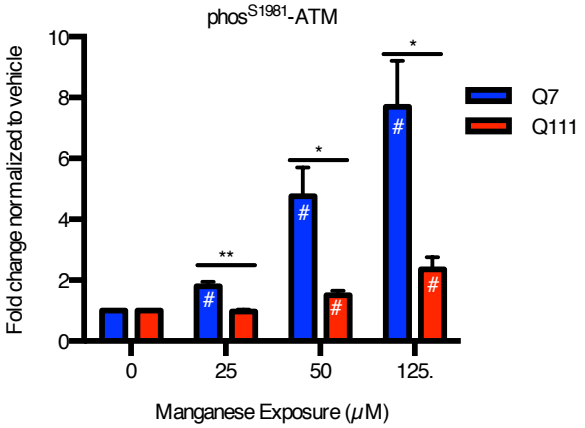

Figure 12. HD striatal cells show reduced manganese-dependent ATM autophosphorylation (S1981). Mouse ST*Hdh* neuroprogenitors (Q7 and Q111) were exposed to 25, 50, or 125 μM manganese or vehicle. Western blot analysis was performed probing for phos(S1981)-ATM. N = 3 for each. # for $p < 0.05$ compared to vehicle-treated by t-test. * $p < 0.05$, ** $p < 0.01$, by t-test. N=3. Bars, mean + SEM.

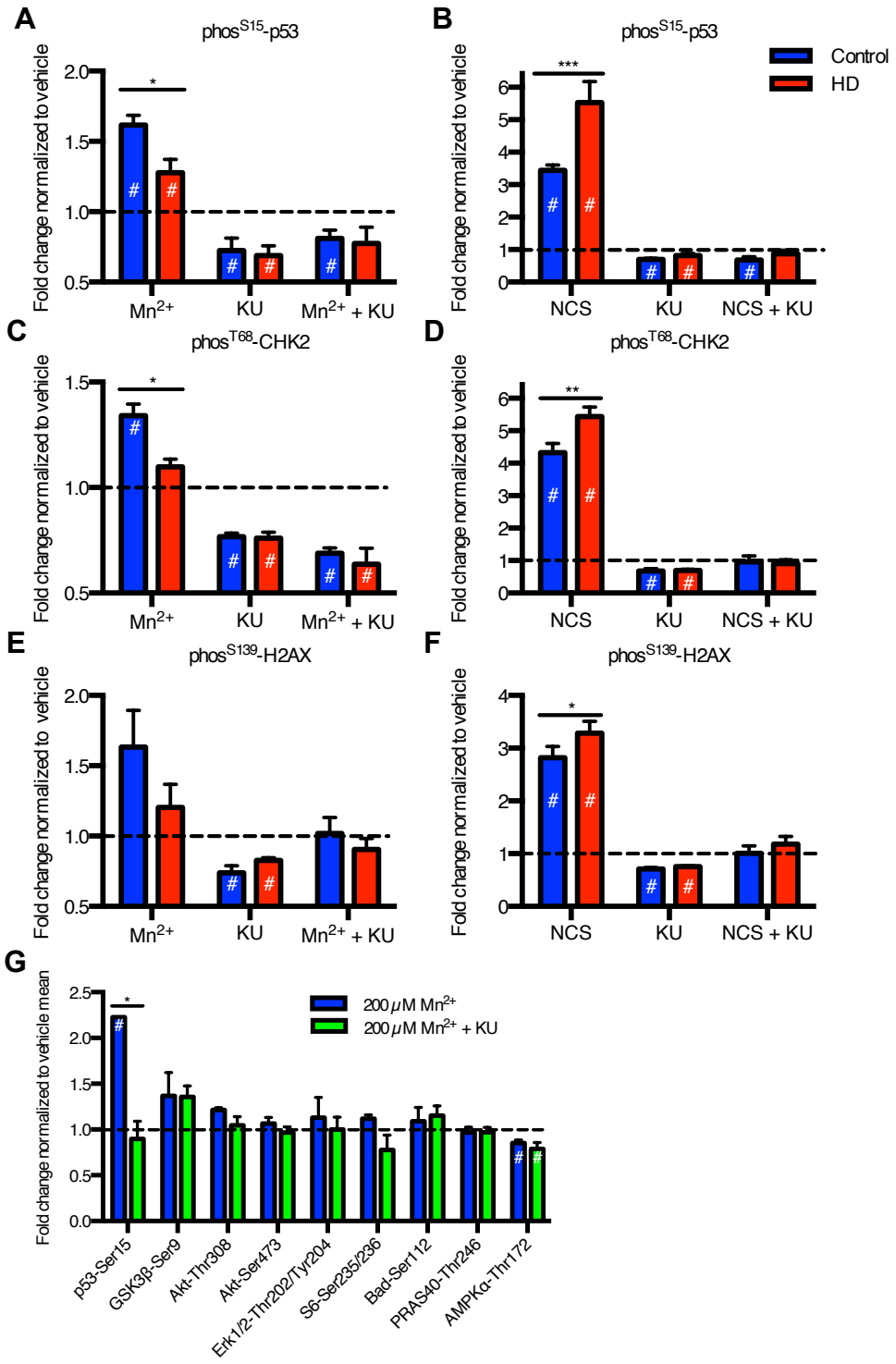

Figure 13. Manganese induces phosphorylation of 3 ATM targets, which is blocked by ATM kinase inhibitor, KU-55933. "In-Cell Western" was performed on human neuroprogenitors for phos^{S15}-p53 (**A,B**), phos^{T68}-CHK2 (**C,D**), and phos^{S139}-H2AX (ie γ-H2AX) (**E,F**) and with exposure to Mn at 200 μM (**A,C,E**) or DNA damaging agent, neocarzinostatin at 100 ng/mL (NCS) (**B,D,F**). The cells were also exposed to ATM inhibitor, KU-55933 at 1 μM. N = 4 for control (CE-6, CF-3; 2 experiments each) and N = 4 for HD (HD70-2, HD180-4; 2 experiments each). (**G**) PathScan data comparing 200 μM Mn^{2+} treated control cells (CE-6 and CF-1) with and without the selective ATM inhibitor, KU-55933 (1 μM). N =2. # for $p < 0.05$ compared to vehicle-treated by t-test. * < 0.05, ** < 0.01 *** < 0.001 for t-test between genotypes.

The effect of the inhibitor was quite specific to p53 phosphorylation, as no significant effects were observed for other signaling proteins on the PathScan array (**Figure 13G**). DNA damage is a canonical activator of the ATM-p53 signaling pathway. To test whether the ATM-p53 pathway is broadly deficient in its ability to respond to any pathway-relevant stressor in HD neuroprogenitors, we exposed the cells to neocarzinostatin, a double-stranded DNA break (DSB)-inducing agent known to activate p53 via ATM (Banin et al., 1998). In contrast to the HD deficit in manganese-induced p53 activation, the human HD neuroprogenitors were hyper-sensitive to p53(S15) activation by neocarzinostatin (**Figure 13B**), and this phosphorylation was completely blocked by the ATM inhibitor, KU-55933, confirming activation occurred via ATM kinase.

To further validate that ATM kinase is activated by manganese, we measured phosphorylation of two other established targets of ATM kinase, CHK2 at threonine-68 (T68) and H2AX at serine-139 (S139, i.e. γ-H2AX). Using the In-Cell Western assay, control neuroprogenitors had a significant increase in phosphorylation of CHK2(T68) with manganese exposure, but CHK2(T68) was non-responsive in HD neuroprogenitors (**Figure 13C**). H2AX(S139) showed the same trend but with greater variance at the same sample size (N=4) (**Figure 13E**). In both cases, the ATM inhibitor KU-55933 completely blocked manganese-dependent phosphorylation. Both ATM kinase targets were activated by the DNA-damaging agent neocarzinostatin with elevated phosphorylation in HD cells compared to control (**Figure 13D,F**). These data demonstrate a deficit in ATM activation by neurologically relevant levels of manganese in HD neuroprogenitors; yet, a fully responsive (or even hyper-responsive in the human HD neuroprogenitors) ATM kinase activity from a canonical activator of this pathway, DSB DNA damage.

<u>The HD-dependent deficit in ATM activation is specific to manganese</u>

Oxidative stress was recently discovered to activate ATM via a mechanism independent from the DNA damage-dependent activation of ATM (Z. Guo et al., 2010). To test whether ATM kinase is responding to manganese via an oxidative stress-dependent mechanism, we exposed the ST*Hdh*$^{Q7/Q7}$ and ST*Hdh*$^{Q111/Q111}$ striatal neuroprogenitors to 250 μM hydrogen peroxide for 1 hour and measured the phosphorylation of p53(S15) and H2AX(S139) by In-Cell Western assay. We observed an equivalent phosphorylation of ATM

targets by hydrogen peroxide in HD and control cells (**Figure 14A,B**), with levels of phosphorylation of p53(S15) and H2AX(S139) equivalent to that observed after neocarzinostatin exposure (100 ng/mL for 1 hour). These observations suggest that hydrogen peroxide and manganese activate ATM via different mechanisms.

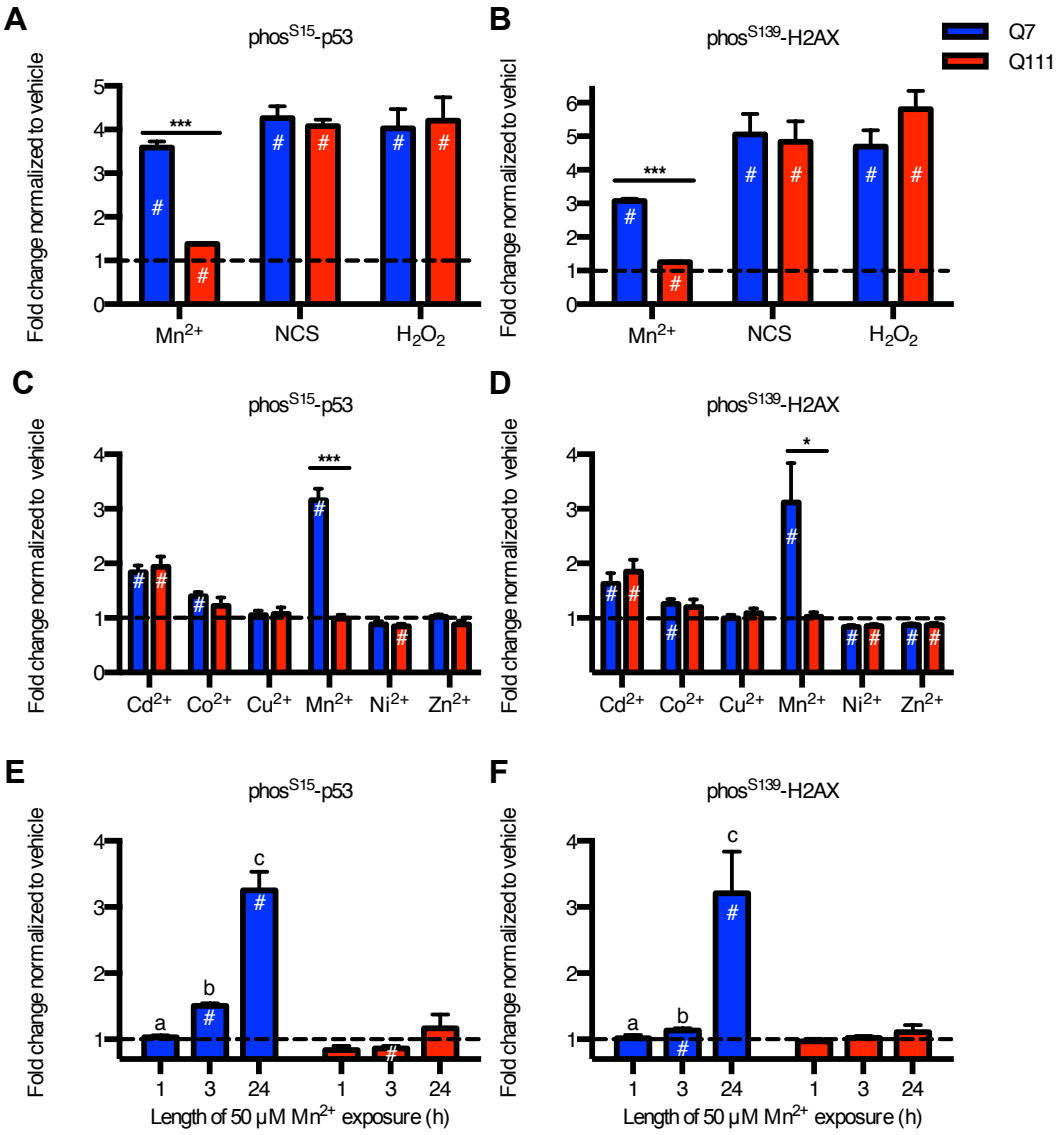

Figure 14. Mutant *Huntingtin* only inhibits manganese-dependent ATM target phosphorylation. (**A,B**) Mouse ST*Hdh* striatal neuroprogenitors (Q7 and Q111) were exposed to manganese (50 μM) for 24 hours, neocarzinostatin (NCS, 100ng/mL) for 1 hour, or hydrogen peroxide (H_2O_2, 250 μM) for 1 h. (**C,D**) Mouse striatal cells were exposed for 24 hours to several divalent metal cations all at 50 μM, except 100 μM Cu^{2+} and 20 μM Cd^{2+}. The means are normalized by the vehicle mean for that line to allow for easier genotype comparisons. (**E,F**) Mouse striatal cells were also exposed to manganese (50 μM) for increasing amounts of time. Significant differences are designated as: *a* is significantly different from *b* and *b* is significantly different from *c*. If no letters are listed, then none of the means are significantly different from on another. # indicates significantly different from vehicle treated ($p < 0.05$ by Tukey's post-hoc). N = 3 for means from 3-5 wells for independent replicate experiments (**A,C,E**). N = 4 for means from 3-5 wells for independent replicate experiments (**B,D,F**). * < 0.05, ** < 0.01 *** < 0.001 for t-test between genotypes. Bars, mean ± SEM.

In the mouse ST*Hdh* neuroprogenitors, the ATM inhibitor, KU-55933, did not effectively block manganese or neocarzinostatin induced p53 phosphorylation at 1 μM (the concentration used in the human neuroprogenitors) but was partially effective at 20 μM (**Figure 15**). At this concentration, the inhibitor likely has off-target effects (Hickson et al., 2004). Nonetheless, we confirmed that KU-55933 decreased manganese-dependent p53 phosphorylation in the mouse striatal neuroprogenitors.

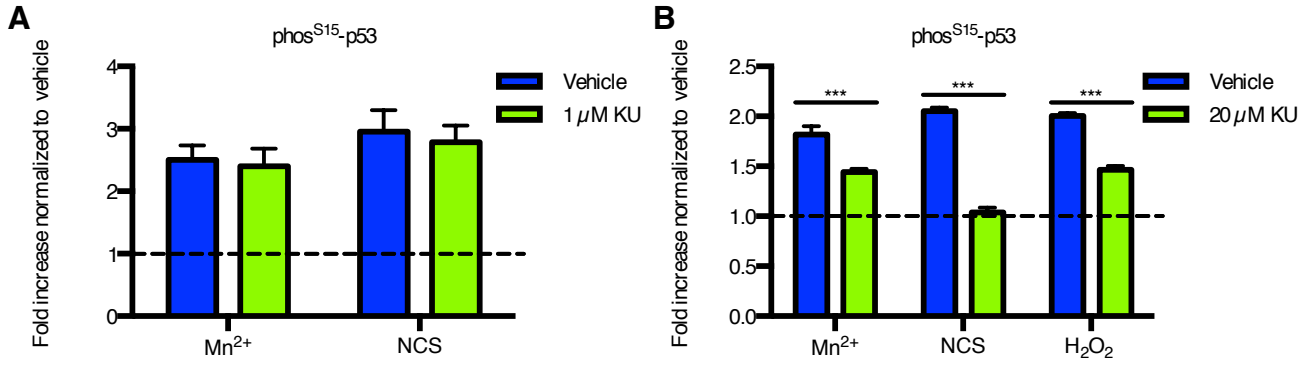

Figure 15. KU-55933 inhibits the ATM dependent target phosphorylation in mouse striatal cells. Mouse ST*Hdh* neuroprogenitors (Q7) were exposed to either manganese (50 μM) for 24 hours, neocarzinostatin (NCS) or hydrogen peroxide (H_2O_2) for 1 hour with or without 1 μM (**A**) or 20 μM (**B**) KU-55933. The mouse phos-p53(S15) antibody was used in **A** and rabbit phos-p53(S15) in **B**. N=5 wells from one independent experiment. *** means $p < 0.001$ by t-test. Bars, mean + SD.

We tested the hypothesis that the HD/manganese interaction effect on the ATM-p53 pathway is related to a generic metal response pathway, by exposing the mouse striatal neuroprogenitors to other divalent metal ions (Cd^{2+}, Co^{2+}, Cu^{2+}, Ni^{2+}, and Zn^{2+}) and assessing ATM phosphorylation targets (**Figure 14C,D**). The same sub-cytotoxic manganese concentration (50 μM) was used for all the metals except copper (100 μM) and cadmium (20 μM), as higher concentrations of cadmium resulted in cytotoxicity (Williams, Li, et al., 2010). We found that other metals either significantly increased (Cd^{2+}, Co^{2+}), decreased (Ni^{2+}, Zn^{2+}), or did not affect (Cu^{2+}) p53(S15) and H2AX(S139) phosphorylation; however, except for cadmium (Cd^{2+}), the changes in p53 phosphorylation were quite small compared to that observed with manganese. None of these other metals, however, showed an HD-dependent deficit in p53(S15) phosphorylation.

We tested the hypothesis that the HD-dependent differences in ATM activity at 24 hours may be due to altered response kinetics to manganese (e.g. peak response of p53 activation occurring at different times post-

exposure). We performed a time-course experiment on the ST*Hdh* striatal neuroprogenitors with 50 μM manganese (see **Figure 14E,F** [for 1, 3, and 24 hour exposures] **and Figure 16** [for 1, 3, 6, and 24 hour exposures]) and saw a continuous accumulation of phosphorylation of p53(S15) and H2AX(S139) over the 24-hour period in the control line (ST*Hdh*$^{Q7/Q7}$). The HD line (ST*Hdh*$^{Q111/Q111}$) did not show manganese-induced phosphorylation of p53 or H2AX at any of the time points, indicating that the difference in ATM activity observed between control and HD lines was not the result of a difference in temporal response patterns. Together, these observations demonstrate a manganese-specific deficit in ATM activation in HD not observed with other known activators of ATM kinase.

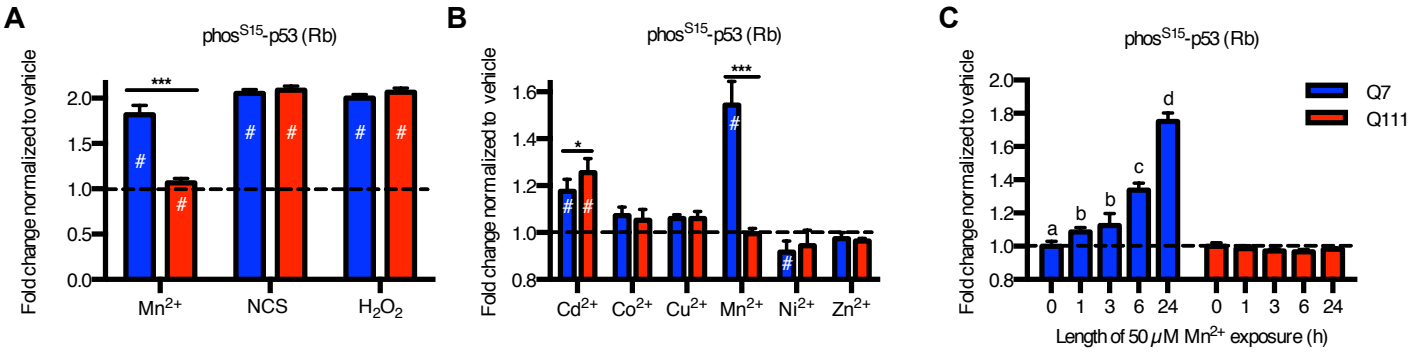

Figure 16. Another antibody for phos-p53(S15) corroborates the specificity of HD-dependent manganese phenotype. Mouse ST*Hdh* neuroprogenitors (Q7 and Q111) were treated identically to **Figure 6A,C,E** for the In-Cell Western assay except using a rabbit polyclonal antibody rather than the monoclonal mouse antibody **Figure 6**. N=5 wells. # is used to indicate significantly different values relative to vehicle-treated cells. For genotype comparisons * < 0.05 and *** < 0.001. Bars, mean + 95% CI.

Cellular manganese accumulation is diminished in HD neuroprogenitors

Because the HD-dependent deficit in manganese-induced ATM activation was remarkably selective to manganese and because manganese is sufficient to induced ATM activity in cell-free kinase assays, we hypothesized that mutant *Huntingtin* alters intracellular manganese homeostasis (Chan et al., 2000; Z. Guo et al., 2010). We have previously reported decreased manganese accumulation in the mouse ST*Hdh*$^{Q111/Q111}$ HD striatal lines compared to the control ST*Hdh*$^{Q7/Q7}$ line (Williams, Kwakye, et al., 2010; Williams, Li, et al., 2010). However, this phenotype occurred with a significant decrease in manganese-induced cytotoxicity and

manganese-induced AKT(S473) phosphorylation in the mutant cells (ST*Hdh*$^{Q111/Q111}$), phenotypes that we did not see in the human neuroprogenitors used in this study (**Figures 7A and 9D**). To measure intracellular manganese content, we used a fluorescence-based assay (CFMEA) that we have previously described (K. K. Kumar et al., 2013; Kwakye, Li, Kabobel, et al., 2011). We found that human HD neuroprogenitors accumulated significantly less manganese (31% versus control cells, $p < 0.01$) after a 24-hour manganese exposure at 200 μM (**Figure 17A**). However, this difference between human control and HD neuroprogenitors was ~2.5 times smaller than observed in mouse neuroprogenitors (78% reduction of manganese in ST*Hdh*$^{Q111/Q111}$ cells versus control cells; **Figure 17B**). Thus, both human and mouse neuroprogenitors with pathogenic alleles of *Huntingtin* display deficits in net manganese accumulation at concentrations associated with deficits in manganese-dependent ATM-p53 signaling.

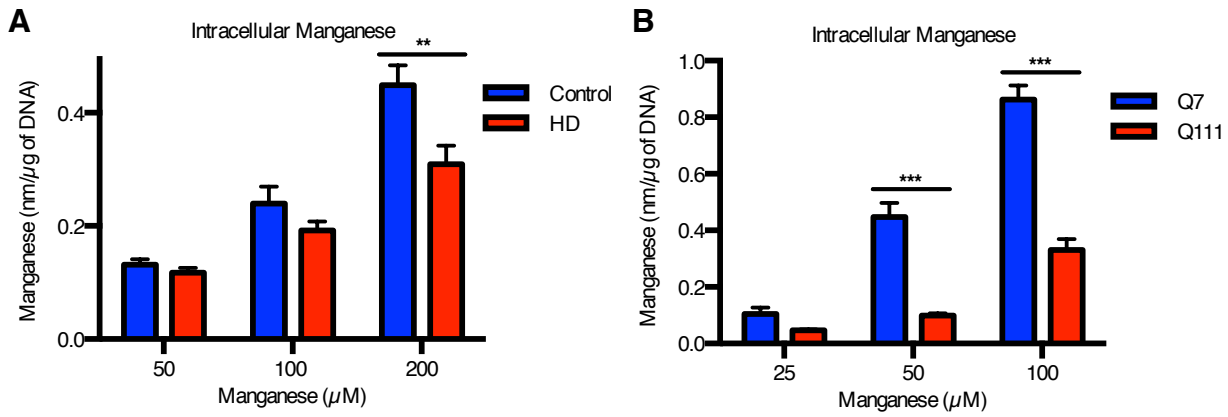

Figure 17. Reduced accumulation of manganese in neuroprogenitors expressing mutant *Huntingtin*. (**A**) Accumulation of intracellular manganese was quantified in human neuroprogenitors that were exposed for 24 hours to manganese by cellular fura-2 manganese extraction assay. For human N = 4 for control (CE-6 and CF-1, twice each) and HD (HD70-2 and HD180-4, twice each). (**B**) The same procedure was performed on mouse ST*Hdh* neuroprogenitors (Q7 and Q111) with N = 3. For genotype comparisons * for $p < 0.05$, ** $p < 0.01$, *** $p < 0.001$ by t-test. Bars, mean + SEM.

<u>Pharmacological equalization of cellular manganese content rescues the ATM-p53 signaling deficit.</u>

To determine if the differential manganese accumulation in HD is the basis of the differential manganese-induced ATM activation, we pharmacologically manipulated intracellular manganese content. To this end, we used the sodium/calcium exchanger (NCX) inhibitor KB-R7943 that blocks manganese efflux in mouse tissues

(Waghorn et al., 2009) to alter cellular manganese content in the control and HD ST*Hdh* neuroprogenitors. Co-incubation of the mouse ST*Hdh* neuroprogenitors with 10 μM KB-R7943 and 50 μM manganese resulted in equivalent manganese accumulation between control ST$Hdh^{Q7/Q7}$ and HD ST$Hdh^{Q111/Q111}$ lines (**Figure 18A**, p = 0.585). Using these conditions to equalize cellular manganese levels, we found that KB-R7943 also equalized the phosphorylation levels of p53(S15) and H2AX(S139) between HD and control neuroprogenitors (**Figure 18B,C;** p = 0.31 for p53[S15] and p = 0.95 for H2AX[S139]). These data demonstrate that normalizing cellular manganese levels mitigates the HD-dependent deficit in manganese-induced ATM target phosphorylation.

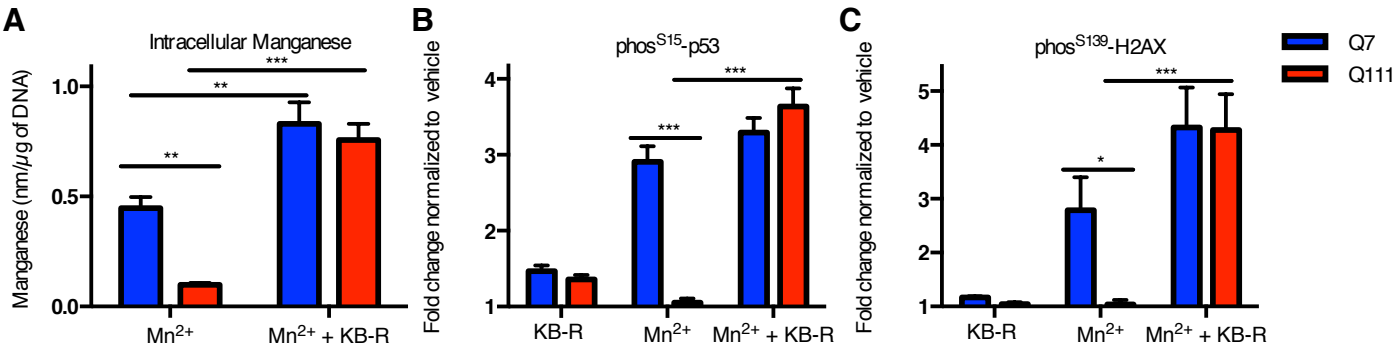

Figure 18. Pharmacological equalization of manganese content results in similar p53(S15) phosphorylation. (**A**) Mouse ST*Hdh* neuroprogenitors (Q7 and Q111) were treated for 24 hours with manganese (50 μM) with or without the NCX inhibitor KB-R7943. Intracellular manganese accumulation was measured by the CFMEA technique. N = 3 independent experiments. (**B,C**) The same treatment paradigm was used for In-Cell Western analysis to quantify the phosphorylation of p53 and H2AX. N = 4 independent experiments for (**B**) and N = 3 independent experiments for (**C**). For genotype comparisons * for $p < 0.05$, ** $p < 0.01$, *** $p < 0.001$ by t-test. Bars, mean + SEM.

Discussion

Our observations demonstrate that a manganese-handling deficit occurs in HD striatal-like neuroprogenitor selectively impairing ATM-p53 signaling under low-level (sub-cytotoxic) manganese exposure levels (>85% viability; **Figure 7**) with no detectable caspase-3 or PARP-1 cleavage (**Figure 8C,D**). We used an ELISA-based array for 18 cellular signaling events and found that phosphorylation of p53(S15) showed the largest response (2.2 fold increase in human; 3.8 fold increase in mouse; **Figure 8**), and this response was significantly reduced in HD neuroprogenitors (~78% decrease in human response [$p < 0.001$]; 69% decrease in mouse response [$p < 0.01$])(**Figure 9B,C**). AKT(S473) phosphorylation was also induced by manganese but to

a lesser extent (1.2 fold for human and mouse, $p < 0.05$) and independent of the HD genotype (**Figure 9D).** Manganese-dependent phosphorylation of CHK2(T68) and H2AX(S139), two canonical targets of ATM kinase, were also found to be deficient in HD cells (**Figure 13A,C,E**). DNA damage and oxidative stress induced by hydrogen peroxide, two known mechanisms to activate ATM activity, did not show HD-dependent differences in the mouse striatal progenitors. DNA-damage resulted in hyper-activation of ATM targets in human HD neuroprogenitors (**Figures 13B,D,F**). Mirroring our findings in the mouse striatal cell line, the human neuroprogenitors had a small but significant defect in cellular manganese accumulation relative to control (**Figure 17A).** However, this difference did not result in manganese cytotoxicity (**Figure 7A**) or manganese-dependent AKT(S473) phosphorylation differences between control and HD cells (**Figure 9D**). Combined, our results demonstrate an altered manganese biology in HD patient-derived neuroprogenitors and identify a novel manganese-responsive cell signaling event, ATM activation, that is impaired in HD. Our data, in both human and mouse model systems, support the hypothesis that a manganese homeostatic defect may occur in HD.

Our data establish ATM-p53 as a major manganese response pathway. Alterations in p53-dependent gene expression following manganese-exposure have been observed in a non-human primate model (Guilarte et al., 2008; Zhao et al., 2012). Here, we provide evidence for manganese-induced p53(S15) phosphorylation by western blot, ELISA, and In-Cell Western assays in both human and mouse neuroprogenitors. Further, this signaling pathway was activated more robustly than several other intracellular signaling events assayed. The identification of ATM as the upstream manganese-induced kinase of p53 is based on both pharmacological inhibition and other established ATM phosphorylation targets (CHK2[T68] and H2AX[S139]). DNA damage and oxidative stress have both been shown to activate ATM, but unlike manganese-dependent ATM activation, DNA damage and hydrogen peroxide had the same or greater response in HD neuroprogenitors compared to controls consistent with previous reports on p53 in HD model systems (Banin et al., 1998; Canman et al., 1998; Z. Guo et al., 2010). Among the metal ions tested, only cadmium induced ATM activation to a similar magnitude as manganese. However, unlike manganese, cadmium is a known DNA damaging agent at micromolar concentrations providing a clearly established route to ATM activation (Dally & Hartwig, 1997). Manganese, on the other hand, is known to activate ATM phosphorylation of p53(S15) in purified kinase

activity assays in the absence of DNA (Chan et al., 2000; Z. Guo et al., 2010). Thus, our data strongly suggest manganese activates ATM via a mechanism independent of DNA damage. Additionally, our results do not support a mechanism via direct redox cycling (Fenton reaction) because many of the other metals, which had minimal effects on ATM activity, are known to be more redox active than manganese (e.g. copper). As neither a DNA damage nor oxidative stress mechanism clearly explains the manganese-dependent ATM activation, we propose that manganese activates ATM via a novel mechanism. Our data demonstrate that manganese mediates the activation of ATM kinase activity at neurologically relevant concentrations (50-200 μM) in living cells (Bowman & Aschner, 2014), much lower than the 5-10 mM used in previously published cell-free purified kinase assays (Chan et al., 2000; Z. Guo et al., 2010).

The HD dependent deficit in manganese induced ATM-p53 activation is one of many examples implicating this pathway with HD pathophysiology. Previous work has shown increased p53 accumulation and phosphorylation in HD patient and mouse brains as well as HD cell lines under basal conditions, while knockdown of p53 can ameliorate both mitochondrial and behavioral HD phenotypes (B.-I. Bae et al., 2005; X. Guo et al., 2013). Possible direct interactions between mutant *Huntingtin* and both p53 and ATM have also been reported ((B.-I. Bae et al., 2005; Ferlazzo et al., 2013; Steffan et al., 2000). Both p53 and ATM phosphorylation have been reported to be elevated in an HD iPSC model (Jung-Il et al., 2012). This pathway was also hyper-activated by DNA damage in our HD neuroprogenitors, mirroring the published findings of camptothecin (a DNA damaging agent) treatment of HD muscle cells (Ehrnhoefer et al., 2014). Genetic variation in the *TP53* gene (which encodes p53 protein) accounts for ~13% of age-of-onset variability in HD not accounted for by the CAG repeat length (Chattopadhyay et al., 2005). The pro-apoptotic function of activated p53 is its best characterized biological role; however, at low levels of activation, p53 transcriptional activity plays a largely pro-survival role by up-regulating genes involved in energetic balance, oxidative defense and metabolic state (Helton & Chen, 2007). The HD-dependent alterations in p53 responsiveness to a non-lethal stressor could provide a mechanism for the age-dependent degeneration seen in HD. Namely, the accumulation of cellular damage over time due to insufficient neuroprotection by the manganese-dependent ATM-p53 pathway.

Our data suggest that mutant *Huntingtin* impinges on the ATM-p53 response to manganese exposure by altering manganese transport/homeostasis. We found lower cellular manganese content in the HD human *ISL1+* neuroprogenitors than control cells following low-level exposures (**Figure 13A**). Equalizing cellular manganese content in HD and control cells by pharmacologically blocking manganese efflux (Waghorn et al., 2009) eliminated the differential response in p53 phosphorylation, providing strong evidence that the deficit in manganese-induced ATM activation in HD cells was dependent on a manganese-handling deficit. Remarkably, the magnitude of the deficit in the ATM-p53 signaling pathways in mouse and human HD models is similar despite the substantially stronger manganese accumulation deficit in the mouse model system. One potential explanation could be differences in compartmentalization of intracellular manganese between the mouse and human models. Manganese has been indicated to accumulate primarily in the nucleus of neurons where a majority of ATM protein is localized (Kalia et al., 2008; Morello et al., 2008).

Epidemiological studies indicate a significant role for environmental factors in HD progression (Wexler, 2004). The defect we observe in manganese-handling/homeostasis in HD patient derived neuroprogenitors substantiates previous reports of reduced accumulation of manganese in both mouse striatal cell models of HD and the striata of manganese-exposed Tg-YAC128Q HD model mice, as well as altered manganese and iron localization in HD patient brains (H Diana Rosas et al., 2012; Williams, Kwakye, et al., 2010; Williams, Li, et al., 2010). Decreased cellular manganese in HD could explain at least some HD pathogenic mechanisms. For example, decreased activity of manganese-dependent enzymes, including superoxide dismutase (MnSOD), arginase, glutamine synthetase, and pyruvate carboxylase could contribute to the oxidative stress, altered neuronal energetics, and excitotoxicity pathological phenotypes reported in HD (Bowman, Kwakye, Herrero Hernández, et al., 2011). Further, differential manganese nutritional status of patients could be an important modifier of disease progression. Manganese deficiency is known to alter glutamate cycling, the urea cycle, insulin signaling, and cellular energetics; all of these biochemical pathways are dependent on manganese-dependent enzymes and have been shown to be dysfunctional in Huntington's disease models (Chiang et al., 2007; Lievens et al., 2001; Podolsky et al., 1972; Seong et al., 2005). In conclusion, these findings suggest the

possibility that alterations in brain manganese homeostasis may contribute to HD pathophysiology, which may open new therapeutic opportunities.

CHAPTER III

GENOMIC INSTABILITY IN HUNTINGTON'S DISEASE CELLS MAY RESULT FROM NUCLEAR MANGANESE DEFICIENCY

Introduction

Huntington's disease neuropathology results from cell death of neurons primarily in the caudate and putamen of the basal ganglia. Although this cell death has been well-characterized, the route by which mutant huntingtin expression leads to cell death is not well understood. Elevated phosphorylation of DNA damage signaling pathway markers such as p53 is a hallmark of HD (B.-I. Bae et al., 2005; Trettel et al., 2000). Mutant huntingtin expressing cells have also been shown to be radiosensitive to X-rays suggesting a potential DNA damage repair defect (Moshell et al., 1980). Recent studies have shown altered DNA repair kinetics of important double strand break (DSB) repair proteins, such as Ku70 and MRE11, and binding of mutant huntingtin to important DNA damage signaling proteins, p53 and ATM (Enokido et al., 2010; Ferlazzo et al., 2013; Moshell et al., 1980; Steffan et al., 2000). Further evidence for altered response to DNA damage and repair is that HD patients have a significantly decreased risk of nearly all forms of cancer compared to control individuals (Sørensen et al., 1999).

We discovered increased genomic instability as evidenced by abnormalities in karypotype analysis in induced pluripotent stem cell (iPSC) lines generated from patients with Huntington's disease as well as elevated DNA damage signaling in HD iPS cells and mouse striatal cells. Previously, our lab has shown a drastic decrease in intracellular manganese levels in HD cells. Manganese is a necessary or putative cofactor for several important proteins involved in DNA damage repair (e.g. MRE11 and ATM). We believe that our data suggesting decreased nuclear manganese in HD could provide a coherent mechanism for increased DNA damage and DNA damage dependent signaling in HD patients and model systems by decreasing the activity of these enzymes. Indeed, supplementation of manganese can restore elevated p53 phosphorylation in HD cells to control levels.

Results and Discussion

Increased genomic instability in HD cells

Our lab has generated induced pluripotent stem cell (iPSC) lines from control subjects and patients with neurodegenerative diseases including juvenile Huntington's disease (HD) (**Chapter II**). Because iPSC (and hESC) lines are known to have frequent genomic abnormalities (Draper et al., 2004; Mayshar et al., 2010), a detailed karyotype analysis (20 metaphase spreads) was performed on each clonal line to ensure genomic integrity. We observed a strikingly high number of HD iPSC lines with genomic abnormalities (10/29 lines from 5 patients) (**Figure 19**). This observation was made all the more stark when we did not identify a single genomic abnormality in any of our control lines (0/13 lines from 4 control subjects). Using a binary logistic regression, disease state was a significant predictor of genomic instability ($p = 0.0017$). Furthermore, the length of the CAG repeat was also a significant predictor of genomic instability in the iPSC lines (all controls were set to 20 CAG repeats) with $p = 0.0025$.

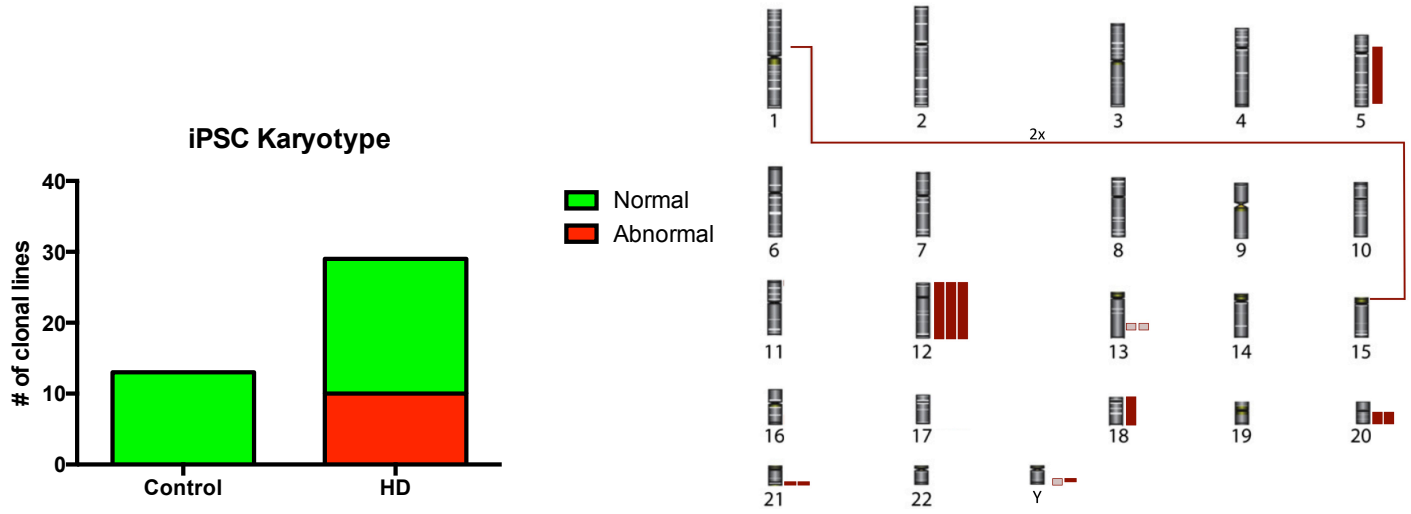

Figure 19. HD iPSC lines have greater propensity for genomic abnormalities than control lines. *Left:* Control lines from 4 individuals (13 total lines) and HD lines from 5 patients (29 total lines) were analyzed by G banding for chromosomal abnormalities. Lines with at least 1 abnormality (deletion, inversion, trisomy etc) out of 20 cells counted were considered abnormal. *Right:* The abnormalities are depicted on a karyogram. Additional chromosomal material is depicted as solid bars, loss as hashed bars, and translocations as lines connecting the translocated regions.

iPSC Line	Patient Phenotype	Abnormal/Total	Passage #	Nature of Abnormalities
CA-11	Control	0/20	?	
CA-24	Control	0/20	9	
CA-26	Control	0/20	6	
CA-30	Control	0/20	8	
CC-1	Control	0/20	7	
CC-2	Control	0/20	6	
CC-3	Control	0/20	6	
CC-5	Control	0/20	7	
CD-2	Control	0/20	6	
CD-3	Control	0/20	6	
CD-10	Control	0/20	9	
CD-12	Control	0/20	9	
CE-6	Control	0/20	6	
HD35-2	HD	20/20	4	i(5)(p13q32)
HD35-5	HD	0/20	4	
HD35-7	HD	0/20	4	
HD35-9	HD	0/20	4	
HD57-1	HD	0/20	4	
HD57-4	HD	0/20	4	
HD57-6	HD	0/20	4	
HD57-7	HD	0/20	4	
HD57-15	HD	0/20	4	
HD58-1	HD	2/20	7	47, X, +12
HD58-1 -shRNA p53	HD	0/20	6	
HD58-3	HD	0/20	6	
HD58-13	HD	4/20	17	i(20)(q10) [2]; idic(q13.3) [2]
HD58-19	HD	0/20	10	
HD58-20	HD	0/20	7	
HD58-21	HD	5/20	10	47, XY, +12
HD58-31	HD	0/20	6	
HD58-34	HD	0/20	6	
HD70-2	HD	0/20	~14	
HD70-5	HD	1/20	~15	47, XX, +12
HD70-11	HD	0/20	8	
HD180-1	HD	20/20	~15	del(13)(q22q32)*
HD180-1 -shRNA p53	HD	20/20	6	del(Y)(q12)
HD180-3	HD	9/20	~15	47, XY, +18
HD180-4	HD	0/20	6	
HD180-6	HD	0/20	11	
HD180-10	HD	20/20	6	del(13)(q22q32)*,add(21)(q22),r(21)(p11.2q22)
HD180-14	HD	20/20	6	46,X,add(Y)?(q11.22)
HD180-16	HD	20/20	6	46,XY,t(1;15)(p10;p10)

Table 1. Karyotype data for control and HD iPSC lines. 20 metaphase spreads were analyzed for each line. Lines are deemed abnormal if they contain one inversion, deletion, or translocation in one or more cell. They are also considered abnormal if they have two or more cells with the same trisomy or monosomy, or 1 cell with a trisomy that commonly occurs in iPSC culture (eg. trisomy 12). Abnormal lines are colored in red. Abnormalities are listed by accepted nomenclature with brackets around the number of cells with a particular abnormality if more than one occurs in a given line. * If an abnormality was seen in subsequent fibroblast analysis, the iPSC line was considered normal.

The HD iPSC genomic abnormalities were from many different classes including trisomies (4), translocations (2), deletions (1), additions (3), inversions (2), isodicentrism (1), and ring formation (2) (**Table 1**). The most common abnormality was trisomy 12 (3), which is known to occur frequently in iPSC lines because the increased expression of important pluripotency genes (ie. Nanog) found on this chromosome provides a growth advantage for these cells (Mayshar et al., 2010). The HD chromosomal abnormalities identified are depicted on a karyogram in **Figure 19** and listed in **Table 1.**

These abnormalities could have arisen in the original fibroblast lines and not during the reprogramming or iPSC state. Therefore, we performed karyotype analysis on two control and three HD fibroblast lines. Instead of our normal 20 metaphase spreads, we performed 100 for each fibroblast lines because the abnormalities' observed in the iPSC lines could have arisen from rare events in the fibroblasts that provided an advantage in the reprogramming process. Each line had a similarly low level of genomic abnormalities (1-2 cells out of 100) in both the control and HD lines (HD58 and HD70), except for HD180 (**Table 2**). This fibroblast line contained 49 abnormal cells out of 100 with 3 different abnormalities of all different classes (deletion [3 cells], translocation [4 cells], and addition [42 cells]). Although all of the fibroblast lines contained at least a low level of genomic structure variation, only one abnormality identified (del(13)(q22q32) from HD180) was identified in any of the iPSC lines (HD180-1 and HD180-10). HD180-1 was considered as normal in the iPSC data analysis in **Figure 19** because the abnormality arose in the fibroblast culture, and HD180-10 was considered abnormal because it contained 2 other abnormalities that did not occur in the fibroblast culture. These results indicate that the vast majority of iPSC genomic abnormalities arise during the reprogramming process or in the iPSC cell state. We have also shown that HD patient cells are vulnerable to genomic instability at both the iPS (all HD lines) and fibroblast (HD180) cell states. ‘

Fibroblast Line	Abnormal/Total	Passage #	Nature of Abnormalities
CA	1/100	7	del(2)(q33)
CF	1/100	< 20	add(4q)
HD58	2/100	7	45, X [2]
HD70	2/100	14	del(8)(q10) [1]; del(18)(p10) [1]
HD180	49/100	17	del(13)(q22q32)[3]; t(3;14)(p13;q11.2)[4];add(4)(q23)[42]

Table 2. Only HD180 fibroblasts have a greater rate of abnormal karyotypes compared to controls. 100 metaphase spreads from each fibroblast line were analyzed for chromosomal abnormalities.

Subsequent experimental use of HD iPSC lines would be confounded if the HD propensity for genomic abnormalities occurs frequently in the stable iPS cell state. Lines would need to be analyzed frequently to ensure genomic integrity. To test for this possibility, we aged several control and HD lines to between 26-33 passages (an average of 16 additional passages from the original analysis). Both control (1/3) and HD (2/4) lines demonstrated a low frequency of abnormalities (average of 1.6 out of 100) not observed in the line during the original analysis (**Table 3**). Although not conclusive, these data suggest a similar slow accumulation of genomic abnormalities in both control and HD cells (p= 0.6576 by binary logistic regression).

iPSC Line	Patient Phenotype	Abnormal/Total	Passage #	Nature of Abnormalities
CA-30	Control	9/100	26(+18)	i(20)(q10) [8]
CF-3	Control	0/100	26 (+20)	
CF-3	Control	0/100	32 (+24)	
HD58-19	HD	0/100	26 (+16)	
HD70-2	HD	0/100	26 (+12)	
HD70-2	HD	2/100	32 (+18)	+12 [1], +22 [1]
HD70-5	HD	3/100	33 (+7)	+12 [2], i(20)(q10) [1]

Table 3. Euploidic HD iPSC lines accumulate abnormalities at the same rate as controls. The iPSC lines were aged in culture fro 7-24 passages greater than when original karyotyping was performed (see Table 1). 100 metaphase spreads from each fibroblast line were analyzed for chromosomal abnormalities.

HD cells show increased DNA damage signaling

Although both hES and iPSC models of Huntington's disease have been reported by several groups, genomic instability has not been previously reported. Here we report the generation of HD iPS lines using p53 siRNA alongside the typical reprogramming factors (Okita et al., 2011). Since p53 is known to suppress iPS generation, p53 knockdown via siRNA is used to increase reprogramming efficiency (Hong et al., 2009). This efficiency comes at a cost by decreasing the genomic integrity of iPSC clonal lines generated with p53 siRNA (Marión et al., 2009). Interestingly, elevated p53 signaling is one of the most consistent phenotypes across HD disease models (B.-I. Bae et al., 2005; X. Guo et al., 2013; J. L. Illuzzi et al., 2011; Jung-Il et al., 2012; Trettel et al., 2000). Many of these studies have also shown concurrent elevation of either H2AX or ATM phosphorylation, indicating an ATM kinase dependent pathway activation of p53. Therefore, elevations in ATM-p53 pathway could indicate an increase in DNA damage in HD cells under basal conditions. We explored whether p53(S15) and H2AX(S139) phosphorylation were increased in our HD iPS lines as well as the mouse ST*Hdh* striatal neuroprogenitor model. Using the HD iPS cells, we performed p53 western blots under basal conditions and with the DNA damaging agent, neocarzinostatin, which is known to increase phosphorylation and accumulation of p53. We show a significant increase in the phosphorylation of p53 at serine-15 and total p53 expression in HD iPS cells compared to controls (**Figure 20A-B)**. DNA damage

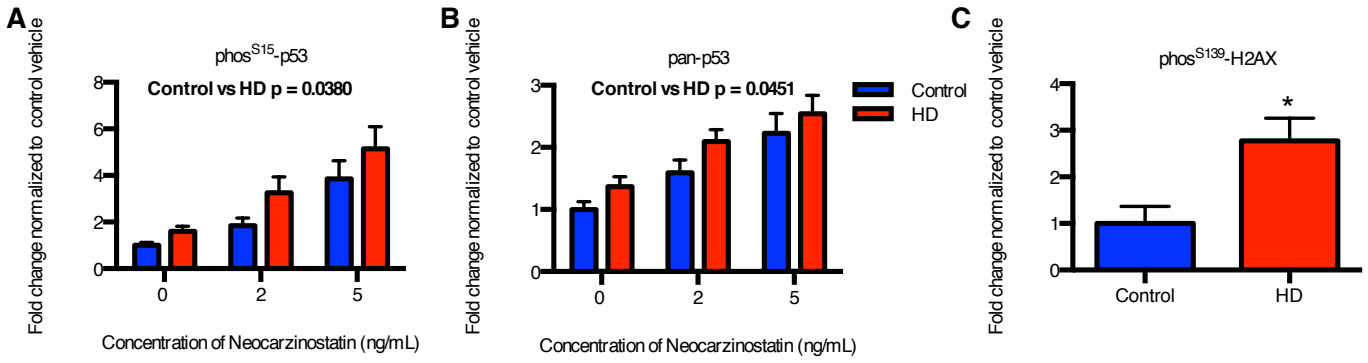

Figure 20. HD iPS cells have elevated basal and DNA damage dependent ATM-p53 signaling. Control and HD iPS cells were treated for 1 hour with DNA damaging agent, neocarzinostatin. Western analysis was performed for phosphorylated p53 at serine 15 (**A**), total p53 (**B**), and phosphorylated histone H2AX at serine 139 (**C**). N = 6 for control (CA-11 = 2, CF-1 = 2, CF-2 = 1) and 6 for HD (HD58-19 = 3, HD70-2 = 1, HD180-4 = 2). Bars = SEM. P value is calculated via 2-way RM-ANOVA (**A,B**) or t test (**C**).

via neocarzinostatin increased p53 phosphorylation and total protein in both cell lines at concentrations that did not significantly decrease cell viability (**Figure 21**). The apparent differences between HD and control cells at each concentration of neocarzinostatin in **Figure 20** was the exact same fold difference as the untreated samples. Additionally, the ratio of phosphorylated p53 total was the same for both lines under basal or treated conditions. This is expected because phosphorylation of p53 inhibits its degradation by the ubiquitin-proteosome system. The HD iPS cells also showed basal elevation of H2AX(S139) phosphorylation (**Figure 20C**). This ATM-dependent phosphorylation is often used as a surrogate measurement for DNA damage (Paull et al., 2000).

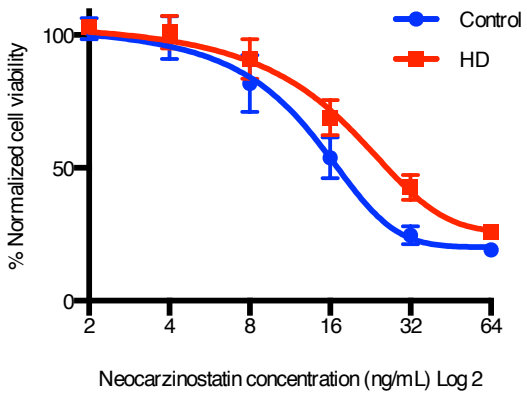

Figure 21. Control and HD iPS cells do not show a significant difference in neocarzinostatin mediated cell viability loss. Control and HD iPS cells were treated for 1 hour with neocarzinostatin followed by 23 hours of recovery time. The MTT assay was then used to quantify cell viability. N = 7 for control (CD-2 = 3, CE-6 = 1, CF-1 = 3) and N = 8 for HD (HD58-19 = 2, HD70-2 = 3, HD180-4 = 3). Points = mean ± SEM.

The mouse ST*Hdh*$^{Q111/Q111}$ striatal cells also showed an increase in p53(S15) and H2AX(S139) phosphorylation under basal conditions (**Figure 22A)**. These differences were not shown in **Chapter II** because they interfere with assessment of the relative effects of manganese on p53 signaling; therefore, we normalized each line to its vehicle-treated control in that chapter.

Interestingly, human *ISL1*+ HD neuroprogenitors show a decrease in p53 and H2AX phosphorylation rather than the increase seen in these other cell types (**Figure 22B**). We believe on possible explanation is the

lack of manganese in the Islet1+ cell medium. The other model systems do contain manganese in there growth medium; therefore, any possible connection between basal p53 phosphorylation and manganese uptake differences would not be apparent in the Islet1+ cells. The elevations in DNA damage signaling in the other cell models likely indicate underlying DNA damage or repair problems caused by the expression of mutant Huntingtin, which may also explain the increased rate of genomic instability seen during reprogramming of HD patient fibroblasts into hiPSCs (**Figure 19)**.

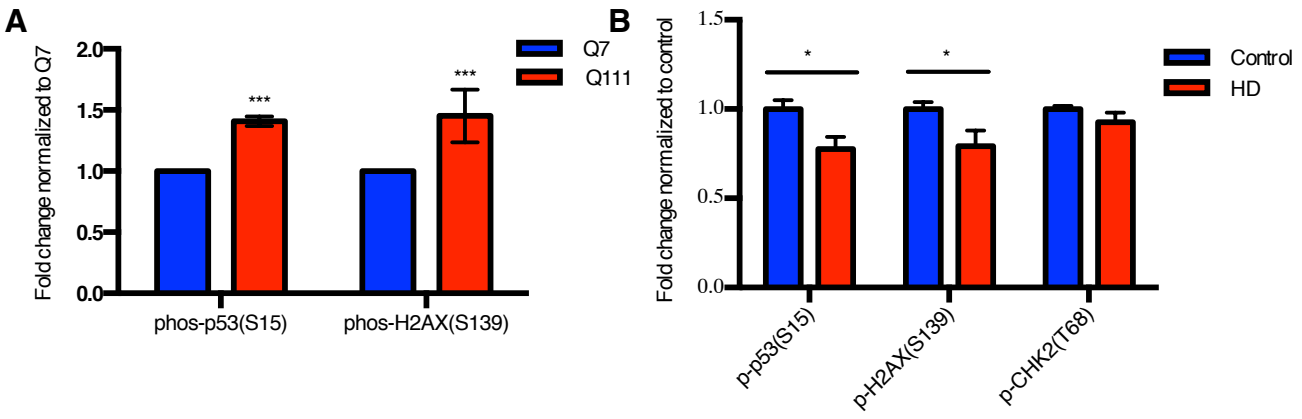

Figure 22. Elevated p53 and H2AX phosphorylation in untreated *Hdh*$^{Q111/Q111}$ cells but not in HD human neuroprogenitors. In-Cell Western assay was used to determine the level phosphorylation of ATM kinase targets p53, H2AX, and CHK2 in *Hdh*$^{Q7/Q7}$ and *Hdh*$^{Q111/Q111}$ striatal cells (**A**) and human neuroprogenitors (**B**). N = 4 for each. Bars = SEM. * for $p < 0.05$, ** for $p < 0.01$, and *** for $p < 0.001$ by t-test.

DNA damage and repair problems in HD cells have been previously identified. Expression of mutant Huntingtin can cause increased DNA DSBs in cells and mouse brain (Enokido et al., 2010; J. Illuzzi et al., 2009; J. L. Illuzzi et al., 2011). Evidence from one HD model, the R6/2 mouse, suggested increased DNA oxidation as key HD disease mechanism (Bogdanov et al., 2001; De Luca et al., 2008). However, studies measuring oxidized DNA in HD patient postmortem brains have provided conflicting results (Alam et al., 2000; Browne et al., 1997; Polidori et al., 1999). Chromosomal abnormalities can occur by DNA damage; DNA double-stranded breaks (DSBs) can be erroneously repaired to cause translocations, other rearrangement events (ie deletions, inversions), and possibly aneuploidy. Huntington's disease cell and animals models have shown increased DNA-damage and DNA-damage induced signaling responses (ie. ATM-p53) (B.-I. Bae et al.,

2005; Bogdanov et al., 2001; De Luca et al., 2008; Ehrnhoefer et al., 2014; Enokido et al., 2010; J. Illuzzi et al., 2009; J. L. Illuzzi et al., 2011; Jung-Il et al., 2012; Trettel et al., 2000).

No evidence of centrosome amplification in HD iPS cells

Alternatively, these genomic aberrations, particularly aneuploidy, can arise from dysregulated chromosomal segregation during cell division (Ganem et al., 2009). Huntington's disease cells have shown disruption to centrosomes and mitotic spindles that could potentially lead to misappropriation of chromosomes during mitosis (Godin et al., 2010; Keryer et al., 2011; Sathasivam et al., 2001). One of these studies identified increased centrosomal amplification in mouse and HD fibroblasts (Sathasivam et al., 2001). This amplification resulted in cells containing more than two centrosomes leading to multipolar mitoses. Having greater than 2 poles segregating chromosomes leads to misappropriation and aneuploidy. However, this study did not provide quantitative data about the rate of centrosome amplification between the two disease groups.

We quantified cells with supernumerary centrosomes (> 2) in both fibrobasts and iPSCs by pericentrin immunolabeling. As expected, actively dividing cells were more likely to be multipolar because under normal circumstances duplication of the centrosome happens just prior to cell division. The rate of mulitpolar cells was much higher in iPS cells compared to fibroblasts (**Figure 23A**). This increased chromosomal amplification has been described previously in human embryonic stem cells (Holubcová et al., 2011). When we further characterized the number of supernumerary centrosomes by genotype, we found no statistical difference between control and HD cell lines (**Figure 23B**). Therefore, we do not believe that centrosomal amplification is a significant process in the selective HD dependent genomic instability.

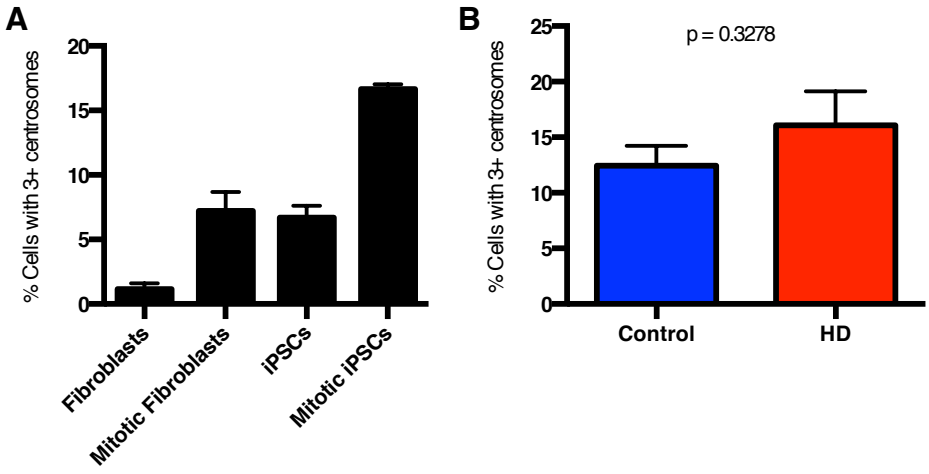

Figure 23. Mutant huntingtin does not alter the incidence of multipolar cells. (**A**) Human fibrobasts and iPS cells were stained pericentrin, a protein marker of centrosomes. 20 mitotic cells for each experiment were identified by Hoechst DNA stain with clear chromosomes. Cells were then scored as either multipolar (3+ centrosomes identified by pericentrin) or normal (1-2 centrosomes. (**B**) Control and HD iPS cells were also analyzed for centrosome amplification. N=6 for each bar. Bars = SEM. P value by t-test.

Decreased manganese levels in detergent permeable cellular compartments of HD mouse striatal cells

We have previously described decreased manganese accumulation in HD human and mouse neuroprogenitors as well as selectively in HD mouse striata upon manganese exposure. However, manganese-dependent phosphorylation events varied in the level of HD dependent response deficit. Primarily, nuclear p53 and H2AX were almost completely unresponsive to manganese-dependent phosphorylation in mutant cells while AKT (a mainly cytoplasmic protein) phosphorylation in humans was not different between controls and mutants (**Chapter II, Figure 9**). This led to the hypothesis that the deficit in manganese accumulation was due to reduced nuclear manganese levels. The nucleus has already been identified as a major site of manganese accumulation in manganese exposed neurons and contains the highest level of manganese in both manganese exposed and unexposed neurons and astrocytes (Kalia et al., 2008; Morello et al., 2008). Unfortunately, our previously published technique (CFMEA) for measuring manganese accumulation only measured total cellular manganese levels (Kwakye, Li, & Bowman, 2011; Kwakye, Li, Kabobel, et al., 2011), but using this same technique with different detergents, we are now able to potentially assess cytoplasmic, nuclear, and mitochondrial manganese levels.

The CFMEA was performed without Triton X-100 detergent to assess both residual extracellular manganese after washes as well as any readily released manganese from the cell via the concentration gradient (**Figure 24A**). We were surprised by the high concentration detected in these wells without a significant difference between Q7 and Q111 cells. We also replaced Triton X-100 (0.1%) with the non-ionic detergent, digitonin (0.001%) (**Figure 24B)**. This replacement had no effect on manganese dependent fura-2 quenching, key to the CFMEA assay (**Figure 24F**). Digitonin is known to permeabilize the plasma membrane but not the mitochondrial membrane or other non-cholesterol containing membranes while Triton X-100 does. The CFMEA was also performed with our standard 0.1% Triton X-100 (**Figure 24C**). As shown in **Figure 18**, KB-R7943 also ameliorated the HD-dependent deficit in manganese accumulation. Here we show that this occurs in both the digitonin and TX-100 permeable fractions (**Figure 24B,C,E**). KB-R7943 treatment also significantly increased the manganese quantified in the detergent free sample (**Figure 24A,** p = 0.0146).

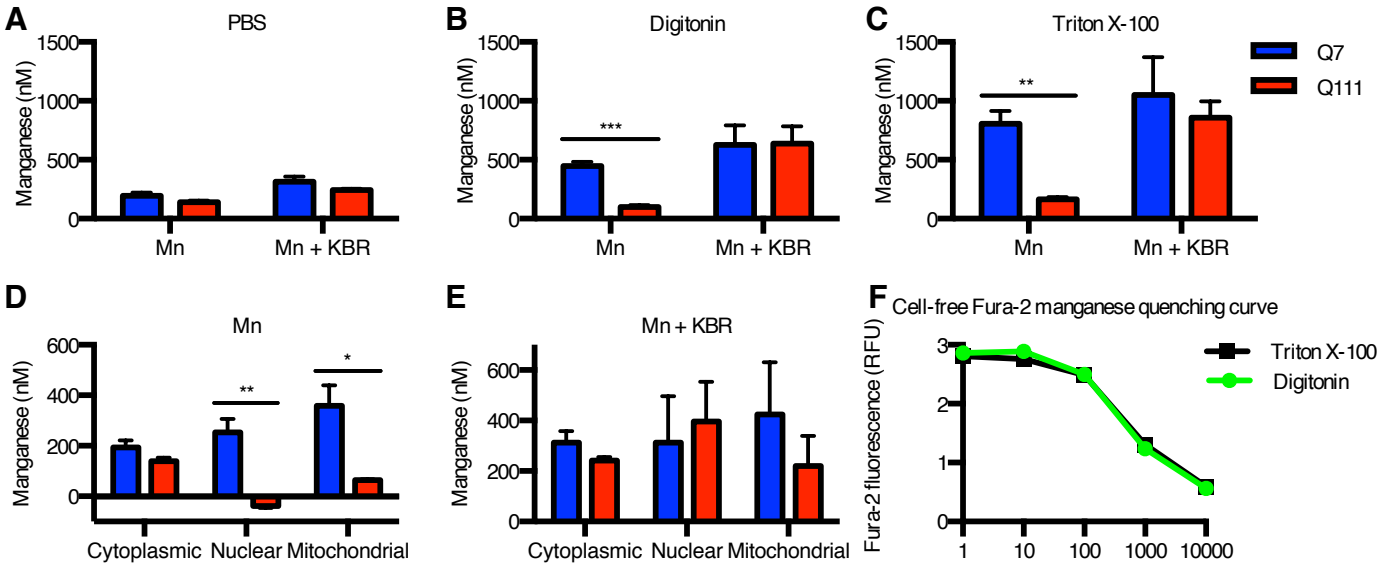

Figure 24. Digitonin permeable fraction has the greatest reduction in Q111 compared to Q7 cells. A-C The CFMEA managanese assay was performed with PBS, digitonin, or Triton X-100, and the resulting manganese concentration in the lysate was calculated. **D-E** Cell fraction concentrations were determined by subtraction for cytoplasmic (PBS), nuclear (digitonin – PBS), and mitochondrial (Trition X-100 – digitonin). N = 3 independent experiments with 2-4 biological replicates each. Bars = SEM.

We have confirmed that both digitonin and Triton X-100 (but not detergent-free PBS) permeabilize the plasma membrane and the nuclear envelope of the *Hdh* mouse striatal cells as measured by the fluorescence of a non-membrane permeable double-strand DNA dye, pico green (**Figure 25**). Therefore, by subtracting the calculated manganese concentration of the PBS from the digitonin permeabilized cells, we are able to estimate the amount of manganese in the nucleus or other digitonin permeable compartments. Likewise, by subtracting the digitonin concentration from the Triton X-100 concentration, we can estimate the manganese found in digitonin resistant compartments. However, the large difference in overall picogreen fluorescence between the TritonX-100 and digitionin may suggest that the nuclear envelope is permeable to picogreen but is completely dissolved with TritonX-100 allowing much more intercalation of the dye with DNA.

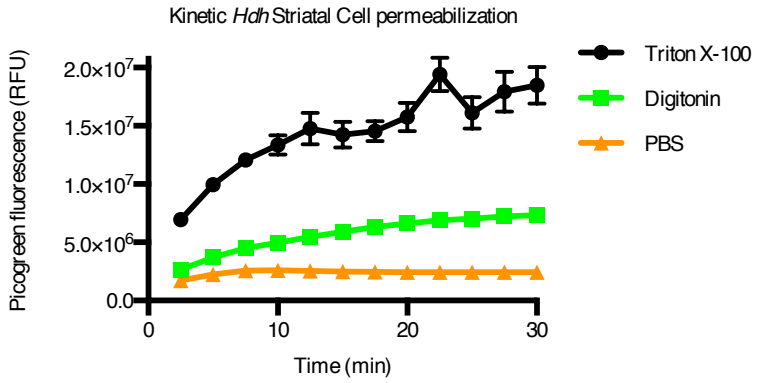

Figure 25. Digitonin and Triton X-100 permeabilize the plasma membrane and nuclear envelope. Kinetic reads were taken of well containing PBS and double-stranded DNA dye, picogreen. Detergents digitonin and Triton X-100 were also added to some wells. The increase in signal in the detergent well but not in the PBS wells demonstrates plasma membrane and nuclear envelope permeabilization (pico green is membrane impermeable). N = 8 wells for Triton X-100 and PBS (4 Q7 and 4 Q111) and N = 16 wells for digitonin (8 for Q7 and 8 for Q111). Error = SEM.

In **Figure 24D,** we see that both the digitonin accessible and digitonin resistant fractions have significantly less manganese in Q111 compared to Q7. The greatest fold difference occurs in the presumed nuclear fraction with 250 nM manganese extracted from the Q7 cells and a negative value calculated from the Q111 cells, that is significantly less than zero. This negative value could be due to dilution of the PBS only manganese and fura-2 by the loss of membrane integrity resulting in release of the cytoplasm. Alternatively,

sequestration of manganese by proteins that which use manganese as a cofactor or by divalent cation binding to the phosphate backbone of nuclear DNA are also possible. In any case, the genotypic difference in nuclear manganese accumulation is severe as we are unable to detect any nuclear manganese in the Q111 cell line with our current techniques.

We believe altered manganese homeostasis could underlie many of the pathological phenotypes in Huntington's disease patients (**Chapter I**). Nuclear manganese deficiency could also potentially lead to genomic instability because manganese is an important co-factor for DNA replication and repair enzymes (Frank & Woodgate, 2007; Hays & Berdis, 2002; Hopfner et al., 2001; Trujillo et al., 1998). For example, MRE11 a necessary part of the DNA repair complex, MRN, has a di-manganese binding pocket, and the presence of manganese is necessary for its nuclease activity, which cannot be substituted by magnesium or calcium (Hopfner et al., 2001; Paull & Gellert, 1998; Trujillo et al., 1998). This activity is necessary for proper repair of double-stranded DNA breaks (DSBs) via homologous recombination; however, nuclease activity-dead MRE11 mutants still undergo MRN complex binding to DSBs and MRE-11 dependent ATM phosphorylation (Limbo et al., 2012).

Additionally, manganese content has been found to regulate the activity of translesion DNA polymerase activity (e.g. DNA polymerase iota) (Hays & Berdis, 2002) . Translesion polymerases allow for replication in DNA with damage lesions increasing cellular tolerance for DNA damage (Waters et al., 2009). Reduced activity due to loss of manganese content may be a reason for increased radio-sensitivity and oxidative stress sensitivity in HD cells (Browne et al., 1999; Moshell et al., 1980). Interestingly, translesion polymerases have high error rates; in fact, DNA polymerase iota has ~ 10,000 times grater rate of single base substitution compared to non translesion eukaryotic polymerases (McCulloch & Kunkel, 2008). Therefore, manganese-dependent increases in activity may be a mechanism for manganese-dependent increases in mutagenesis, a result of high manganese exposure (Beckman et al., 1985). Reduced translesion polymerase activity in HD could also be a potential mechanism for reduced risk for all cancers in HD patients (Sørensen et al., 1999).

Manganese exposure rescues the elevated p53 phosphorylation in HD cells

As we showed earlier, the HD model Q111 cells had elevated p53 phosphorylation. When we exposed these cells to 50 μM manganese and measured p53 phosphorylation at 1 and 3 hours, we found that at both time points the elevated p53 phosphorylation returned to statistically the same levels as untreated Q7 cells (**Figure 26A**). We did not see the same effect on H2AX phosphorylation (**Figure 26B**). This may suggest two different kinases are responsible for the elevated phosphorylation of these two proteins. We also did not see the same effect in the human Islet1^{+} cells since they did not have elevated basal p53 phsophorylation (**Figure 22B** and data not shown).

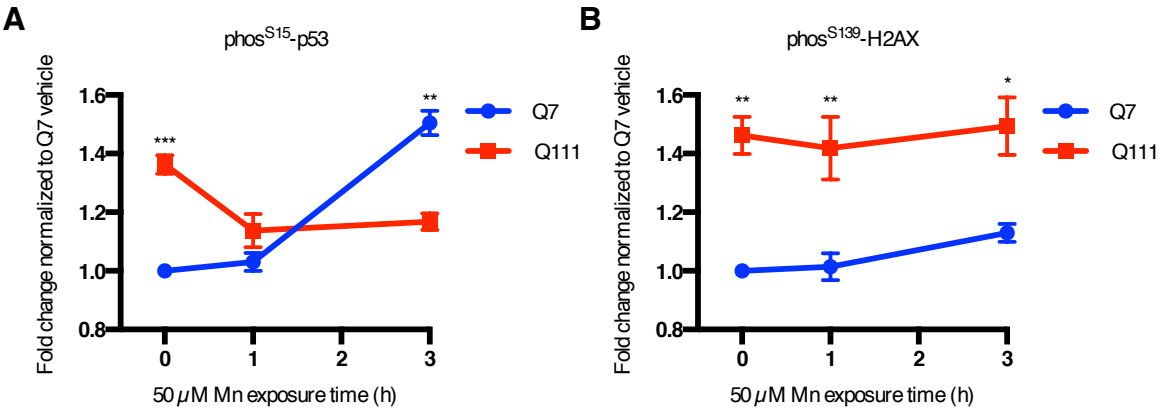

Figure 26. Manganese exposure returns Q111 to the same level of p53 but not H2AX phosphorylation seen in Q7. In-cell western was used to quantify phosphorylation of p53 at serine 15 (**A**) and H2AX at serine 139 (**B**) in the *Hdh*$^{Q7/Q7}$ (Q7) and *Hdh*$^{Q111/Q111}$ (Q111) cells after various times of manganese exposure. All values were normalized within experiment to the vehicle treated (0 hour) Q7 control cells. N = 3 in (**A**) and 4 in **(B**). Bars, mean ± SEM. For genotype comparisons, * for $p < 0.05$, ** for $p < 0.01$, and *** for $p < 0.001$ by two-way ANOVA with Sidak's *post-hoc* analysis. N = 3 independent experiments.

Although we have discussed many manganese dependent enzymes whose restored function may ultimately decrease p53 phosphorylation (see **Chapter I**), one obvious possibility is MRE11. We hypothesize that reduced nuclease activity due to loss of manganese would result in stalled DSB strand repair. MRE11 foci would have a longer active time to phosphorylate ATM increasing its DNA damage response in HD cells (which we saw in **Chapter I, Figure 12**). By supplementing the Q111 cells with high levels of manganese, the MRE11

nuclease function could be restored leading to reduced ATM phosphorylation and subsequent p53 phosphorylation. This is only possible if p53 phosphorylation dynamics are significantly faster than those of H2AX since we do not see the same rescue of its elevated basal phosphorylation (**Figure 26B**).

Conclusions and Future Directions

We can conclude several important findings from these data. 1.) HD iPS cells have increased genomic instability and DNA damage signaling. 2.) The HD dependent cellular manganese deficiency is greatest in digitonin permeabilized compartments including but not limited to the nucleus. 3.) Manganese can return p53 phosphorylation levels in HD to control levels in 1 hour in the *STHdh* model system presumably due to rescue of manganese dependent enzyme activity.

The necessary experiments needed to conclusively connect manganese deficiency, DNA damage signaling, and genomic instability should center around the activity of manganese dependent enzymes, MRE11 and polymerase iota. We are not yet aware of an *in situ* activity assay for polymerase iota, but there are some for MRE11. When double-stranded DNA breaks occur, the MRN complex binds to these site causing a dispersed nuclear staining via MRE11 immunofluroescence (Mirzoeva & Petrini, 2001). As repair progresses MRE11 foci give way to Rad51 foci, by measure the rate of pattern change of these two protein foci after DNA damage, the rate of DNA repair can be indirectly assessed. In fact, MRE11 foci retention has already been shown in one HD model (Ferlazzo et al., 2013).

Additionally, DNA damage and repair kinetics can be measured directly by pulsed-field gel electrophoresis or indirectly by the Comet method. In short, pulsed-field gel electrophoresis uses high voltage pulses to pull large genomic DNA fragments into smears in a gel lane. By measuring the relative amounts of DNA in the smear, the relative DNA damage and repair rates can be assayed between different samples (Collins, 2004). The comet assay uses single-cell gel electrophoresis to pull loops of DNA out of the lysed nucleus. The more DNA damage, the more unwound the DNA is from its histones allowing for longer loops. Therefore, measuring the length and intensity of the tails is an indirect measure of DNA damage(Ager et al., 1990).

CHAPTER IV

MANGANESE ACCUMULATION DEFICIENCY IN HUNTINGTON'S DISEASE MAY RESULT FROM LOSS OF Na^+/Ca^{2+} EXCHANGER EXPRESSION

Introduction

Huntington's disease human and mouse cell lines as well as mouse striata have reduce manganese accumulation compared with wild type controls (Williams, Kwakye, et al., 2010) (**Chapters 2 and 3**). Although Huntington's disease models have previously been shown to have altered iron and calcium homeostasis (**Chapter 1**), the mechanisms behind the alterations in these divalent metal cations does not explained the apparent alterations in manganese homeostasis (Williams, Kwakye, et al., 2010). In **Figure 18**, I showed that the drug KB-R7943 normalizes the amount of manganese taken up in HD model Q111 striatal cells to control levels with minimal effect on the Q7 control cells. Therefore, we believed that the target of this drug plays an important role in the etiology of the manganese-handling deficit in mutant huntingtin expressing cells.

KB-R7943 is known to be an inhibitor of the sodium-calcium exchanger (NCX) (Iwamoto & Shigekawa, 1998). The three NCX genes encode for ion antiporters that rely on Na influx down the concentration gradient to propagate Ca efflux that is vital for the normal functioning of cells (Niggli & Lederer, 1991). These antiporters also work in the "reverse" mode in which calcium is pumped into the cell and sodium is released (Matsuda et al., 1997). To our knowledge, manganese transport via NCX has not been investigated in an *in vitro* model; however, many lines of evidence point to NCX transporting manganese. NCX is a particularly important protein in cardiac function, and manganese is often used as a calcium surrogate given its divalency, similar ionic radius, and ability to be detected by MRI (Y. Chen et al., 2012; Waghorn et al., 2009). Two NCX inhibitors KB-R7943 and SEA0400 have been shown to increase manganese concentration in heart tissue as measured by manganese-enhance MRI (Y. Chen et al., 2012; Waghorn et al., 2009). Manganese and many other divalent

metals have also been shown to inhibit radio-labeled calcium uptake through the NCX protein potentially via competition for the channel (Iwamoto & Shigekawa, 1998). In this study, manganese inhibition of calcium uptake showed specificity in these studies for NCX1 and NCX2 over NCX3. Although we originally hypothesized that KB-R7943 normalized manganese levels by blocking excess efflux for the HD Q111 cells, we found that it actually normalized the expression of NCX1, the most highly expressed NCX in this cell line and that KB-R7943 increased its expression.

Results and Discussion

We have previously identified a severe deficit in manganese accumulation in the HD murine model *Hdh*$^{Q111/Q111}$ (Q111) immortalized cell line compared to control *Hdh*$^{Q7/Q7}$ (Q7) (Williams, Li, et al., 2010). We also discovered that 24 hours of co-incubation of the sodium calcium exchange inhibitor, KB-R7943, and manganese resulted in the same manganese accumulation between the two genotypes (control and HD) (**Figure 27A**). We hypothesized that the Q111 cell line had excess manganese efflux via NCX that was blocked by the inhibitor. However, when we performed the same experiment for only 3 hours, we saw same reduction in Q111 cells but no effect of the KB-R7943 (**Figure 27B**).

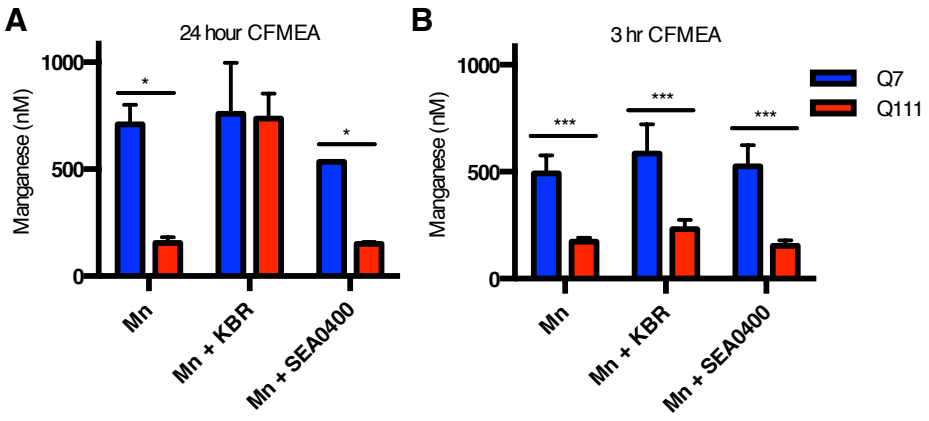

Figure 27. KB-R7943 but not SEA0400 normalizes manganese uptake at 24 but not 3 hours. Cells were exposed to either 50 μM manganese for 24 hours in basal medium (DMEM + 10 % FBS) (**A**) or to 125 μM manganese for 3 hours in HBSS (**B**) with DMSO, 10 μM KB-R7943 (KBR), or 10 μM SEA0400. Statistical comparisons between bars was performed by two-way ANOVA with LSD *post-hoc* test with * for $p < 0.05$ and *** for $p < 0.01$. N = 2 for (**A**) and 4 for (**B**). Bars, means + SEM.

Additionally, the more specific NCX inhibitor, SEA0400, does not significantly affect manganese accumulation at either time point. These data suggest that KB-R7943 must be altering gene expression, or some other long-term effect, rather then an immediate, direct blockade of the NCX channel.

We, therefore, investigated the expression level of the three mammalian NCX isoforms: NCX1, NCX2, and NCX3. All three have been shown to be expressed in brain tissue (Canitano et al., 2002). Using quantitative RT-PCR, we found that only NCX1 and NCX3 expression could be detected and that NCX1 was expressed ~60 times greater than NCX3 based on CT values. NCX1 expression was significantly diminished in Q111 cells compared to Q7 by approximately 15 fold, and expression was unaffected by manganese exposure (**Figure 28A**). NCX3 expression was also reduced in Q111 by approximately 40% compared to Q7 (**Figure 28B**). Interestingly, NCX3 expression increased due to manganese exposure by 50% in Q7 but not in Q111. This is possibly due to manganese dependent p53 activity discussed in **Chapter 2** because NCX3 has a p53 consensus site on its promoter region, but NCX1 does not (genecards.org).

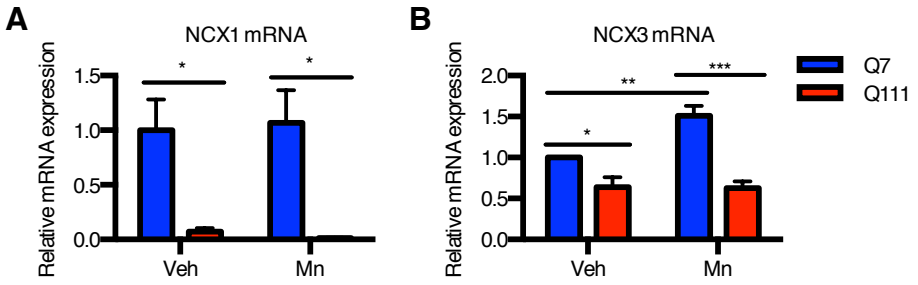

Figure 28. NCX1 and NCX3 mRNA expression are diminished in Q111 cells. Quantitative RT-PCR for NCX1 (**A**) and NCX3 (**B**) was performed on Q7 and Q111 cells exposed to 50 μM manganese or vehicle for 24 hours. Values were normalized to actin expression. N = 3 for (**A**) and N = 6 for (**B**). * for $p < 0.05$, ** for $p < 0.01$, and *** for $p < 0.001$ by two-way ANOVA with LSD *post-hoc* test. Bars = SEM.

These data gave the first evidence of a putative mechanism of the underlying manganese handling defect in HD cells. However, the effect of KB-R7943 became all the more intriguing since it only alters manganese accumulation in Q111, which has reduced expression of both NCX1 and NCX3. One recent publication demonstrated that chronic (48 hour) exposure to KB-R7943 up-regulated expression of NCX1 through the

formation of an NCX1-p38 complex, activating p38 to increase NCX1 expression (Xu et al., 2009). We hypothesized that KB-R7943 was up-regulating NCX1expression levels in Q111 to normal levels and thereby ameliorating the manganese-handling defect. To test this hypothesis, we performed quantitative RT-PCR on Q7 and Q11 cells exposed to 50 μM manganese and/or 10 μM KB-R7943 measuring NCX1 (**Figure 29**) expression. Again, we saw a severe reduction in NCX1 mRNA expression in Q111 cells regardless of exposure, which averaged approximately a 400 fold decrease (**Figure 29A**). Combined exposure of manganese and KB-R743 in Q7 cells led to a significant 2.3 fold increase in NCX1 mRNA expression (**Figure 29B**). In Q111 cells, KB-R7943 significantly increased NCX1 mRNA expression 5-fold (**Figure 29D**) regardless of manganese exposure (**Figure 29C**).

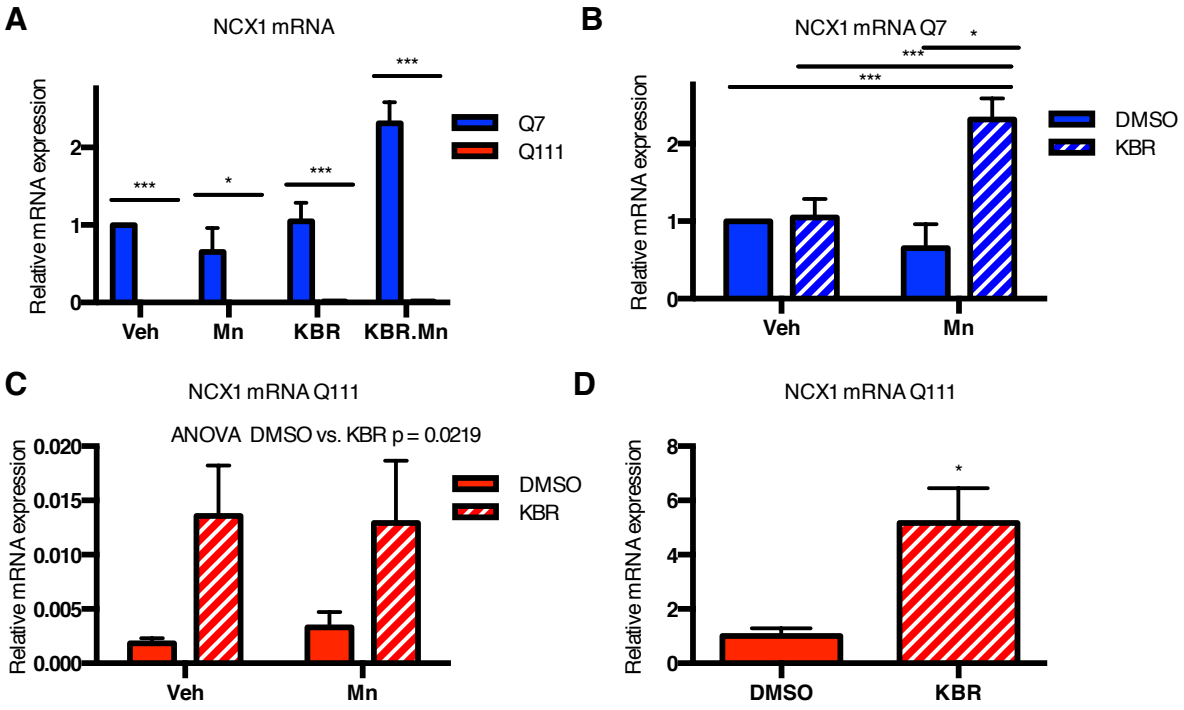

Figure 29. KB-R7943 significantly increases NCX1 expression in Q7 and Q111 cells. Quantitative RT-PCR was performed on Q7 and Q111 cells treated with 50 μM manganese and/or 10 μM KB-R7943. Values were normalized to actin expression. Data for both genotypes is presented in (**A**), each genotype individually in (**B,C**) to use different scaling, and Q111 in (**D**) without separating by manganese treatment which had no significant effect on NCX1 expression. N = 3 independent experiments for (**A-C**) and N = 6 for (**D**).

Although we confirmed our hypothesis that KB-R7943 treatment was leading to an increase in NCX1 expression, this expression change did not bring Q111 expression levels to those seen in Q7 despite normalization of manganese levels. One possibility is that NCX1 surface protein expression is non-existent in Q111 cells and our detected mRNA is either an artifact or expression is to low for significant translation into protein. The apparent 5 fold increase in NCX1 mRNA may be allowing NCX1 production, and over the 24 hour manganese exposure time, intracellular manganese levels will reach a maximal level equal to the extracellular concentration of manganese regardless of the exact number of NCX1 channels on the plasma membrane.

Conclusions and Future Directions

We can conclude that Q111 cells have reduced NCX1 and NCX3 expression with NCX1 expression increasing with KB-R7943 exposure. Future experiments are needed to measure the expression of NCX1 protein and its subcellular localization in Q7 and Q111 cells with and without KB-R7943 exposure. We have also generated expression plasmids the cloned NCX1 and NCX3 cDNA from Q7 cells. By transfecting Q111 with these genes, we will assess whether the manganese-handling deficit in Q111 is rescued to control levels.

However, these conclusions and proposed experiments would not explain the NCX1 expression deficit. Recently, NCX1 has been shown to be a target of the REST/NRSF transcription factor complex (Formisano et al., 2013), and one of the major expression alterations in Huntington's disease is expression loss of genes controlled by this complex (Zuccato et al., 2003). Therefore, it is possible that NCX1 expression is decreased in other HD model systems as well. Alternatively, ERK and p38 have been shown to regulate expression and activity of the NCX proteins (Sirabella et al., 2012) . ERK1/2 signaling has been shown to be reduced in Q111 cells due to reduced BDNF signaling and has been found to be protective against mutant huntingtin-associated toxicity in striatal cells (Apostol et al., 2006; Gines et al., 2003). Therefore, reduced ERK1/2 levels in Huntington's disease may result in lower NCX1 levels.

CHAPTER V

CONCLUSIONS

Manganese-dependent ATM activity

The identification of manganese responsive ATM kinase activity in an intact cellular model system is a novel finding. We have yet to probe the full relevance of this phenomenon, but in this discussion, I will highlight some of the likely possibilities. First, our finding fits well with previous literature findings (Guilarte et al., 2008). Namely that in non-human primate models chronically exposed to manganese have increased immunoreactivity for p53 and altered expression of p53 transcriptional targets (Guilarte et al., 2008). However, this study did not investigate the upstream kinase responsible for the increase in p53-dependent transcription. Importantly, manganese deficiency in the HD cells did not alter ATM activation by DNA damage. In fact, the manganese deplete HD cells (Q111) had elevated doubled stranded DNA break dependent ATM target phosphorylation, calling into question the literature claim that ATM is a manganese-dependent enzyme. This may not be that surprising since the original publications making this claim showed ATM becoming active when manganese was present regardless of the presence of DNA. Based on this literature and our findings, I hypothesize that ATM is activated through a novel Mn-dependent mechanism. One possible route is the disulfide bridge formation caused by oxidative stress shown in Guo et al 2010. In fact, this paper showed that high manganese concentrations (5 mM) alone can catalyze the dimerization of ATM. A 2+ redox state could allow manganese to potentially interact with the 2 polar sulfhydral groups that are in close proximity within the ATM dimer. This may catalyze the disulfide bond formation. Interestingly, the manganese specificity over other divalent metals suggests that whatever mechanism causes ATM activation is manganese specific. Perhaps the pocket near the sulfhydral groups is selective to manganese based on its distinct ionic radius.

Interestingly, the ability of ATM to respond to manganese may constitute a manganese-sensing kinase that could be an important aspect of cellular manganese homeostasis. But what are the possible reasons for ATM to be responsive to manganese levels and the potential outcomes? It is known that p53 has a complex

relationship with manganese superoxide dismutase (MnSOD), one of the most highly expressed manganese containing enzymes. Increased p53 activity leads to a decrease in MnSOD expression, and when p53 signaling reaches apoptotic levels, p53 translocates from the nucleus to the mitochondria where it inhibits MnSOD activity (Pani et al., 2000). Therefore, basally elevated p53 in HD cells could result in the increased sensitivity to oxidative stress seen in many model systems (Bogdanov et al., 2001; Browne & Beal, 2006; Polidori et al., 1999) as could decreased manganese via the same mechanism of decrease MnSOD activity (**Chapter I**). If the elevated basal p53 phosphorylation in Huntington's disease results from a deficit in intracellular manganese (as **Figure 25** suggests), the function of this elevation may be to decrease the expression of MnSOD in order to use available manganese sparingly. Therefore, the ability of ATM to respond to excess manganese leading to p53 phosphorylation may provide an additional layer of regulation to this network.

Another possible regulation by a manganese-sensing ATM-p53 pathway is arginase. Arginase is one of the most abundant manganese-dependent enzymes, and p53 is known to bind to the promoter region of the arginase I, ARG1 (SABiosceinces DECODE database). Although we have not published these data here, previous work by our group has demonstrated increased arginase activity and expression with manganese exposure. The ATM-p53 pathway may be an important part of arginase regulation by sensing availability of manganese.

In any case, ATM is a keep kinase balancing DNA damage, insulin, oxidative stress, and apoptotic signaling pathways. Even a small alteration in its biology due to reduced intracellular manganese could have profound effects over the lifetime of an organism. Each of these signaling pathways and processes has altered function in Huntington's disease. Connecting the increased CAG repeat length in mutant Huntingtin to reduced manganese levels is an important direction of this research and will be discussed in the next section; however, it is possible that the purported interaction between ATM and mutant Huntingtin is the proximal cause for reduced manganese levels if ATM is a manganese sensor that can regulate manganese homeostasis (Ferlazzo et al., 2013). In fact, more recent experiments from the Bowman lab (not shown here) show that inhibition of ATM kinase activity can lead to a dramatic decrease in manganese uptake over time.

Mutant Huntingtin-dependent manganese deficiency

Throughout this thesis, I have demonstrated altered manganese homeostasis seen in Huntington's disease mouse striatal cells (*Hdh*$^{Q111/Q111}$). This deficit also occurred in human cells but to a lesser degree; however, the deficiency in manganese induced ATM kinase target phosphorylation was almost as pronounced as the mouse cells. Since this phosphorylation event was an outcome of intracellular manganese levels one of two options is possible. (1) Either the deficit is compartment specific or (2) the relationship between the level of ATM target phosphorylation and manganese concentration is not linear. A manganese-handling defect that is strongest in the nucleus (where the majority of p53, H2AX, and CHK2 are in the cell) would possibly give the results seen in the human cells. We have shown just such a exaggerated nuclear defect in the mouse striatal cell model.

The differential extraction CFMEA provides us with an easy tool to assess intracellular manganese accumulation in a rapid fashion; however, it will be important to further validate what compartments each detergent is extracting. This can be addressed by western blot of the supernatant from the digitonin treated cells compared to the Triton X-100 and PBS samples with probing for compartment specific protein markers. Additionally, the high level of manganese in the PBS-only CFMEA needs to be addressed. This data either indicates a large extracellular background concentration that is not sufficiently washed away by 3 PBS washes or rapid efflux of manganese out of the cytoplasm. The former will call into question the exact amounts of manganese calculated in previous published work, and the later would provide an additional compartment specific assessment of intracellular manganese levels. We have yet to perform the CFMEA manganese quantification assay with the different detergents in the human cells, and these experiments will be critical to validate our finding from the mouse model.

If the nuclear manganese localization is deficient in both human and mouse cells, this provides potential rational for the genomic instability and increased DNA damage and DNA damage signaling shown in this thesis and the literature. Indeed, the fact that manganese exposure rescues the elevated p53 in the HD mouse cells provides further evidence that loss nuclear manganese is the root cause. As I have already stated, it is now

important to assay the function of manganese dependent enzymes in the HD and control cells (both mouse and human) to more deeply understand the effects of manganese deficiency. To address the genomic instability, manganese dependent DNA enzymes, MRE11 and DNA polymerase iota are two good candidates. Good immunofluorescence pattern readouts exist for MRE11 DNA damage repair but DNA polymerases activity is often assayed in lysates or purified protein experiments. Before these experiments, it may be good to assay manganese dependent enzymes that are more abundant with easily measured activity. We are currently assaying the activity of the manganese-dependent enzyme, arginase (**Chapter I**). Unpublished work from prior lab members has shown alterations in both expression and activity in *in vivo* mouse models, and the HD mouse striatal cells should also have a robust difference in arginase activity.

One of the more confusing aspects of this work is the dual nature of the ATM-p53 pathway in the context of manganese and Huntington's disease. In control cells, manganese exposure leads to an increase in ATM target phosphorylation including p53. This effect is severely diminished in HD cells and is often not significant in our exposure paradigm (50 μM manganese for 24 hours). On the other hand, HD cells have elevated p53 phosphorylation under basal conditions and in the human cells have exaggerated responses to DNA damaging agents. In this context, manganese exposure was actually shown to *decrease* p53 phosphorylation in HD cells. I hypothesize that small amount of manganese taken up into the HD cells was not enough to elicit a ATM response but was enough to restore the activity of manganese dependent enzymes. In particular, returning proper MRE11 activity could possibily decrease MRN dependent ATM activation because MRN foci would be able to mature once MRE11 nuclease activity is restored. Therefore, ATM activity can be increased with either too little or too much manganese present.

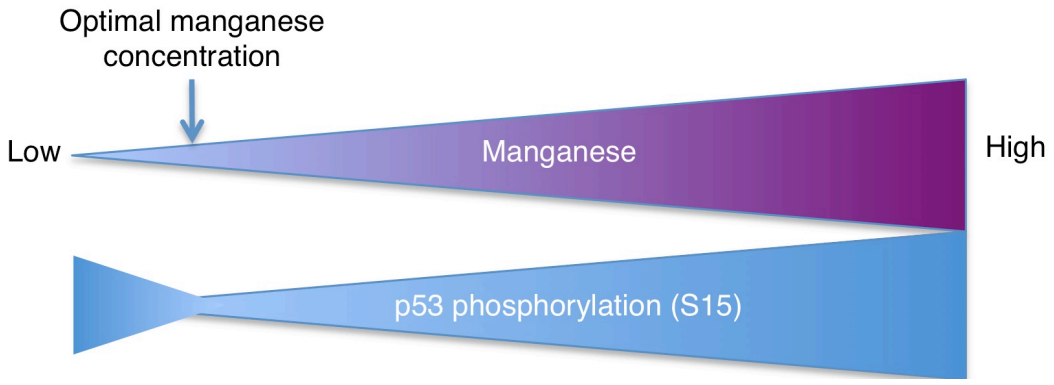

Figure 30. Conceptual diagram of the relationship between intracellular manganese and p53 phosphorylation.

Lastly, one of the ultimate remaining questions of this thesis work is whether the NCX1 expression deficit is truly the reason for the manganese accumulation deficit, and if so, does this deficiency occur in *in vivo* or human models as well? Many of the possible explanations of the effect KB-R7943 has on manganese uptake via NCX is through alterations to cell signaling pathways, including ERK1/2 and p38. Using the Pathscan assay from **Chapter II**, we could assess the effects of KB-R7943 exposure on a wide range of cell signaling pathways.

Comparison of model systems

One unique aspect of this study was the parallel modeling of Huntington's disease in both the murine striatal $Hdh^{Q7/Q7}$/ $Hdh^{Q111/Q111}$ and the human induced pluripotent stem cell derived neuroprogenitors. Each model system provided distinct advantages and challenges during experimentation and together they cement our findings in an already widely accepted disease model (Q7/Q11) and a patient-specific model (iPSCs).

The striatal cells ($Hdh^{Q7/Q7}$/ $Hdh^{Q111/Q111}$) are readily available through cell biorepositories (catalog.coriell.org). By nature, they are immortalized and in a static cell stage. This is in contrast to our iPSC-derived neural progenitors, which are still in the process of differentiation during the experimental phase. The striatal cells also grow quickly as single cells that can be easily passaged by trypsinization prior to confluency. The iPSC-derived cultures are heterogenous containing other cells in addition the characterized "striatal-like" neuroprogenitors. The iPSCs take between 1-2 months from thawing a vial until experiments can be performed

on the differentiated neuroprogenitors. Experiments can begin in as little as 4 days after thawing the murine striatal cells. For these reasons, the experimental variation is also much less in the striatal cells than the iPSC-derived cells. Therefore, the striatal cells serve greater utility when screening a large number of variables (such as the metals in **Figure 14,** while the human neuroprogenitors provide evidence that phenotypes found in the murine cells are artifacts of the model system and that they occur in human disease.

CHAPTER VI

MATERIALS AND METHODS

Reagents and plasmids

The immortalized murine striatal cell line models of HD, both wild-type (ST*Hdh*$^{Q7/Q7}$) and mutant (ST*Hdh*$^{Q111/Q111}$), were obtained from Coriell Cell Repository (Cambden, NJ). The ATM kinase inhibitor, KU55933, was from Tocris (Bristol, UK), hydrogen peroxide was from Sigma-Aldrich (St. Louis, MO), neocarzinostatin was from Sigma-Aldrich (St. Louis, MO). Heavy metal cations used in this study were Cd (Cd^{2+} as $CdCl_2$ hydrate), Cu (Cu^{2+} as $CuSO_4$ pentahyrdate), Mn (Mn^{2+} as $MnCl_2$ tetrahydrate), Ni (Ni^{2+} as $NiCl_2$ hexahydrate), Co (Co^{2+} as $CoCl_2$ hexahydrate), and Zn (Zn^{2+} as $ZnCl_2$). Plasmids used for reprogramming (#s 27077, 27078, and 27080) were obtained from Addgene (Cambridge, MA).

Antibodies

Antigen	Species	Clone name	Company	Model system	WB	ICW	IF
Islet 1 & 2	Mo	39.4D5	DSHB	Hu			1:100
Nanog	Gt		R&D Systems	Hu			1:20
Oct3/4	Rb		Cell Signaling	Hu			1:200
PAX6	Rb		Covance	Hu			1:100
Pericentrin	Rb		Abcam	Hu			1:1000
phospho-p53(Ser15)	Mo	16GB	Cell Signlaing	Hu, Mo	1:1000	1:400	
phospho-p53(Ser15)	Rb		Cell Signaling	Hu, Mo	1:1000	1:400	
p53	Mo	DO-1	Santa Cruz	Hu	1:1000		
p53	Rb	FL-393	Santa Cruz	Mo	1:1000		
phospho-H2A.X	Mo	JBW301	EMD Millipore	Hu, Mo	1:1000	1:400	
phospho-CHK2(Thr68)	Rb		Cell Signaling	Hu		1:400	
SSEA3	Rt	MC-631	Millipore	Hu			1:500
SSEA4	Mo	MC-813-70	DSHB				1:500
antiMouse IRDYE 800CW	Dk		LI-COR		1:10,000	1:800	
antiRabbit IRDYE 800CW	Dk		LI-COR			1:800	
antiRabbit IRDye 680LT	Dk		LI-COR		1:10,000		
anti(mo, rb, gt, or rt) Dylight 488 or 549	Dk		Jackson				1:800

Table 5. Antibodies. Antibodies used in this study are listed above with the species used to produce the antibody, clone name of all monoclonal antibodies, the company of origin, the model system that the antibody was used in, and the concentration used for each type of experiment. **WB** = western blot, **ICW** = In-Cell western, and **IF** = immunofluroescence microscopy.

Generation of human iPSC lines

Human dermal fibroblasts were obtained from either Dr. Kevin Ess (CD, CE, CF, and HD58) or from Coriell Cell Repository (Cambden, NJ) (GM21756 and GM09197 which are HD70 and HD180 respectively). Primary dermal fibroblasts were obtained by skin biopsy from healthy adult subjects (CD, CE, and CF) with no known family history of neurodegenerative disease after appropriate patient consent/assent under the guidelines of an approved IRB protocol (Vanderbilt #080369). Cells were grown to ~ 80% confluency, trypsinized, and counted. 6x10^5 cells were then electroporated with the CXLE plasmid vectors using the Neon Transfection System (Life Technologies, Carlsbad, CA) according to the conditions described in Okita et al 2011. Cells were replated in normal 10% FBS medium (formulation described in "Cell Culture" section) and grown with daily media changes for 7 days. The cells were then trypsinized and replated at 1x10^5 cells per 100 mm dish on top of SNL feeder cells. The next day, the medium was changed to KOSR ES medium (described in (Neely et al., 2011)) and replaced daily for ~30 days before colonies were picked and propagated.

Karyotype Analysis

Human iPSC lines were submitted for standard g-band karyotype analysis by Genetics Associates, Inc., (Nashville, TN). For each line, 20 metaphase spreads were analyzed and normal lines used in this study has euploid in 20 of 20 cells. For additional experiments the number of metaphase spreads was increased to 100.

Pluritest

All iPSC lines used in this study were validated using the bioinformatics assay, "Pluritest", developed by Muller F and collaborators (Müller et al., 2011). Human iPSC mRNA was isolated using the Qiagen RNeasy kit according to the manufacturer's recommendations (Qiagen, Valencia, CA). Microarrays were performed by Expression Analysis, Inc., (Durham, NC) on Illumina Human HT-12 v4.0 expression BeadChips (Illumina, Inc., San Diego, CA). Pluripotency of the iPSC lines was determined by uploading binary micro-array scanner output files (.idat file) into the freely available Pluritest Internet application (http://www.pluritest.org).

Cell culture

ST*Hdh*$^{Q7/Q7}$ and ST*Hdh*$^{Q111/Q111}$ immortalized murine striatal cells and human dermal fibroblasts were cultured in Dulbecco's Modified Eagle Medium [D6546, Sigma-Aldrich, St. Louis MO] supplemented with 10% FBS [Atlanta Biologicals, Flowery Branch, GA], 2 mM GlutaMAX (Life Technologies, Carlsbad, CA), Penicillin-Streptomycin, 0.5 mg/mL G418 Sulfate (Life Technologies, Carlsbad, CA), MEM non-essential amino acids solution (Life Technologies, Carlsbad, CA), 14mM HEPES (Life Technologies, Carlsbad, CA). They were incubated at 33°C and 5% CO_2. Cells were passaged before reaching greater than 90% confluency. The cells were split by trypsinization using 0.05% Trypsin-EDTA solution (Life Technologies, Carlsbad, CA) incubated for five minutes. One day prior to exposure, cells were plated in the appropriate cell culture plate type at $8x10^5$ cells/mL for Q7 and $1x10^6$ cells/mL for Q111.

Human iPSC lines were maintained in mTeSR1 medium (StemCell technologies, Vancouver, BC) on Matrigel (BD Biosciences, San Jose, CA) coated 6-well plates. Media was replaced daily. Cells were passaged at ~50% confluency. Before passage, spontaneously differentiated cells were manually removed using a specific home-made glass scraper (add our book chapter reference). Then colonies were washed once in DMEM/F12 (Life Technologies, Carlsbad, CA) and incubated for 5-10 min with dispase (StemCell Technologies, Vancouver, BC). The colonies were then washed twice with DMEM/F12. The colonies were then scrapped into mTeSR1 and triturated several times to achieve smaller cell clump size and replated at a dilution of 3-5 onto Matrigel.

Neural progenitor differentiation

Human iPSC colonies grown on Matrigel in mTeSR1 were dissociated by incubating for 15 minutes in Accutase (Innovative Cell Technologies, San Diego, CA). Cells were diluted, centrifuged, and resuspended in mTeSR1 medium containing 10 μM ROCK inhibitor, Y-27632 (Tocris, Bristol, UK). Cells were then replated onto Matrigel coated 12-well plates at a concentration of 1x10^5 cells/mL. The medium was changed 24 hours later to mTeSr1 without ROCK inhibitor and the cells were fed each subsequent day until cells reach > 90% confluency

(typically on 4 days later). Medium was then replaced with Knockout DMEM/F12 (Life Technologies, Carlsbad, CA) supplemented with 20% Knockout Serum Replacement (Life Tech), 2 mM Glutamax (Life Tech), MEM non-essential amino acids (Life Tech), and 55 μM 2-mercaptoethanol) containing 0.5 μM DMH1 (gift of Dr. Charles C. Hong) and 10 μM SB431542 (Tocris, Bristol, UK). After 72 hours, the medium was supplemented with 25% N2 medium (DMEM/F12 [with L-glutamine and HEPES] (Life Tech), 1x N2 supplement (Life Tech), and 4.5 g/L D-glucose) and 0.65 μM purmorphamine (Stemgent, Cambridge, MA), and SB431542 was no longer added. After an additional 48 hours, the N2 medium content was increased to 50%, and DMH1 was no longer added. After another 48 hours, an additional 25% N2 medium was added (25% neuralization medium, 75% N2 medium). Cultures were dissociated 10 days after the initial addition of neuralization medium via a 20 minute incubation with Accutase. For all experiments using human iPS-derived neural progenitors, cells were replated onto Matrigel-coated dishes at $7x10^5$ cells/mL in 100% N2 medium containing 0.65 μM purmorphamine and 10 μM ROCK inhibitor, Y-27632. The next day the experimental exposure was added in 100% N2 medium containing purmorphamine without ROCK inhibitor. Assays were performed 24 hours later.

CellTiterBlue Cytotoxicity Assay

Human neural progenitors or mouse striatal cells (*STHdh*$^{Q7/Q7}$, *STHdh*$^{Q111/Q111}$) were grown on 96-well plates. The day after replating, they were exposed to toxicants in the cell type appropriate neuralization medium. At 2 hours prior to the completion of the 24-hour exposure period or after toxicant removal and washes following 1-hour exposures, 20 μL of CellTiterBlue reagent (Promega, Madison, WI) was added to each well. Prior to this addition, cell lysis buffer was added to several wells to provide an accurate fluorescence background for 0% viable cells. The plates were then incubated for 2 hours at 37° C. Fluorescence was measured using excitation of 570 nm and emission of 600 nm on a POLARstar Omega microplate reader (BMG Labtech, Ortenberg, Germany).

MTT Assay

For the neocarzinostatin treatment viability assay, induced pluripotent stem cells were plated at 100,000 cells/mL in mTeSR1 with Rho-kinase inhibitor, Y-27632 (Tocris, Bristol, UK). Cells were exposed to neocarzinostatin in mTeSR1 for 1 hour followed by washing twice in PBS and replacing with fresh mTesr1 medium. Cells were then placed back in the incubator for an additional 23 hours. MTT, (3-(4,5-Dimethylthiazol-2-yl)-2,5-diphenyltetrazolium bromide, was added to each well for a final concentration of 0.5 % MTT. After 2 hours of incubation, the medium was removed and cells with formazan crystal were dissolved in a solution of 10% Sorenson's buffer in 90% DMSO. Absorbance readings were taken at 570-590 nm.

Cellular Fura-2 Manganese Extraction Assay (CFMEA)

CFMEA was performed exactly as described previously (K. K. Kumar et al., 2013). In short, cells grown in 96-well plates were exposed to either 50 μM $MnCl_2$ in cell culture medium for 24 hours or 125 μM $MnCl_2$ for 3 hours in Hank's buffered salt solution (HBSS). The wells were then washed 3 times with PBS. PBS was then added containing 0.75 μM Fura-2 , 0.1% Triton X-100, and Alexa Fluor 568 (dextran conjugate). Cells were incubated at room temperature in the dark for > 20 min. Fura-2 fluorescence was measure on a Beckman-Coulter DTX 880 multimode plate reader excitation/emission 360/535 nM. Manganese concentration was calculated based on a manganese-dependent quenching curve of Fura-2 fluorescence. Alexa Fluor 568 fluorescence was used as a volumetric control. Matrigel-coated wells show a manganese concentration dependent background that is not observed in uncoated wells. A manganese concentration-specific background was therefore subtracted from the experimental signals of wells containing matrigel. Manganese content was normalized to DNA content of each culture unless otherwise specified. This was performed by the Quant-iT PicoGreen dsDNA Assay kit.

DNA Polymerase Chain Reaction (PCR)

PCR was performed for both validation of the loss of the episomal plasmid vector and for validating the HD mutation in the iPSC lines. DNA was isolated using the DNeasy kit (Qiagen, Valencia, CA) and quantified using a Nanodrop 1000 spectrophotometer (Nanodrop Instruments). Primers and template DNA were mixed with

GoTaq Green 2X Master Mix (Promega, Madison, WI). The PCR amplification was performed on a MyCycler Thermal Cycler (Bio-Rad, Hercules, CA). For amplification of the mutant *Huntingtin* gene CAG repeat region, 1X Q buffer (Qiagen, Valencia, CA) and 5% DMSO were added. DNA products were run on 1 or 2% agarose gels in TBE buffer and stained with ethidium bromide.

Quantitative Reverse Transcriptase PCR

Cells were lysed using RLT buffer with 1% BME and homogenized on QIAshredder columns (Qiagen, Valencia, CA). Total RNA was isolated using the RNeasy kit with on column RNase-free DNase treatment (Qiagen, Valencia, CA). Total RNA was quantified using a Nanodrop 1000 spectrophotometer (Thermo Scientific, Waltham, MA). First strand cDNA synthesis reactions were performed on 1 μg of total RNA using the SuperScript III kit with random hexamers (Life Technologies, Carlsbad, CA). Quantitative PCR was performed using the Power SYBR Green Master Mix (Life Technologies, Carlsbad, CA) as 10 μL reactions in 384-well plates with 10 ng of cDNA on a 7900HT fast real-time PCR system (Applied Biosystems, Carlsbad, CA). Primers are listed in **Table 4**. Actin was used as a normalizing control gene.

Primer Name	Gene	Sequence	Tm	Product Size
AT83	FOXG1 F	CAACGGCATCTACGAGTTCA	59.9	57
AT84	FOXG1 R	TGCTTGTTCTCGCGGTAGTA	59.7	
AT95	PAX6 F	CAGCTTCACCATGGCAAATA	59.7	77
AT96	PAX6 R	GCAGCATGCAGGAGTATGAG	59.6	
AT103	Actin F	CTGTGGCATCCACGAAACTA	59.7	84
AT104	Actin R	AGCACTGTGTTGGCGTACAG	60.0	
AT277	Islet-1 F	ACGGTGGCTTACAGGCTAAC	59.3	56
AT278	Islet-1 R	TTTCCAAGGTGGCTGGTAAC	60.0	
1594	HTT CAG Repeat F	CCGCTCAGGTTCTGCTTTTA	60.5	278
1595	HTT CAG Repeat R	GGCTGAGGAAGCTGAGGAG	60.2	(19 CAG repeats)
Insertion1	WPRE F	CAGGCAACGTGGCGTGGTGT	70.0	265
Insertion2	WPRE R	GGACGTCCCGCGCAGAATCC	71.5	
AT335	Mouse Actin F	CAGCCTTCCTTCTTGGGTAT	58.3	83
AT336	Mouse Actin R	CGGATGTCAACGTCACACTT	59.6	
AT327	Mouse p21 F	GAGGCCCAGTACTTCCTCTG	58.9	78
AT328	Mouse p21 R	AGAGTGCAAGACAGCGACAA	59.8	
AT321	Mouse NCX1	CGACTTGAGCACCACTGTGT	59.9	108
AT322	Mouse NCX1	TCCCCTGGTTTGAAGATCAC	59.9	
AT323	Mouse NCX2	TCAACCAAGGGAATGGAGAC	59.9	75
AT324	Mouse NCX2	GCTTGCCCATCTCTGCTATC	59.9	
AT325	Mouse NCX3	CCCATGTTCCTGCTTGTTTT	60	115
AT326	Mouse NCX3	CCTGGATTCTTTGGCAATGT	59.9	

Table 4. Primer sequences for PCR and quantitative reverse transcriptase PCR. Identifying numbers were assigned to each new primer designed for human and mouse (where noted) genes listed. The melt temperature was calculated via the Breslauer et al 1986 table of thermodynamic properties and the Schildkraut and Lifson 1965 salt correction formula. Expected product sizes are from a mRNA library not necessarily genomic DNA because some primer sets span exon-intron boundaries.

PathScan ELISA Array

The assay was performed following the manufacturers instructions. In brief, cells were washed once with ice-cold PBS and lysed with ice-cold sandwich ELISA array lysis buffer (Cell Signaling, Danvers, MA) containing 1 mM PMSF for 5 minutes on ice. The lysates were then pipetted into pre-chilled tubes. Lysate protein concentration was calculated using the DC protein assay (Promega, Madison, WI). After diluting to equivalent concentrations, lysates were added to the prepared PathScan Intracellular signaling array (Cell Signaling, Danvers, MA). The fluorescent signal was assessed using the Odyssey Infrared Imaging system (LI-COR, Lincoln, NE). Two wells were incubated in dilution buffer only and provided the background signal for each pathway. Only signal intensities ≥ 3 fold the background signal are reported, except for cleavage of caspase-3 and PARP-1. Since human data was generated on a single slide, the data was divided by the mean of the

untreated sample intensities to achieve a fold change value. For the mouse PathScan, each of the three data points for each signaling pathway were generated on a separate slide on separate days. Therefore, the values for each day were divided by the untreated sample intensity for that day. Therefore, the untreated means have no variance since all values are 1. 95% confidence intervals were used to calculate statistical significance. Human cell analysis was performed by t test.

Immunoblot analysis

Protein samples were prepared by scraping cells into ice-cold PBS, centrifuging, and adding RIPA buffer containing protease (Sigma-Aldrich, St. Louis, MO) and phosphatase inhibitor cocktails 2 & 3 (Sigma, Sigma-Aldrich, St. Louis, MO) to the pellet. After gentle homogenization, cells were centrifuged at 4 C for 10 minutes at 20,000 *g*. The resulting DNA containing pellet was removed from the lysate, and the protein concentration was quantified using the DC assay (BioRad, Hercules, CA) with a BSA standard curve. Samples were mixed with 5x SDS loading buffer containing 1% 2-mercaptoethanol and boiled for 5 minutes. 15 μg of protein was loaded for each sample onto a 4-15% pre-cast gel SDS-PAGE gel (BioRad, Hercules, CA) and run at 90V for 120 minutes. The protein bands were then transferred onto nitrocellulose membranes using iBlot Gel Transfer Device (Life Technologies), and the protein was transferred onto a nitrocellulose membrane. The remaining gel was stained with IRDye Blue protein stain (LI-COR, Lincoln, NE). Since the gels retained ~1/3 of the original protein after transferring with the iBlot, we imaged the stained gel on the Li-Cor Odyssey Imaging System and quantified the intensity entire lane from ~150-20 kDa. This value was used to normalize the values of immunostained bands. The membrane was blocked in Odyssey Blocking Buffer for one hour prior to the addition of the primary antibodies. The primary antibodies were diluted in Odyssey Blocking Buffer containing 0.1% TWEEN and incubated overnight. After washing 5 times for 5 minutes in TBST, membranes were incubated with secondary antibodies at 1:10,000 (LiCor, Lincoln, NE) for 1 hour. Membranes were imaged using the Li-Cor Odyssey Imaging System, and quantification was performed using Image Studio Lite (LiCOR, Lincoln, NE).

In-Cell Western Assay

Cells were plated in 96-well μClear black-walled plates (Greiner Bio-One, Frickenhausen, Germany) at the appropriate density for the particular line. After exposing cells to toxicants, they were washed once in room temperature PBS (without calcium and magnesium). The cells were then fixed with 4% paraformaldehyde in PBS for 30 minutes at room temperature, washed 5 times for in PBS with 0.1% Triton-X 100, and blocked for 1.5 hours in 150 μL of Odyssey blocking buffer. The cells were then incubated with primary antibody at 1:400 in Odyssey blocking buffer (LiCor, Lincoln, NE) with 50 μL in each well for 2.5 hours. After washing 4 times in PBS with 0.1% Tween-20 for 5 minutes, cells were incubated for 1 hour in the appropriate LiCor IRdye800 secondary antibody at 1:800 dilution in Odyssey blocking buffer along with 1:500 of CellTag normalization dye (LI-COR, Lincoln, NE). An additional round of 5 washes for 5 minutes in PBS with Tween-20 was performed after which all buffer was removed. Plates were imaged with the Li-Cor Odyssey Imaging System and intensities were calculated for each well with Image Studio software. Cultures that were no incubated with primary antibodies served as backgound. Antibody signals were normalized using the CellTag signal (a measure of total cells). We have included exemplary images from both human and In-Cell Western assays in the appendix.

Immunofluorescence microscopy

Cells were fixed in paraformaldehyde for 30 min at room temperature. After permeabilization with 0.2% Triton-X100 for 20 min at room temperature, cells were incubated in PBS containing 5% donkey serum and 0.05% Triton-X100 for 2 h at room temperature or overnight. Cell were incubated in primary antibody overnight (see table to antibody dilutions), washed in PBS with 0.05% Triton-X100 and incubated for 3 hours with secondary antibody. Images were obtained with a Zeiss ObserverZ1 microscope and AxioVs40 software (version 4.7.2).

Centrosome counting

Fibroblasts and iPS cells were grown on Nunc Lab-Tek I Chamber slides (Thermo Scientific,). Cells were immunostained for immunofluorescence microscopy as described above for pericentrin (Abcam, 1:1000).

Coverslips were mounted over the cells using Prolong Gold Antifade Reagent with DAPI (Life Technologies). Using a Zeiss ObserverZ1 microscope, cells undergoing mitosis were identified by loss of nuclear envelope and distinct chromosome morphology. While blinded to genotype, these cells were then scored for the number of centrosomes by focusing up and down in the channel stained by the pericentrin antibody. Cells with 1 or 2 distinct centrosomes were scored as normal, while those with 3 or more were counted as abnormal. Each line in each experiment had 20 cells scored.

APPENDIX

In-Cell Western Images

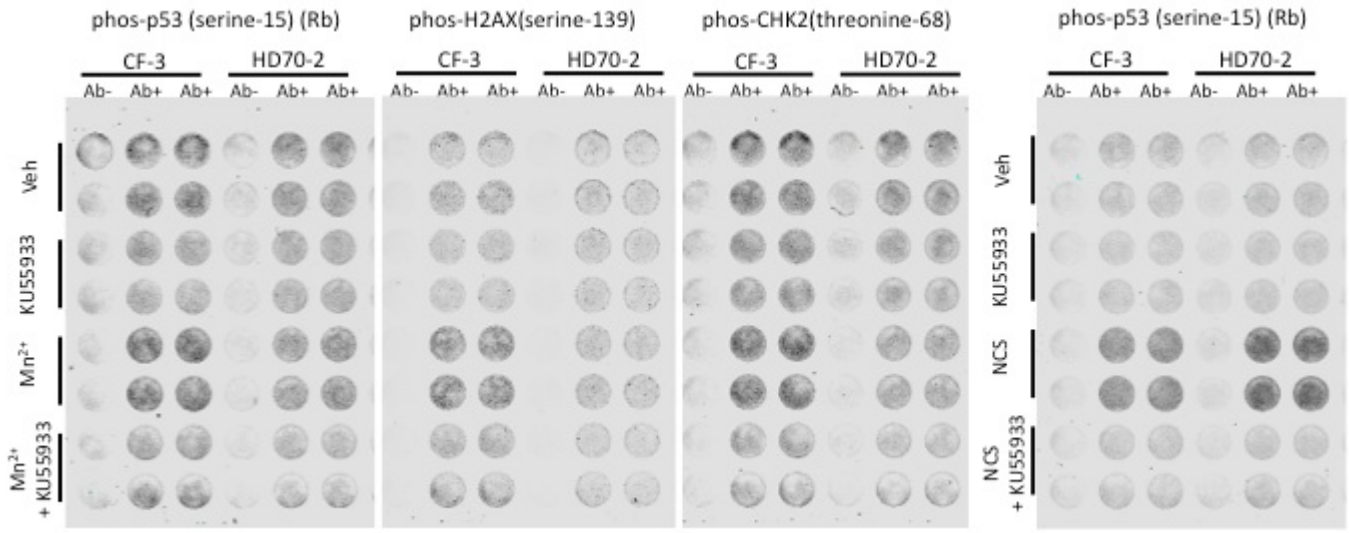

Appendix Figure 1. Image of In-Cell Western assays for ATM targets in CF-3 and HD70-2 human neuroprogenitors. Human neuroprogenitors plated onto 96-well plates were exposed for 24 hours to manganese (50 μM), 1 hour neocarzinostatin (100 ng/mL), and/or KU-55933 (1 μM). The In-Cell Western assay was then used to quantify the expression of several phosphorylation events as list above the figure. Columns of wells labeled as (Ab-) did not receive a primary antibody and served as a background/non-specific binding control, for the columns of wells labeled as (Ab+).

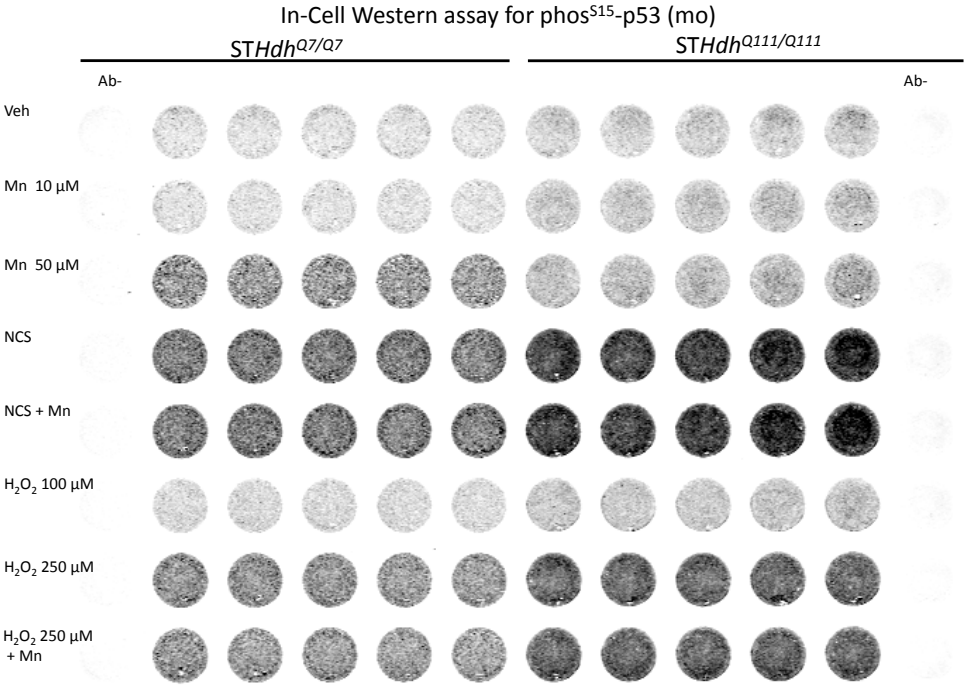

Appendix Figure 2. Image of In-Cell Western assay for phospho-p53(S15)(mo). Mouse ST*Hdh* neuroprogentiors plated onto 96-well plates were exposed for 24 hours to manganese (50 μM), 1 hour neocarzinostatin (100 ng/mL), or 1 hour H_2O_2 (250 μM). The In-Cell Western assay was then performed to quantify the expression of several phosphorylation events as list above the figure. Columns labeled (Ab-) did not receive a primary antibody and served as a background/non-specific binding control for the other wells.

REFERENCES

Ager, D., Dewey, W., Gardiner, K., Harvey, W., Johnson, R., & Waldren, C. (1990). Measurement of radiation-induced DNA double-strand breaks by pulsed-field gel electrophoresis. *Radiation research, 122*(2), 181-187.

Ala, A., Walker, A. P., Ashkan, K., Dooley, J. S., & Schilsky, M. L. (2007). Wilson's disease. *The Lancet, 369*(9559), 397-408.

Alam, Z. I., Halliwell, B., & Jenner, P. (2000). No evidence for increased oxidative damage to lipids, proteins, or DNA in Huntington's disease. *Journal of neurochemistry, 75*(2), 840-846.

An, M. C., Zhang, N., Scott, G., Montoro, D., Wittkop, T., Mooney, S., . . . Ellerby, L. M. (2012). Genetic correction of Huntington's disease phenotypes in induced pluripotent stem cells. *Cell Stem Cell*.

Anca, M., Gazit, E., Loewenthal, R., Ostrovsky, O., Frydman, M., & Giladi, N. (2004). Different phenotypic expression in monozygotic twins with Huntington disease. *American Journal of Medical Genetics Part A, 124*(1), 89-91.

Andreassen, O. A., Dedeoglu, A., Ferrante, R. J., Jenkins, B. G., Ferrante, K. L., Thomas, M., . . . Borchelt, D. R. (2001). Creatine increases survival and delays motor symptoms in a transgenic animal model of Huntington's disease. *Neurobiology of disease, 8*(3), 479-491.

Andreassen, O. A., Ferrante, R. J., Dedeoglu, A., Albers, D. W., Klivenyi, P., Carlson, E. J., . . . Beal, M. F. (2001). Mice with a partial deficiency of manganese superoxide dismutase show increased vulnerability to the mitochondrial toxins malonate, 3-nitropropionic acid, and MPTP. *Experimental neurology, 167*(1), 189-195.

Andreassen, O. A., Ferrante, R. J., Dedeoglu, A., & Beal, M. F. (2001). Lipoic acid improves survival in transgenic mouse models of Huntington's disease. *Neuroreport, 12*(15), 3371-3373.

Andrew, S. E., Goldberg, Y. P., Kremer, B., Telenius, H. k., Theilmann, J., Adam, S., . . . Kalchman, M. A. (1993). The relationship between trinucleotide (CAG) repeat length and clinical features of Huntington's disease. *Nature genetics, 4*(4), 398-403.

Apostol, B. L., Illes, K., Pallos, J., Bodai, L., Wu, J., Strand, A., . . . Marsh, J. L. (2006). Mutant huntingtin alters MAPK signaling pathways in PC12 and striatal cells: ERK1/2 protects against mutant huntingtin-associated toxicity. *Human molecular genetics, 15*(2), 273-285.

Armstrong, L., Tilgner, K., Saretzki, G., Atkinson, S. P., Stojkovic, M., Moreno, R., . . . Lako, M. (2010). Human induced pluripotent stem cell lines show stress defense mechanisms and mitochondrial regulation similar to those of human embryonic stem cells. *Stem Cells, 28*(4), 661-673. doi: 10.1002/stem.307

Aschner, J. L., & Aschner, M. (2005). Nutritional aspects of manganese homeostasis. *Molecular aspects of medicine, 26*(4), 353-362.

Aschner, M., & Aschner, J. L. (1991). Manganese neurotoxicity: cellular effects and blood-brain barrier transport. *Neuroscience & Biobehavioral Reviews, 15*(3), 333-340.

Aubry, L., Bugi, A., Lefort, N., Rousseau, F., Peschanski, M., & Perrier, A. L. (2008). Striatal progenitors derived from human ES cells mature into DARPP32 neurons in vitro and in quinolinic acid-lesioned rats. *Proc Natl Acad Sci USA, 105*(43), 16707-16712. doi: 10.1073/pnas.0808488105

Azevedo, F. A., Carvalho, L. R., Grinberg, L. T., Farfel, J. M., Ferretti, R. E., Leite, R. E., . . . Herculano‚ÄêHouzel, S. (2009). Equal numbers of neuronal and nonneuronal cells make the human brain an isometrically scaled‚Äêup primate brain. *Journal of Comparative Neurology, 513*(5), 532-541.

Bae, B.-I., Xu, H., Igarashi, S., Fujimuro, M., Agrawal, N., Taya, Y., . . . Ross, C. A. (2005). p53 mediates cellular dysfunction and behavioral abnormalities in Huntington's disease. *Neuron, 47*(1), 29-41.

Bae, J.-H., Jang, B.-C., Suh, S.-I., Ha, E., Baik, H. H., Kim, S.-S., . . . Shin, D.-H. (2006). Manganese induces inducible nitric oxide synthase (iNOS) expression via activation of both MAP kinase and PI3K/Akt pathways in BV2 microglial cells. *Neuroscience letters, 398*(1), 151-154.

Baly, D. L., Curry, D. L., Keen, C. L., & Hurley, L. S. (1984). Effect of manganese deficiency on insulin secretion and carbohydrate homeostasis in rats. *The Journal of nutrition, 114*(8), 1438-1446.

Baly, D. L., Keen, C. L., & Hurley, L. S. (1985). Pyruvate carboxylase and phosphoenolpyruvate carboxykinase activity in developing rats: effect of manganese deficiency. *The Journal of nutrition, 115*(7), 872.

Banin, S., Moyal, L., Shieh, S.-Y., Taya, Y., Anderson, C., Chessa, L., . . . Shiloh, Y. (1998). Enhanced phosphorylation of p53 by ATM in response to DNA damage. *Science, 281*(5383), 1674-1677.

Baquer, N. Z., Sinclair, M., Kunjara, S., Yadav, U. C., & McLean, P. (2003). Regulation of glucose utilization and lipogenesis in adipose tissue of diabetic and fat fed animals: Effects of insulin and manganese. *Journal of biosciences, 28*(2), 215-221.

Bartzokis, G., Cummings, J., Perlman, S., Hance, D. B., & Mintz, J. (1999). Increased basal ganglia iron levels in Huntington disease. *Archives of neurology, 56*(5), 569.

Beal, M., Brouillet, E., Jenkins, B., Ferrante, R., Kowall, N., Miller, J., . . . Hyman, B. (1993). Neurochemical and histologic characterization of striatal excitotoxic lesions produced by the mitochondrial toxin 3-nitropropionic acid. *The Journal of neuroscience, 13*(10), 4181-4192.

Beard, J. (2003). Iron deficiency alters brain development and functioning. *The Journal of nutrition, 133*(5), 1468S-1472S.

Beckman, R. A., Mildvan, A. S., & Loeb, L. A. (1985). On the fidelity of DNA replication: manganese mutagenesis in vitro. *Biochemistry, 24*(21), 5810-5817.

Bédard, A., Gravel, C., & Parent, A. (2006). Chemical characterization of newly generated neurons in the striatum of adult primates. *Exp Brain Res, 170*(4), 501-512. doi: 10.1007/s00221-005-0233-5

Behrens, P., Franz, P., Woodman, B., Lindenberg, K., & Landwehrmeyer, G. (2002). Impaired glutamate transport and glutamate,Äiglutamine cycling: downstream effects of the Huntington mutation. *Brain, 125*(8), 1908-1922.

Betarbet, R., Sherer, T. B., MacKenzie, G., Garcia-Osuna, M., Panov, A. V., & Greenamyre, J. T. (2000). Chronic systemic pesticide exposure reproduces features of Parkinson's disease. *Nature neuroscience, 3*(12), 1301-1306.

Birken, D. L., & Oldendorf, W. H. (1989). N-Acetyl-L-Aspartic acid: A literature review of a compound prominent in< sup> 1</sup> H-NMR spectroscopic studies of brain. *Neuroscience & Biobehavioral Reviews, 13*(1), 23-31.

Bjokoy, G., Lamark, T., Brech, A., Outzen, H., Perander, M., Overvatn, A., . . . Johansen, T. (2005). p62/SQSTM1 forms protein aggregates degraded by autophagy and has a protective effect on huntingtin-induced cell death. *The Journal of cell biology, 171*(4), 603-614.

Bogdanov, M. B., Andreassen, O. A., Dedeoglu, A., Ferrante, R. J., & Beal, M. F. (2001). Increased oxidative damage to DNA in a transgenic mouse model of Huntington's disease. *Journal of neurochemistry, 79*(6), 1246-1249.

Boll, M.-C., Alcaraz-Zubeldia, M., Montes, S., & Rios, C. (2008). Free copper, ferroxidase and SOD1 activities, lipid peroxidation and NO x content in the CSF. A different marker profile in four neurodegenerative diseases. *Neurochemical research, 33*(9), 1717-1723.

Bonilla, E., Estevez, J., Suarez, H., Morales, L., de Bonilla, L. C., Villalobos, R., & Davila, J. (1991). Serum ferritin deficiency in Huntington's disease patients. *Neuroscience letters, 129*(1), 22-24.

Bowman, A. B., & Aschner, M. (2014). Considerations on manganese (Mn) treatments for< i> in vitro</i> studies. *Neurotoxicology, 41*, 141-142.

Bowman, A. B., Kwakye, G. F., Herrero Hern√°ndez, E., & Aschner, M. (2011). Role of manganese in neurodegenerative diseases. *Journal of Trace Elements in Medicine and Biology, 25*(4), 191-203.

Bowman, A. B., Kwakye, G. F., Herrero Hernández, E., & Aschner, M. (2011). Role of manganese in neurodegenerative diseases. *Journal of Trace Elements in Medicine and Biology, 25*(4), 191-203.

Braissant, O., Gotoh, T., Loup, M., Mori, M., & Bachmann, C. (1999). l-arginine uptake, the citrulline‚ÄìNO cycle and arginase II in the rat brain: an in situ hybridization study. *Molecular brain research, 70*(2), 231-241.

Brock, A. A., Chapman, S. A., Ulman, E. A., & Wu, G. (1994). Dietary manganese deficiency decreases rat hepatic arginase activity. *The Journal of nutrition, 124*(3), 340-344.

Brouillet, E., Condé, F., Beal, M. F., & Hantraye, P. (1999). Replicating Huntington's disease phenotype in experimental animals. *Prog Neurobiol, 59*(5), 427-468.

Browne, S. E., & Beal, M. F. (2006). Oxidative damage in Huntington's disease pathogenesis. *Antioxidants & redox signaling, 8*(11-12), 2061-2073.

Browne, S. E., Bowling, A. C., Macgarvey, U., Baik, M. J., Berger, S. C., Muquit, M. M., . . . Beal, M. F. (1997). Oxidative damage and metabolic dysfunction in Huntington's disease: selective vulnerability of the basal ganglia. *Annals of neurology, 41*(5), 646-653.

Browne, S. E., Ferrante, R. J., & Beal, M. F. (1999). Oxidative stress in Huntington's disease. *Brain Pathology, 9*(1), 147-163.

Brustovetsky, N., Brustovetsky, T., Jemmerson, R., & Dubinsky, J. M. (2002). Calcium-induced cytochrome c release from CNS mitochondria is associated with the permeability transition and rupture of the outer membrane. *Journal of neurochemistry, 80*(2), 207-218.

Brustovetsky, N., Brustovetsky, T., Purl, K. J., Capano, M., Crompton, M., & Dubinsky, J. M. (2003). Increased susceptibility of striatal mitochondria to calcium-induced permeability transition. *The Journal of neuroscience, 23*(12), 4858-4867.

Buecker, C., Chen, H.-H., Polo, J. M., Daheron, L., Bu, L., Barakat, T. S., . . . Geijsen, N. (2010). A murine ESC-like state facilitates transgenesis and homologous recombination in human pluripotent stem cells. *Cell Stem Cell, 6*(6), 535-546. doi: 10.1016/j.stem.2010.05.003

Butterworth, J. (1986). Changes in nine enzyme markers for neurons, glia, and endothelial cells in agonal state and Huntington's disease caudate nucleus. *Journal of neurochemistry, 47*(2), 583-587.

Calabrese, V., Mancuso, C., Calvani, M., Rizzarelli, E., Butterfield, D. A., & Stella, A. M. G. (2007). Nitric oxide in the central nervous system: neuroprotection versus neurotoxicity. *Nature Reviews Neuroscience, 8*(10), 766-775.

Camnasio, S., Carri, A. D., Lombardo, A., Grad, I., Mariotti, C., Castucci, A., . . . Zuccato, C. (2012). The first reported generation of several induced pluripotent stem cell lines from homozygous and heterozygous Huntington's disease patients demonstrates mutation related enhanced lysosomal activity. *Neurobiology of disease, 46*(1), 41-51.

Canitano, A., Papa, M., Boscia, F., Castaldo, P., Sellitti, S., Taglialatela, M., & Annunziato, L. (2002). Brain Distribution of the Na+/Ca2+ Exchanger-Encoding Genes NCX1, NCX2, and NCX3 and Their Related Proteins in the Central Nervous System. *Annals of the New York Academy of Sciences, 976*(1), 394-404.

Canman, C. E., Lim, D.-S., Cimprich, K. A., Taya, Y., Tamai, K., Sakaguchi, K., . . . Siliciano, J. D. (1998). Activation of the ATM kinase by ionizing radiation and phosphorylation of p53. *Science, 281*(5383), 1677-1679.

Carmichael, J., Sugars, K. L., Bao, Y. P., & Rubinsztein, D. C. (2002). Glycogen synthase kinase-3β inhibitors prevent cellular polyglutamine toxicity caused by the Huntington's disease mutation. *Journal of Biological Chemistry, 277*(37), 33791-33798.

Carri, A. D., Onorati, M., Lelos, M. J., Castiglioni, V., Faedo, A., Menon, R., . . . Talpo, F. (2013). Developmentally coordinated extrinsic signals drive human pluripotent stem cell differentiation toward authentic DARPP-32+ medium-sized spiny neurons. *Development, 140*(2), 301-312.

Carter, C. (1982). Glutamine synthetase activity in Huntington's disease. *Life Sciences, 31*(11), 1151-1159.

Carvajal, L. A., & Manfredi, J. J. (2013). Another fork in the road—life or death decisions by the tumour suppressor p53. *EMBO reports, 14*(5), 414-421.

Castiglioni, V., Onorati, M., Rochon, C., & Cattaneo, E. (2012). Induced pluripotent stem cell lines from Huntington's disease mice undergo neuronal differentiation while showing alterations in the lysosomal pathway. *Neurobiology of disease, 46*(1), 30-40.

Chamberlain, S. J., Li, X.-J., & Lalande, M. (2008). Induced pluripotent stem (iPS) cells as in vitro models of human neurogenetic disorders. *Neurogenetics, 9*(4), 227-235. doi: 10.1007/s10048-008-0147-z

Chambers, S. M., Fasano, C. A., Papapetrou, E. P., Tomishima, M., Sadelain, M., & Studer, L. (2009). Highly efficient neural conversion of human ES and iPS cells by dual inhibition of SMAD signaling. *Nature biotechnology, 27*(3), 275-280.

Chan, D. W., Son, S.-C., Block, W., Ye, R., Khanna, K. K., Wold, M. S., . . . Taya, Y. (2000). Purification and Characterization of ATM from Human Placenta A MANGANESE-DEPENDENT, WORTMANNIN-SENSITIVE SERINE/THREONINE PROTEIN KINASE. *Journal of Biological Chemistry, 275*(11), 7803-7810.

Chattopadhyay, B., Baksi, K., Mukhopadhyay, S., & Bhattacharyya, N. P. (2005). Modulation of age at onset of Huntington disease patients by variations in TP53 and human caspase activated DNase (hCAD) genes. *Neuroscience letters, 374*(2), 81-86.

Chen, J., Hardy, P., Kucharczyk, W., Clauberg, M., Joshi, J., Vourlas, A., . . . Henkelman, R. (1993). MR of human postmortem brain tissue: correlative study between T2 and assays of iron and ferritin in Parkinson and Huntington disease. *American journal of neuroradiology, 14*(2), 275-281.

Chen, Y., Payne, K., Perara, V. S., Huang, S., Baba, A., Matsuda, T., & Yu, X. (2012). Inhibition of the sodium–calcium exchanger via SEA0400 altered manganese-induced T1 changes in isolated perfused rat hearts. *NMR in Biomedicine, 25*(11), 1280-1285.

Chiang, M.-C., Chen, H.-M., Lai, H.-L., Chen, H.-W., Chou, S.-Y., Chen, C.-M., . . . Chern, Y. (2009). The A2A adenosine receptor rescues the urea cycle deficiency of Huntington's disease by enhancing the activity of the ubiquitin‚Äìproteasome system. *Human molecular genetics, 18*(16), 2929-2942.

Chiang, M.-C., Chen, H.-M., Lee, Y.-H., Chang, H.-H., Wu, Y.-C., Soong, B.-W., . . . Niu, D.-M. (2007). Dysregulation of C/EBPalpha by mutant Huntingtin causes the urea cycle deficiency in Huntington's disease. *Human molecular genetics, 16*(5), 483-498.

Chinnery, P. F., Crompton, D. E., Birchall, D., Jackson, M. J., Coulthard, A., Lomb√®s, A., . . . Mottershead, J. P. (2007). Clinical features and natural history of neuroferritinopathy caused by the FTL1 460InsA mutation. *Brain, 130*(1), 110-119.

Chiosa, L., Niculescu, V., Bonciocat, C., & Stancu, C. (1965). The protective action of N-acetyl and N-carbamyl derivatives of glutamic and aspartic acids against ammonia intoxication. *Biochemical Pharmacology, 14*(11), 1635-1643.

Chmielnicki, E., Benraiss, A., Economides, A. N., & Goldman, S. A. (2004). Adenovirally expressed noggin and brain-derived neurotrophic factor cooperate to induce new medium spiny neurons from resident progenitor cells in the adult striatal ventricular zone. *Journal of Neuroscience, 24*(9), 2133-2142. doi: 10.1523/JNEUROSCI.1554-03.2004

Clegg, M. S., Donovan, S. M., Monaco, M. H., Baly, D. L., Ensunsa, J. L., & Keen, C. L. (1998). *The influence of manganese deficiency on serum IGF-1 and IGF binding proteins in the male rat.* Paper presented at the Proceedings of the Society for Experimental Biology and Medicine. Society for Experimental Biology and Medicine (New York, NY).

Clifford, J. J., Drago, J., Natoli, A. L., Wong, J. Y. F., Kinsella, A., Waddington, J. L., & Vaddadi, K. S. (2002). Essential fatty acids given from conception prevent topographies of motor deficit in a transgenic model of Huntington's disease. *Neuroscience, 109*(1), 81-88.

Colin, E., Régulier, E., Perrin, V., Dürr, A., Brice, A., Aebischer, P., . . . Saudou, F. (2005). Akt is altered in an animal model of Huntington's disease and in patients. *European Journal of Neuroscience, 21*(6), 1478-1488.

Collins, A. R. (2004). The comet assay for DNA damage and repair. *Molecular biotechnology, 26*(3), 249-261.

Colton, C., Xu, Q., Burke, J., Bae, S., Wakefield, J., Nair, A., . . . Vitek, M. (2004). Disrupted spermine homeostasis: a novel mechanism in polyglutamine-mediated aggregation and cell death. *The Journal of neuroscience, 24*(32), 7118-7127.

Consortium, H. I. (2012). Induced pluripotent stem cells from patients with Huntington's disease show CAG-repeat-expansion-associated phenotypes. *Cell Stem Cell, 11*(2), 264-278.

Cooper, A. J. (2001). Role of glutamine in cerebral nitrogen metabolism and ammonia neurotoxicity. *Mental retardation and developmental disabilities research reviews, 7*(4), 280-286.

Cordova, F. M., Aguiar Jr, A. S., Peres, T. V., Lopes, M. W., Gonçalves, F. M., Remor, A. P., . . . Prediger, R. D. (2012). In vivo manganese exposure modulates Erk, Akt and Darpp-32 in the striatum of developing rats, and impairs their motor function. *PloS one, 7*(3), e33057.

Crooks, D. R., Welch, N., & Smith, D. R. (2007). Low-level manganese exposure alters glutamate metabolism in GABAergic AF5 cells. *Neurotoxicology, 28*(3), 548-554.

Curtis, A. R., Fey, C., Morris, C. M., Bindoff, L. A., Ince, P. G., Chinnery, P. F., . . . McHale, D. P. (2001). Mutation in the gene encoding ferritin light polypeptide causes dominant adult-onset basal ganglia disease. *Nature genetics, 28*(4), 350-354.

Dally, H., & Hartwig, A. (1997). Induction and repair inhibition of oxidative DNA damage by nickel (II) and cadmium (II) in mammalian cells. *Carcinogenesis, 18*(5), 1021-1026.

Damiano, M., Galvan, L., Déglon, N., & Brouillet, E. (2010). Mitochondria in Huntington's disease. *Biochim Biophys Acta, 1802*(1), 52-61. doi: 10.1016/j.bbadis.2009.07.012

Davies, S. W., Turmaine, M., Cozens, B. A., DiFiglia, M., Sharp, A. H., Ross, C. A., . . . Bates, G. P. (1997). Formation of neuronal intranuclear inclusions underlies the neurological dysfunction in mice transgenic for the HD mutation. *cell, 90*(3), 537-548.

Davis, C. D., & Greger, J. (1992). Longitudinal changes of manganese-dependent superoxide dismutase and other indexes of manganese and iron status in women. *The American journal of clinical nutrition, 55*(3), 747-752.

Dawson, V. L., Dawson, T. M., London, E. D., Bredt, D. S., & Snyder, S. H. (1991). Nitric oxide mediates glutamate neurotoxicity in primary cortical cultures. *Proceedings of the National Academy of Sciences, 88*(14), 6368-6371.

De Luca, G., Russo, M. T., Degan, P., Tiveron, C., Zijno, A., Meccia, E., . . . Crescenzi, M. (2008). A Role for Oxidized DNA Precursors in Huntington's Disease–Like Striatal Neurodegeneration. *PLoS genetics, 4*(11), e1000266.

Deckel, A. W. (2001). Nitric oxide and nitric oxide synthase in Huntington's disease. *Journal of neuroscience research, 64*(2), 99-107.

Deckel, A. W., Tang, V., Nuttal, D., Gary, K., & Elder, R. (2002). Altered neuronal nitric oxide synthase expression contributes to disease progression in Huntington‚Äôs disease transgenic mice. *Brain research, 939*(1), 76-86.

Deng, K., He, H., Qiu, J., Lorber, B., Bryson, J. B., & Filbin, M. T. (2009). Increased synthesis of spermidine as a result of upregulation of arginase I promotes axonal regeneration in culture and in vivo. *The Journal of neuroscience, 29*(30), 9545-9552.

Dexter, D., Carayon, A., Javoy-Agid, F., Agid, Y., Wells, F., Daniel, S., . . . Marsden, C. (1991). Alterations in the levels of iron, ferritin and other trace metals in Parkinson's disease and other neurodegenerative diseases affecting the basal ganglia. *Brain, 114*(4), 1953-1975.

Dhara, S. K., & Stice, S. L. (2008). Neural differentiation of human embryonic stem cells. *J Cell Biochem, 105*(3), 633-640. doi: 10.1002/jcb.21891

Dimos, J. T., Rodolfa, K. T., Niakan, K. K., Weisenthal, L. M., Mitsumoto, H., Chung, W., . . . Eggan, K. (2008). Induced pluripotent stem cells generated from patients with ALS can be differentiated into motor neurons. *Science, 321*(5893), 1218-1221. doi: 10.1126/science.1158799

Dipaolo, R. V., Kanfer, J. N., & Newberne, P. M. (1974). Copper deficiency and the central nervous system: myelination in the rat: morphological and biochemical studies. *Journal of Neuropathology & Experimental Neurology, 33*(2), 226-236.

Dobson, A. W., Erikson, K. M., & Aschner, M. (2004). Manganese neurotoxicity. *Annals of the New York Academy of Sciences, 1012*(1), 115-128.

Drane, P., Bravard, A., Bouvard, V., & May, E. (2001). Reciprocal down-regulation of p53 and SOD2 gene expression-implication in p53 mediated apoptosis. *Oncogene, 20*(4), 430-439.

Draper, J. S., Smith, K., Gokhale, P., Moore, H. D., Maltby, E., Johnson, J., . . . Andrews, P. W. (2004). Recurrent gain of chromosomes 17q and 12 in cultured human embryonic stem cells. *Nature biotechnology, 22*(1), 53-54.

Duan, W., Guo, Z., Jiang, H., Ware, M., Li, X.-J., & Mattson, M. P. (2003). Dietary restriction normalizes glucose metabolism and BDNF levels, slows disease progression, and increases survival in huntingtin mutant mice. *Proceedings of the National Academy of Sciences, 100*(5), 2911-2916.

Duan, W., Lee, J., Guo, Z., & Mattson, M. P. (2001). Dietary restriction stimulates BDNF production in the brain and thereby protects neurons against excitotoxic injury. *J Mol Neurosci, 16*(1), 1-12. doi: 10.1385/JMN:16:1:1

Dupont, C., & Tanaka, Y. (1985). Blood manganese levels in children with convulsive disorder. *Biochemical medicine, 33*(2), 246-255.

Durante, W., Johnson, F. K., & Johnson, R. A. (2007). Arginase: a critical regulator of nitric oxide synthesis and vascular function. *Clinical and Experimental Pharmacology and Physiology, 34*(9), 906-911.

Duyao, M. P., Auerbach, A. B., Ryan, A., Persichetti, F., Barnes, G. T., McNeil, S. M., . . . Joyner, A. L. (1995). Inactivation of the mouse Huntington's disease gene homolog Hdh. *Science, 269*(5222), 407-410.

Ebert, A. D., Yu, J., Rose, F. F., Mattis, V. B., Lorson, C. L., Thomson, J. A., & Svendsen, C. N. (2009). Induced pluripotent stem cells from a spinal muscular atrophy patient. *Nature, 457*(7227), 277-280. doi: 10.1038/nature07677

Ehrnhoefer, D. E., Skotte, N. H., Ladha, S., Nguyen, Y. T., Qiu, X., Deng, Y., . . . Becanovic, K. (2014). p53 increases caspase-6 expression and activation in muscle tissue expressing mutant huntingtin. *Human molecular genetics, 23*(3), 717-729.

Eid, T., Ghosh, A., Wang, Y., Beckstr√∂m, H., Zaveri, H. P., Lee, T.-S. W., . . . de Lanerolle, N. C. (2008). Recurrent seizures and brain pathology after inhibition of glutamine synthetase in the hippocampus in rats. *Brain, 131*(8), 2061-2070.

Eid, T., Thomas, M., Spencer, D., Runden-Pran, E., Lai, J., Malthankar, G., . . . De Lanerolle, N. (2004). Loss of glutamine synthetase in the human epileptogenic hippocampus: possible mechanism for raised extracellular glutamate in mesial temporal lobe epilepsy. *The Lancet, 363*(9402), 28-37.

Enokido, Y., Tamura, T., Ito, H., Arumughan, A., Komuro, A., Shiwaku, H., . . . Ishiguro, H. (2010). Mutant huntingtin impairs Ku70-mediated DNA repair. *The Journal of cell biology, 189*(3), 425-443.

Ensunsa, J. L., Symons, J. D., Lanoue, L., Schrader, H. R., & Keen, C. L. (2004). Reducing arginase activity via dietary manganese deficiency enhances endothelium-dependent vasorelaxation of rat aorta. *Experimental Biology and Medicine, 229*(11), 1143-1153.

Erikson, K. M., & Aschner, M. (2003). Manganese neurotoxicity and glutamate-GABA interaction. *Neurochemistry international, 43*(4), 475-480.

Erikson, K. M., Syversen, T., Steinnes, E., & Aschner, M. (2004). Globus pallidus: a target brain region for divalent metal accumulation associated with dietary iron deficiency. *The Journal of nutritional biochemistry, 15*(6), 335-341.

Erway, L., Hurley, L. S., & Fraser, A. S. (1970). Congenital ataxia and otolith defects due to manganese deficiency in mice. *J. Nutr, 100*(6), 643-654.

Estevez, A. G., Sahawneh, M. A., Lange, P. S., Bae, N., Egea, M., & Ratan, R. R. (2006). Arginase 1 regulation of nitric oxide production is key to survival of trophic factor-deprived motor neurons. *The Journal of neuroscience, 26*(33), 8512-8516.

Fan, J., Gladding, C. M., Wang, L., Zhang, L. Y., Kaufman, A. M., Milnerwood, A. J., & Raymond, L. A. (2012). P38 MAPK is involved in enhanced NMDA receptor-dependent excitotoxicity in YAC transgenic mouse model of Huntington disease. *Neurobiology of disease, 45*(3), 999-1009.

Farrer, L. A. (1985). Diabetes mellitus in Huntington disease. *Clinical genetics, 27*(1), 62-67.

Feng, Z., Hu, W., De Stanchina, E., Teresky, A. K., Jin, S., Lowe, S., & Levine, A. J. (2007). The regulation of AMPKalpha, TSC2, and PTEN expression by p53: stress, cell and tissue specificity, and the role of these gene products in modulating the IGF-1-AKT-mTOR pathways. *Cancer research, 67*(7), 3043-3053.

Feng, Z., & Levine, A. J. (2010). The regulation of energy metabolism and the IGF-1/mTOR pathways by the p53 protein. *Trends in cell biology, 20*(7), 427-434.

Ferlazzo, M. L., Sonzogni, L., Granzotto, A., Bodgi, L., Lartin, O., Devic, C., . . . Foray, N. (2013). Mutations of the Huntington's Disease Protein Impact on the ATM-Dependent Signaling and Repair Pathways of the Radiation-Induced DNA Double-Strand Breaks: Corrective Effect of Statins and Bisphosphonates. *Molecular neurobiology*, 1-12.

Fernandes, H. B., Baimbridge, K. G., Church, J., Hayden, M. R., & Raymond, L. A. (2007). Mitochondrial sensitivity and altered calcium handling underlie enhanced NMDA-induced apoptosis in YAC128 model of Huntington's disease. *The Journal of neuroscience, 27*(50), 13614-13623.

Ferrante, R. J., Andreassen, O. A., Jenkins, B. G., Dedeoglu, A., Kuemmerle, S., Kubilus, J. K., . . . Beal, M. F. (2000). Neuroprotective effects of creatine in a transgenic mouse model of Huntington's disease. *The Journal of neuroscience, 20*(12), 4389-4397.

Filipov, N. M., & Dodd, C. A. (2012). Role of glial cells in manganese neurotoxicity. *Journal of Applied Toxicology, 32*(5), 310-317.

Fitsanakis, V. A., Au, C., Erikson, K. M., & Aschner, M. (2006). The effects of manganese on glutamate, dopamine and gamma-aminobutyric acid regulation. *Neurochemistry international, 48*(6), 426-433.

Folstein, S. E. (1989). *Huntington's disease: a disorder of families*: Johns Hopkins University Press.

Formisano, L., Guida, N., Valsecchi, V., Pignataro, G., Vinciguerra, A., Pannaccione, A., . . . Sisalli, M. J. (2013). NCX1 is a new rest target gene: Role in cerebral ischemia. *Neurobiology of disease, 50*, 76-85.

Fossale, E., Seong, I. S., Coser, K. R., Shioda, T., Kohane, I. S., Wheeler, V. C., . . . Lee, J.-M. (2011). Differential effects of the Huntington's disease CAG mutation in striatum and cerebellum are quantitative not qualitative. *Human molecular genetics, 20*(21), 4258-4267. doi: 10.1093/hmg/ddr355

Fox, J. H., Kama, J. A., Lieberman, G., Chopra, R., Dorsey, K., Chopra, V., . . . Hersch, S. (2007). Mechanisms of copper ion mediated Huntington's disease progression. *PloS one, 2*(3), e334.

Frank, E. G., & Woodgate, R. (2007). Increased catalytic activity and altered fidelity of human DNA polymerase ι in the presence of manganese. *Journal of Biological Chemistry, 282*(34), 24689-24696.

Friedman, J. H., Trieschmann, M. E., Myers, R. H., & Fernandez, H. H. (2005). Monozygotic twins discordant for Huntington disease after 7 years. *Archives of neurology, 62*(6), 995.

Gaeta, A., & Hider, R. C. (2005). The crucial role of metal ions in neurodegeneration: the basis for a promising therapeutic strategy. *British journal of pharmacology, 146*(8), 1041-1059.

Gambardella, A., Muglia, M., Labate, A., Magariello, A., Gabriele, A., Mazzei, R., . . . Valentino, P. (2001). Juvenile Huntington‚Äôs disease presenting as progressive myoclonic epilepsy. *Neurology, 57*(4), 708-711.

Ganem, N. J., Godinho, S. A., & Pellman, D. (2009). A mechanism linking extra centrosomes to chromosomal instability. *Nature, 460*(7252), 278-282.

Gaspard, N., Bouschet, T., Hourez, R., Dimidschstein, J., Naeije, G., van den Ameele, J., . . . Vanderhaeghen, P. (2008). An intrinsic mechanism of corticogenesis from embryonic stem cells. *Nature, 455*(7211), 351-357. doi: 10.1038/nature07287

Gavin, C., Gunter, K., & Gunter, T. (1998). Manganese and calcium transport in mitochondria: implications for manganese toxicity. *Neurotoxicology, 20*(2-3), 445-453.

Georgiou, N., Bradshaw, J. L., Chiu, E., Tudor, A., O'Gorman, L., & Phillips, J. G. (1999). Differential clinical and motor control function in a pair of monozygotic twins with Huntington's disease. *Movement disorders, 14*(2), 320-325.

Gines, S., Seong, I. S., Fossale, E., Ivanova, E., Trettel, F., Gusella, J. F., . . . MacDonald, M. E. (2003). Specific progressive cAMP reduction implicates energy deficit in presymptomatic Huntington's disease knock-in mice. *Human molecular genetics, 12*(5), 497-508.

Glass, M., Van Dellen, A., Blakemore, C., Hannan, A., & Faull, R. (2004). Delayed onset of huntington′ s disease in mice in an enriched environment correlates with delayed loss of cannabinoid CB1 receptors. *Neuroscience, 123*(1), 207-212.

Godin, J. D., Colombo, K., Molina-Calavita, M., Keryer, G., Zala, D., Charrin, B. C., . . . Dragatsis, I. (2010). Huntingtin is required for mitotic spindle orientation and mammalian neurogenesis. *Neuron, 67*(3), 392-406.

Gomez-Esteban, J., Lezcano, E., Zarranz, J., Velasco, F., Garamendi, I., Perez, T., & Tijero, B. (2006). Monozygotic twins suffering from Huntington‚Äôs disease show different cognitive and behavioural symptoms. *European Neurology, 57*(1), 26-30.

Gottlieb, T. M., Leal, J., Seger, R., Taya, Y., & Oren, M. (2002). Cross-talk between Akt, p53 and Mdm2: possible implications for the regulation of apoptosis. *Oncogene, 21*(8), 1299-1303.

Grison, A., Mantovani, F., Comel, A., Agostoni, E., Gustincich, S., Persichetti, F., & Del Sal, G. (2011). Ser46 phosphorylation and prolyl-isomerase Pin1-mediated isomerization of p53 are key events in p53-dependent apoptosis induced by mutant huntingtin. *Proceedings of the National Academy of Sciences, 108*(44), 17979-17984.

Gruber, B., Kłaczkow, G., Jaworska, M., Krzysztoń-Russjan, J., Anuszewska, E., Zielonka, D., . . . Marcinkowski, J. (2013). Huntington's disease - imbalance of amino acid levels in plasma of patients and mutation carriers. *Annals of agricultural and environmental medicine: AAEM, 20*(4), 779.

Guilarte, T. R., Burton, N. C., Verina, T., Prabhu, V. V., Becker, K. G., Syversen, T., & Schneider, J. S. (2008). Increased APLP1 expression and neurodegeneration in the frontal cortex of manganese‚Äêexposed non‚Äêhuman primates. *Journal of neurochemistry, 105*(5), 1948-1959.

Guilarte, T. R., & Chen, M.-K. (2007). Manganese inhibits NMDA receptor channel function: implications to psychiatric and cognitive effects. *Neurotoxicology, 28*(6), 1147-1152.

Guillemot, F. (2005). Cellular and molecular control of neurogenesis in the mammalian telencephalon. *Curr Opin Cell Biol, 17*(6), 639-647. doi: 10.1016/j.ceb.2005.09.006

Guo, X., Disatnik, M.-H., Monbureau, M., Shamloo, M., Mochly-Rosen, D., & Qi, X. (2013). Inhibition of mitochondrial fragmentation diminishes Huntington’s disease–associated neurodegeneration. *The Journal of clinical investigation, 123*(12), 5371.

Guo, Z., Kozlov, S., Lavin, M. F., Person, M. D., & Paull, T. T. (2010). ATM activation by oxidative stress. *Science, 330*(6003), 517-521.

Gutekunst, C.-A., Norflus, F., & Hersch, S. M. (2002). The neuropathology of Huntington's disease. *Oxford Monographs on Medical Genetics, 45*, 251-275.

Ha, H. C., Sirisoma, N. S., Kuppusamy, P., Zweier, J. L., Woster, P. M., & Casero, R. A. (1998). The natural polyamine spermine functions directly as a free radical scavenger. *Proceedings of the National Academy of Sciences, 95*(19), 11140-11145.

Häberle, J., Görg, B., Rutsch, F., Schmidt, E., Toutain, A., Benoist, J.-F. ß., . . . Schliess, F. (2005). Congenital glutamine deficiency with glutamine synthetase mutations. *New England Journal of Medicine, 353*(18), 1926-1933.

Hands, S. L., Mason, R., Umar Sajjad, M., Giorgini, F., & Wyttenbach, A. (2010). Metallothioneins and copper metabolism are candidate therapeutic targets in Huntington‚Äôs disease. *Biochemical Society Transactions, 38*, 552-558.

Harms, L., Meierkord, H., Timm, G., Pfeiffer, L., & Ludolph, A. (1997). Decreased N-acetyl-aspartate/choline ratio and increased lactate in the frontal lobe of patients with Huntington's disease: a proton magnetic resonance spectroscopy study. *Journal of Neurology, Neurosurgery & Psychiatry, 62*(1), 27-30.

Hassanein, M., Ghaleb, H., Haroun, E., Hegazy, M., & Khayyal, M. (1966). Chronic manganism: preliminary observations on glucose tolerance and serum proteins. *British journal of industrial medicine, 23*(1), 67-70.

Hays, H., & Berdis, A. J. (2002). Manganese substantially alters the dynamics of translesion DNA synthesis. *Biochemistry, 41*(15), 4771-4778.

Hébert, J. M., & Fishell, G. (2008). The genetics of early telencephalon patterning: some assembly required. *Nat Rev Neurosci, 9*(9), 678-685. doi: 10.1038/nrn2463

Helton, E. S., & Chen, X. (2007). p53 modulation of the DNA damage response. *Journal of cellular biochemistry, 100*(4), 883-896.

Hickson, I., Zhao, Y., Richardson, C. J., Green, S. J., Martin, N. M., Orr, A. I., . . . Smith, G. C. (2004). Identification and characterization of a novel and specific inhibitor of the ataxia-telangiectasia mutated kinase ATM. *Cancer research, 64*(24), 9152-9159.

Hiney, J. K., Srivastava, V. K., & Les Dees, W. (2011). Manganese induces IGF-1 and cyclooxygenase-2 gene expressions in the basal hypothalamus during prepubertal female development. *Toxicological Sciences, 121*(2), 389-396.

Hockly, E., Cordery, P. M., Woodman, B., Mahal, A., Van Dellen, A., Blakemore, C., . . . Bates, G. P. (2002). Environmental enrichment slows disease progression in R6/2 Huntington's disease mice. *Annals of neurology, 51*(2), 235-242.

Hodges, A., Strand, A. D., Aragaki, A. K., Kuhn, A., Sengstag, T., Hughes, G., . . . Thu, D. (2006). Regional and cellular gene expression changes in human Huntington's disease brain. *Human molecular genetics, 15*(6), 965-977.

Holubcová, Z., Matula, P., Sedláčková, M., Vinarský, V., Doležalová, D., Bárta, T., . . . Hampl, A. (2011). Human embryonic stem cells suffer from centrosomal amplification. *Stem Cells, 29*(1), 46-56.

Hong, H., Takahashi, K., Ichisaka, T., Aoi, T., Kanagawa, O., Nakagawa, M., . . . Yamanaka, S. (2009). Suppression of induced pluripotent stem cell generation by the p53–p21 pathway. *Nature, 460*(7259), 1132-1135.

Hopfner, K.-P., Karcher, A., Craig, L., Woo, T. T., Carney, J. P., & Tainer, J. A. (2001). Structural biochemistry and interaction architecture of the DNA double-strand break repair Mre11 nuclease and Rad50-ATPase. *Cell, 105*(4), 473-485.

Hou, Z., Zhang, Y., Propson, N. E., Howden, S. E., Chu, L.-F., Sontheimer, E. J., & Thomson, J. A. (2013). Efficient genome engineering in human pluripotent stem cells using Cas9 from Neisseria meningitidis. *Proceedings of the National Academy of Sciences, 110*(39), 15644-15649.

Hu, B.-Y., Weick, J. P., Yu, J., Ma, L.-X., Zhang, X.-Q., Thomson, J. A., & Zhang, S.-C. (2010). Neural differentiation of human induced pluripotent stem cells follows developmental principles but with variable potency. *Proc Natl Acad Sci USA, 107*(9), 4335-4340. doi: 10.1073/pnas.0910012107

Hu, W., Zhang, C., Wu, R., Sun, Y., Levine, A., & Feng, Z. (2010). Glutaminase 2, a novel p53 target gene regulating energy metabolism and antioxidant function. *Proceedings of the National Academy of Sciences, 107*(16), 7455-7460.

Huang, L.-s., Sun, G., Cobessi, D., Wang, A. C., Shen, J. T., Tung, E. Y., . . . Berry, E. A. (2006). 3-nitropropionic acid is a suicide inhibitor of mitochondrial respiration that, upon oxidation by complex II, forms a covalent adduct with a catalytic base arginine in the active site of the enzyme. *Journal of Biological Chemistry, 281*(9), 5965-5972.

Humbert, S., Bryson, E. A., Cordelières, F. P., Connors, N. C., Datta, S. R., Finkbeiner, S., . . . Saudou, F. (2002a). The IGF-1/Akt pathway is neuroprotective in Huntington's disease and involves Huntingtin phosphorylation by Akt. *Developmental cell, 2*(6), 831-837.

Humbert, S., Bryson, E. A., Cordelières, F. P., Connors, N. C., Datta, S. R., Finkbeiner, S., . . . Saudou, F. d. r. (2002b). The IGF-1/Akt pathway is neuroprotective in Huntington's disease and involves Huntingtin phosphorylation by Akt. *Developmental cell, 2*(6), 831-837.

Huntington, G. (2003). On chorea. George Huntington, M.D. *J Neuropsychiatry Clin Neurosci, 15*(1), 109-112.

Hurlbert, M. S., Zhou, W., Wasmeier, C., Kaddis, F., Hutton, J., & Freed, C. (1999). Mice transgenic for an expanded CAG repeat in the Huntington's disease gene develop diabetes. *Diabetes, 48*(3), 649-651.

Hurley, L. S., Theriault, L. L., & Dreosti, I. E. (1970). Liver mitochondria from manganese-deficient and pallid mice: function and ultrastructure. *Science, 170*(3964), 1316-1318.

Hurley, L. S., Woolley, D. E., Rosenthal, F., & Timiras, P. S. (1963). Influence of manganese on susceptibility of rats to convulsions. *American Journal of Physiology--Legacy Content, 204*(3), 493-496.

Illuzzi, J., Yerkes, S., Parekh-Olmedo, H., & Kmiec, E. B. (2009). DNA breakage and induction of DNA damage response proteins precede the appearance of visible mutant huntingtin aggregates. *Journal of neuroscience research, 87*(3), 733-747.

Illuzzi, J. L., Vickers, C. A., & Kmiec, E. B. (2011). Modifications of p53 and the DNA damage response in cells expressing mutant form of the protein huntingtin. *Journal of Molecular Neuroscience, 45*(2), 256-268.

Iwamoto, T., & Shigekawa, M. (1998). Differential inhibition of Na+/Ca2+ exchanger isoforms by divalent cations and isothiourea derivative. *American Journal of Physiology-Cell Physiology, 275*(2), C423-C430.

Jain, M., Armstrong, R. J., Barker, R. A., & Rosser, A. E. (2001). Cellular and molecular aspects of striatal development. *Brain Res Bull, 55*(4), 533-540.

Jenkins, B. G., Koroshetz, W. J., Beal, M. F., & Rosen, B. R. (1993). Evidence for irnnairment of energy metabofism in vivo in Huntington's disease using localized 1H NMR spectroscopy. *Neurology, 43*(12), 2689-2689.

Jeon, I., Lee, N., Li, J. Ä., Park, I. Ä., Park, K. S., Moon, J., . . . Kwon, J. (2012). Neuronal Properties, In Vivo Effects, and Pathology of a Huntington's Disease Patient-Derived Induced Pluripotent Stem Cells. *Stem Cells, 30*(9), 2054-2062.

Jia, F., Wilson, K. D., Sun, N., Gupta, D. M., Huang, M., Li, Z., . . . Wu, J. C. (2010). A nonviral minicircle vector for deriving human iPS cells. *Nat Meth, 7*(3), 197-199. doi: 10.1038/nmeth.1426

Jomova, K., Vondrakova, D., Lawson, M., & Valko, M. (2010). Metals, oxidative stress and neurodegenerative disorders. *Molecular and cellular biochemistry, 345*(1-2), 91-104.

Jones, R. G., Plas, D. R., Kubek, S., Buzzai, M., Mu, J., Xu, Y., . . . Thompson, C. B. (2005). AMP-activated protein kinase induces a p53-dependent metabolic checkpoint. *Molecular cell, 18*(3), 283-293.

Josefsen, K., Nielsen, S., Campos, A., Seifert, T., Hasholt, L., Nielsen, J. r. E., . . . Quistorff, B. r. (2010). Reduced gluconeogenesis and lactate clearance in Huntington's disease. *Neurobiology of disease, 40*(3), 656-662.

Ju, T.-C., Chen, H.-M., Lin, J.-T., Chang, C.-P., Chang, W.-C., Kang, J.-J., . . . Chang, C. (2011). Nuclear translocation of AMPK-α1 potentiates striatal neurodegeneration in Huntington's disease. *The Journal of cell biology, 194*(2), 209-227.

Jung-Il, C., Dong-Wook, K., Nayeon, L., Young-Joo, J., Iksoo, J., Jihye, K., . . . Kang, S. S. (2012). Quantitative proteomic analysis of induced pluripotent stem cells derived from a human Huntington's disease patient. *Biochemical Journal, 446*(3), 359-371.

Juopperi, T. A., Kim, W. R., Chiang, C.-H., Yu, H., Margolis, R. L., Ross, C. A., . . . Song, H. (2012). Astrocytes generated from patient induced pluripotent stem cells recapitulate features of Huntington,Äôs disease patient cells. *Mol Brain, 5*(1), 17.

Kalia, K., Jiang, W., & Zheng, W. (2008). Manganese accumulates primarily in nuclei of cultured brain cells. *Neurotoxicology, 29*(3), 466-470.

Kanyo, Z. F., Scolnick, L. R., Ash, D. E., & Christianson, D. W. (1996). Structure of a unique binuclear manganese cluster in arginase.

Keen, C. L., Ensunsa, J. L., & Clegg, M. S. (2000). Manganese metabolism in animals and humans including the toxicity of manganese. *Met Ions Biol Syst, 37*(2), 89-121.

Keen, C. L., Uriu-Hare, J. Y., Hawk, S. N., Jankowski, M. A., Daston, G. P., Kwik-Uribe, C. L., & Rucker, R. B. (1998). Effect of copper deficiency on prenatal development and pregnancy outcome. *The American journal of clinical nutrition, 67*(5), 1003S-1011S.

Kenney, C., Powell, S., & Jankovic, J. (2007). Autopsy-proven Huntington's disease with 29 trinucleotide repeats. *Mov Disord, 22*(1), 127-130. doi: 10.1002/mds.21195

Keryer, G., Pineda, J. R., Liot, G., Kim, J., Dietrich, P., Benstaali, C., . . . Ferrante, R. J. (2011). Ciliogenesis is regulated by a huntingtin-HAP1-PCM1 pathway and is altered in Huntington disease. *The Journal of clinical investigation, 121*(11), 4372.

Kim, D.-S., Lee, J. S., Leem, J. W., Huh, Y. J., Kim, J. Y., Kim, H.-S., . . . Kim, D.-W. (2010). Robust Enhancement of Neural Differentiation from Human ES and iPS Cells Regardless of their Innate Difference in Differentiation Propensity. *Stem cell reviews*. doi: 10.1007/s12015-010-9138-1

Koretsky, A. P., & Silva, A. C. (2004). Manganese-enhanced magnetic resonance imaging (MEMRI). *NMR in Biomedicine, 17*(8), 527-531.

Ku, S., Soragni, E., Campau, E., Thomas, E. A., Altun, G., Laurent, L. C., . . . Gottesfeld, J. M. (2010). Friedreich's ataxia induced pluripotent stem cells model intergenerational GAA· TTC triplet repeat instability. *Cell Stem Cell, 7*(5), 631-637.

Kumar, K. K., Aboud, A. A., Patel, D. K., Aschner, M., & Bowman, A. B. (2013). Optimization of Fluorescence Assay of Cellular Manganese Status for High Throughput Screening. *Journal of biochemical and molecular toxicology, 27*(1), 42-49.

Kumar, P., Kalonia, H., & Kumar, A. (2010). Huntington's disease: pathogenesis to animal models. *Pharmacol Rep, 62*(1), 1-14.

Kwakye, G. F., Li, D., & Bowman, A. B. (2011). Novel high-throughput assay to assess cellular manganese levels in a striatal cell line model of Huntington's disease confirms a deficit in manganese accumulation. *Neurotoxicology, 32*(5), 630-639.

Kwakye, G. F., Li, D., Kabobel, O. A., & Bowman, A. B. (2011). Cellular fura-2 Manganese Extraction Assay (CFMEA). *Current Protocols in Toxicology*, 12.18. 11-12.18. 20.

Laeng, P., Pitts, R. L., Lemire, A. L., Drabik, C. E., Weiner, A., Tang, H., . . . Altar, C. A. (2004). The mood stabilizer valproic acid stimulates GABA neurogenesis from rat forebrain stem cells. *J Neurochem, 91*(1), 238-251. doi: 10.1111/j.1471-4159.2004.02725.x

Langbehn, D., Brinkman, R., Falush, D., Paulsen, J., & Hayden, M. (2004). A new model for prediction of the age of onset and penetrance for Huntington's disease based on CAG length. *Clinical genetics, 65*(4), 267-277.

Larsen, N. A., Pakkenberg, H., Damsgaard, E., & Heydorn, K. (1979). Topographical distribution of arsenic, manganese, and selenium in the normal human brain. *Journal of the neurological sciences, 42*(3), 407-416.

Lee, G., Papapetrou, E. P., Kim, H., Chambers, S. M., Tomishima, M. J., Fasano, C. A., . . . Studer, L. (2009). Modelling pathogenesis and treatment of familial dysautonomia using patient-specific iPSCs. *Nature, 461*(7262), 402-406. doi: 10.1038/nature08320

Lee, J.-M., Ivanova, E. V., Seong, I. S., Cashorali, T., Kohane, I., Gusella, J. F., & MacDonald, M. E. (2007). Unbiased gene expression analysis implicates the huntingtin polyglutamine tract in extra-mitochondrial energy metabolism. *PLoS genetics, 3*(8), e135.

Levi, S., Cozzi, A., & Arosio, P. (2005). Neuroferritinopathy: a neurodegenerative disorder associated with L-ferritin mutation. *Best Practice & Research Clinical Haematology, 18*(2), 265-276.

Levine, A. J., Feng, Z., Mak, T. W., You, H., & Jin, S. (2006). Coordination and communication between the p53 and IGF-1,ÄìAKT,ÄìTOR signal transduction pathways. *Genes & development, 20*(3), 267-275.

Li, D. W., Liu, J., Schmid, P., Schlosser, R., Feng, H., Liu, W., . . . Deng, M. (2006). Protein serine/threonine phosphatase-1 dephosphorylates p53 at Ser-15 and Ser-37 to modulate its transcriptional and apoptotic activities. *Oncogene, 25*(21), 3006-3022.

Li, X.-J., Zhang, X., Johnson, M. A., Wang, Z.-B., Lavaute, T., & Zhang, S.-C. (2009). Coordination of sonic hedgehog and Wnt signaling determines ventral and dorsal telencephalic neuron types from human embryonic stem cells. *Development, 136*(23), 4055-4063. doi: 10.1242/dev.036624

Lievens, J.-C., Woodman, B., Mahal, A., Spasic-Boscovic, O., Samuel, D., Kerkerian-Le Goff, L., & Bates, G. (2001). Impaired glutamate uptake in the R6 Huntington's disease transgenic mice. *Neurobiology of disease, 8*(5), 807-821.

Limbo, O., Moiani, D., Kertokalio, A., Wyman, C., Tainer, J. A., & Russell, P. (2012). Mre11 ATLD17/18 mutation retains Tel1/ATM activity but blocks DNA double-strand break repair. *Nucleic acids research, 40*(22), 11435-11449.

Lin, T., Ambasudhan, R., Yuan, X., Li, W., Hilcove, S., Abujarour, R., . . . Ding, S. (2009). A chemical platform for improved induction of human iPSCs. *Nat Meth, 6*(11), 805-808. doi: 10.1038/nmeth.1393

López-Bendito, G., Cautinat, A., Sánchez, J. A., Bielle, F., Flames, N., Garratt, A. N., . . . Marín, O. (2006). Tangential neuronal migration controls axon guidance: a role for neuregulin-1 in thalamocortical axon navigation. *Cell, 125*(1), 127-142.

Lumsden, A. L., Henshall, T. L., Dayan, S., Lardelli, M. T., & Richards, R. I. (2007). Huntingtin-deficient zebrafish exhibit defects in iron utilization and development. *Human molecular genetics, 16*(16), 1905-1920.

Lupo, G., Harris, W. A., & Lewis, K. E. (2006). Mechanisms of ventral patterning in the vertebrate nervous system. *Nat Rev Neurosci, 7*(2), 103-114. doi: 10.1038/nrn1843

Ma, L., Hu, B., Liu, Y., Vermilyea, S. C., Liu, H., Gao, L., . . . Zhang, S.-C. (2012). Human embryonic stem cell-derived GABA neurons correct locomotion deficits in quinolinic acid-lesioned mice. *Cell Stem Cell, 10*(4), 455-464.

MacDonald, M. E., Ambrose, C. M., Duyao, M. P., Myers, R. H., Lin, C., Srinidhi, L., . . . Groot, N. (1993). A novel gene containing a trinucleotide repeat that is expanded and unstable on Huntington's disease chromosomes. *cell, 72*(6), 971-983.

Madison, J. L., Wegrzynowicz, M., Aschner, M., & Bowman, A. B. (2012). Disease-toxicant interactions in manganese exposed Huntington disease mice: early changes in striatal neuron morphology and dopamine metabolism. *PloS one, 7*(2), e31024.

Maglione, V., Marchi, P., Di Pardo, A., Lingrell, S., Horkey, M., Tidmarsh, E., & Sipione, S. (2010). Impaired ganglioside metabolism in Huntington's disease and neuroprotective role of GM1. *The Journal of neuroscience, 30*(11), 4072-4080.

Mangiarini, L., Sathasivam, K., Seller, M., Cozens, B., Harper, A., Hetherington, C., . . . Davies, S. W. (1996). Exon 1 of the *HD* Gene with an Expanded CAG Repeat Is Sufficient to Cause a Progressive Neurological Phenotype in Transgenic Mice. *Cell, 87*(3), 493-506.

Manley, K., Shirley, T. L., Flaherty, L., & Messer, A. (1999). Msh2 deficiency prevents in vivo somatic instability of the CAG repeat in Huntington disease transgenic mice. *Nature genetics, 23*(4), 471-473.

Marión, R. M., Strati, K., Li, H., Murga, M., Blanco, R., Ortega, S., . . . Blasco, M. A. (2009). A p53-mediated DNA damage response limits reprogramming to ensure iPS cell genomic integrity. *Nature, 460*(7259), 1149-1153.

Marklund, M., Sjödal, M., Beehler, B. C., Jessell, T. M., Edlund, T., & Gunhaga, L. (2004). Retinoic acid signalling specifies intermediate character in the developing telencephalon. *Development, 131*(17), 4323-4332. doi: 10.1242/dev.01308

Martinez-Vicente, M., Talloczy, Z., Wong, E., Tang, G., Koga, H., Kaushik, S., . . . Sulzer, D. (2010). Cargo recognition failure is responsible for inefficient autophagy in Huntington's disease. *Nature neuroscience, 13*(5), 567-576.

Matsuda, T., Takuma, K., & Baba, A. (1997). Na (+)-Ca2+ exchanger: physiology and pharmacology. *Japanese journal of pharmacology, 74*(1), 1-20.

Matsuoka, M., & Igisu, H. (2001). Cadmium induces phosphorylation of p53 at serine 15 in MCF-7 cells. *Biochemical and Biophysical Research Communications, 282*(5), 1120-1125.

Mayshar, Y., Ben-David, U., Lavon, N., Biancotti, J.-C., Yakir, B., Clark, A. T., . . . Benvenisty, N. (2010). Identification and classification of chromosomal aberrations in human induced pluripotent stem cells. *Cell stem cell, 7*(4), 521-531.

Mazziotta, J. C., Phelps, M. E., Pahl, J. J., Huang, S.-C., Baxter, L. R., Riege, W. H., . . . Wapenski, J. A. (1987). Reduced cerebral glucose metabolism in asymptomatic subjects at risk for Huntington's disease. *New England Journal of Medicine, 316*(7), 357-362.

McCulloch, S. D., & Kunkel, T. A. (2008). The fidelity of DNA synthesis by eukaryotic replicative and translesion synthesis polymerases. *Cell research, 18*(1), 148-161.

Meplan, C., Richard, M.-J., & Hainaut, P. (2000). Metalloregulation of the tumor suppressor protein p53: zinc mediates the renaturation of p53 after exposure to metal chelators in vitro and in intact cells. *Oncogene, 19*(46), 5227-5236.

Mihara, M., Erster, S., Zaika, A., Petrenko, O., Chittenden, T., Pancoska, P., & Moll, U. M. (2003). p53 has a direct apoptogenic role at the mitochondria. *Molecular cell, 11*(3), 577-590.

Mirzoeva, O. K., & Petrini, J. H. (2001). DNA damage-dependent nuclear dynamics of the Mre11 complex. *Molecular and cellular biology, 21*(1), 281-288.

Mochel, F., DeLonlay, P., Touati, G., Brunengraber, H., Kinman, R. P., Rabier, D., . . . Saudubray, J.-M. (2005). Pyruvate carboxylase deficiency: clinical and biochemical response to anaplerotic diet therapy. *Molecular genetics and metabolism, 84*(4), 305-312.

Mochel, F., Durant, B., Meng, X., O'Callaghan, J., Yu, H., Brouillet, E., . . . Durr, A. (2012). Early alterations of brain cellular energy homeostasis in Huntington disease models. *Journal of Biological Chemistry, 287*(2), 1361-1370.

Molero, A. E., Gokhan, S., Gonzalez, S., Feig, J. L., Alexandre, L. C., & Mehler, M. F. (2009). Impairment of developmental stem cell-mediated striatal neurogenesis and pluripotency genes in a knock-in model of Huntington's disease. *Proceedings of the National Academy of Sciences, 106*(51), 21900-21905.

Molina-Holgado, F., Hider, R. C., Gaeta, A., Williams, R., & Francis, P. (2007). Metals ions and neurodegeneration. *Biometals, 20*(3-4), 639-654.

Morello, M., Canini, A., Mattioli, P., Sorge, R., Alimonti, A., Bocca, B., . . . Sancesario, G. (2008). Sub-cellular localization of manganese in the basal ganglia of normal and manganese-treated rats: an electron spectroscopy imaging and electron energy-loss spectroscopy study. *Neurotoxicology, 29*(1), 60-72.

Moshell, A., Barrett, S., Tarone, R., & Robbins, J. (1980). Radiosensitivity in Huntington's disease: implications for pathogenesis and presymptomatic diagnosis. *The Lancet, 315*(8158), 9-11.

Müller, F.-J., Schuldt, B. M., Williams, R., Mason, D., Altun, G., Papapetrou, E. P., . . . Schmidt, N. O. (2011). A bioinformatic assay for pluripotency in human cells. *Nature methods, 8*(4), 315-317.

Muñoz-Sanjuán, I., & Brivanlou, A. H. (2002). Neural induction, the default model and embryonic stem cells. *Nat Rev Neurosci, 3*(4), 271-280. doi: 10.1038/nrn786

Nagata, E., Sawa, A., Ross, C. A., & Snyder, S. H. (2004). Autophagosome-like vacuole formation in Huntington's disease lymphoblasts. *Neuroreport, 15*(8), 1325-1328.

Nance, M. A., & Myers, R. H. (2001). Juvenile onset Huntington's disease --clinical and research perspectives. *Mental retardation and developmental disabilities research reviews, 7*(3), 153-157.

Nasir, J., Floresco, S. B., O'Kusky, J. R., Diewert, V. M., Richman, J. M., Zeisler, J., . . . Hayden, M. R. (1995). Targeted disruption of the Huntington's disease gene results in embryonic lethality and behavioral and morphological changes in heterozygotes. *cell, 81*(5), 811-823.

Neely, M. D., Litt, M. J., Tidball, A. M., Li, G. G., Aboud, A. A., Hopkins, C. R., . . . Bowman, A. B. (2012). DMH1, a highly selective small molecule BMP inhibitor promotes neurogenesis of hiPSCs: comparison of PAX6 and Sox1 expression during neural induction. *ACS chemical neuroscience, 3*(6), 482-491.

Neely, M. D., Tidball, A. M., Aboud, A. A., Ess, K. C., & Bowman, A. B. (2011). Induced Pluripotent Stem Cells (iPSCs): an emerging model system for the study of human neurotoxicology *Cell Culture Techniques* (pp. 27-61): Springer.

Nguyen, T., Hamby, A., & Massa, S. M. (2005). Clioquinol down-regulates mutant huntingtin expression in vitro and mitigates pathology in a Huntington's disease mouse model. *Proceedings of the National Academy of Sciences of the United States of America, 102*(33), 11840-11845.

Niggli, E., & Lederer, W. (1991). Molecular operations of the sodium–calcium exchanger revealed by conformation currents.

Nithianantharajah, J., & Hannan, A. J. (2006). Enriched environments, experience-dependent plasticity and disorders of the nervous system. *Nat Rev Neurosci, 7*(9), 697-709. doi: 10.1038/nrn1970

Normandin, L., & Hazell, A. S. (2002). Manganese neurotoxicity: an update of pathophysiologic mechanisms. *Metabolic brain disease, 17*(4), 375-387.

Okita, K., Matsumura, Y., Sato, Y., Okada, A., Morizane, A., Okamoto, S., . . . Tezuka, K.-i. (2011). A more efficient method to generate integration-free human iPS cells. *Nature methods, 8*(5), 409-412.

Ostrakhovitch, E., & Cherian, M. (2004). Differential regulation of signal transduction pathways in wild type and mutated p53 breast cancer epithelial cells by copper and zinc. *Archives of biochemistry and biophysics, 423*(2), 351-361.

Pang, T., Stam, N., Nithianantharajah, J., Howard, M., & Hannan, A. (2006). Differential effects of voluntary physical exercise on behavioral and brain-derived neurotrophic factor expression deficits in Huntington,Äôs disease transgenic mice. *Neuroscience, 141*(2), 569-584.

Pani, G., Bedogni, B., Anzevino, R., Colavitti, R., Palazzotti, B., Borrello, S., & Galeotti, T. (2000). Deregulated manganese superoxide dismutase expression and resistance to oxidative injury in p53-deficient cells. *Cancer research, 60*(16), 4654-4660.

Panickar, K., Jayakumar, A., Rao, K., & Norenberg, M. (2009). Ammonia-induced activation of p53 in cultured astrocytes: role in cell swelling and glutamate uptake. *Neurochemistry international, 55*(1), 98-105.

Papavasiliou, P. S., Kutt, H., Miller, S. T., Rosal, V., Wang, Y. Y., & Aronson, R. B. (1979). Seizure disorders and trace metals Manganese tissue levels in treated epileptics. *Neurology, 29*(11), 1466-1466.

Park, I.-H., Arora, N., Huo, H., Maherali, N., Ahfeldt, T., Shimamura, A., . . . Daley, G. Q. (2008). Disease-specific induced pluripotent stem cells. *cell, 134*(5), 877-886.

Paull, T. T., & Gellert, M. (1998). The 3′ to 5′ exonuclease activity of Mre11 facilitates repair of DNA double-strand breaks. *Molecular cell, 1*(7), 969-979.

Paull, T. T., Rogakou, E. P., Yamazaki, V., Kirchgessner, C. U., Gellert, M., & Bonner, W. M. (2000). A critical role for histone H2AX in recruitment of repair factors to nuclear foci after DNA damage. *Current Biology, 10*(15), 886-895.

Peng, T.-I., & Greenamyre, J. T. (1998). Privileged Access to Mitochondria of Calcium Influx throughN-Methyl-d-Aspartate Receptors. *Molecular pharmacology, 53*(6), 974-980.

Podolsky, S., Leopold, N., & Sax, D. (1972). Increased frequency of diabetes mellitus in patients with Huntington's chorea. *The Lancet, 299*(7765), 1356-1359.

Polidori, M. C., Mecocci, P., Browne, S. E., Senin, U., & Beal, M. F. (1999). Oxidative damage to mitochondrial DNA in Huntington's disease parietal cortex. *Neuroscience letters, 272*(1), 53-56.

Pouladi, M. A., Morton, A. J., & Hayden, M. R. (2013). Choosing an animal model for the study of Huntington's disease. *Nature Reviews Neuroscience, 14*(10), 708-721.

Prohaska, J. R. (1987). Functions of trace elements in brain metabolism. *Physiological reviews, 67*(3), 858-901.

Rallu, M., Corbin, J. G., & Fishell, G. (2002). Parsing the prosencephalon. *Nat Rev Neurosci, 3*(12), 943-951. doi: 10.1038/nrn989

Rauskolb, S., Zagrebelsky, M., Dreznjak, A., Deogracias, R., Matsumoto, T., Wiese, S., . . . Barde, Y.-A. (2010). Global Deprivation of Brain-Derived Neurotrophic Factor in the CNS Reveals an Area-Specific Requirement for Dendritic Growth. *Journal of Neuroscience, 30*(5), 1739-1749. doi: 10.1523/JNEUROSCI.5100-09.2010

Ravikumar, B., Vacher, C., Berger, Z., Davies, J. E., Luo, S., Oroz, L. G., . . . O'Kane, C. J. (2004). Inhibition of mTOR induces autophagy and reduces toxicity of polyglutamine expansions in fly and mouse models of Huntington disease. *Nature genetics, 36*(6), 585-595.

Rodriguez, M. C., MacDonald, J. R., Mahoney, D. J., Parise, G., Beal, M. F., & Tarnopolsky, M. A. (2007). Beneficial effects of creatine, CoQ10, and lipoic acid in mitochondrial disorders. *Muscle & nerve, 35*(2), 235-242.

Rosas, H. D., Chen, Y. I., Doros, G., Salat, D. H., Chen, N.-k., Kwong, K. K., . . . Hersch, S. M. (2012). Alterations in brain transition metals in Huntington disease: an evolving and intricate story. *Archives of neurology, 69*(7), 887-893.

Rosas, H. D., Koroshetz, W. J., Chen, Y. I., Skeuse, C., Vangel, M., Cudkowicz, M. E., . . . Goldstein, J. M. (2003). Evidence for more widespread cerebral pathology in early HD: an MRI-based morphometric analysis. *Neurology, 60*(10), 1615-1620.

Ross, C. A., Aylward, E. H., Wild, E. J., Langbehn, D. R., Long, J. D., Warner, J. H., . . . Paulsen, J. S. (2014). Huntington disease: natural history, biomarkers and prospects for therapeutics. *Nature Reviews Neurology*.

Roth, J. A. (2006). Homeostatic and toxic mechanisms regulating manganese uptake, retention, and elimination. *Biological research, 39*(1), 45.

Rubinsztein, D. C., Leggo, J., Chiano, M., Dodge, A., Norbury, G., Rosser, E., & Craufurd, D. (1997). Genotypes at the GluR6 kainate receptor locus are associated with variation in the age of onset of Huntington disease. *Proc Natl Acad Sci USA, 94*(8), 3872-3876.

Rubinsztein, D. C., Leggo, J., Coles, R., Almqvist, E., Biancalana, V., Cassiman, J.-J., . . . Curtis, A. (1996). Phenotypic characterization of individuals with 30,Äì40 CAG repeats in the Huntington disease (HD) gene reveals HD cases with 36 repeats and apparently normal elderly individuals with 36,Äì39 repeats. *American journal of human genetics, 59*(1), 16.

Santamaria, A. (2008). Manganese exposure, essentiality & toxicity. *Indian Journal of Medical Research, 128*(4).

Sathasivam, K., Woodman, B., Mahal, A., Bertaux, F., Wanker, E. E., Shima, D. T., & Bates, G. P. (2001). Centrosome disorganization in fibroblast cultures derived from R6/2 Huntington's disease (HD) transgenic mice and HD patients. *Human molecular genetics, 10*(21), 2425-2435.

Schinder, A. F., Olson, E. C., Spitzer, N. C., & Montal, M. (1996). Mitochondrial dysfunction is a primary event in glutamate neurotoxicity. *The Journal of neuroscience, 16*(19), 6125-6133.

Scrutton, M. C., Utter, M. F., & Mildvan, A. S. (1966). Pyruvate carboxylase VI. The presence of tightly bound manganese. *Journal of Biological Chemistry, 241*(15), 3480-3487.

Seki, T., Yuasa, S., Oda, M., Egashira, T., Yae, K., Kusumoto, D., . . . Fukuda, K. (2010). Generation of induced pluripotent stem cells from human terminally differentiated circulating T cells. *Cell Stem Cell, 7*(1), 11-14. doi: 10.1016/j.stem.2010.06.003

Seong, I. S., Ivanova, E., Lee, J.-M., Choo, Y. S., Fossale, E., Anderson, M., . . . Lesort, M. (2005). HD CAG repeat implicates a dominant property of huntingtin in mitochondrial energy metabolism. *Human molecular genetics, 14*(19), 2871-2880.

Shank, R. P. (1983). Ornithine as a precursor of glutamate and GABA: uptake and metabolism by neuronal and glial enriched cellular material. *Journal of neuroscience research, 9*(1), 47-57.

She, Q.-B., Chen, N., & Dong, Z. (2000). ERKs and p38 kinase phosphorylate p53 protein at serine 15 in response to UV radiation. *Journal of Biological Chemistry, 275*(27), 20444-20449.

Simmons, D. A., Casale, M., Alcon, B., Pham, N., Narayan, N., & Lynch, G. (2007). Ferritin accumulation in dystrophic microglia is an early event in the development of Huntington's disease. *Glia, 55*(10), 1074-1084.

Sipione, S., & Cattaneo, E. (2001). Modeling Huntington's disease in cells, flies, and mice. *Mol Neurobiol, 23*(1), 21-51. doi: 10.1385/MN:23:1:21

Sirabella, R., Secondo, A., Pannaccione, A., Molinaro, P., Formisano, L., Guida, N., . . . Cataldi, M. (2012). ERK1/2, p38, and JNK regulate the expression and the activity of the three isoforms of the Na+/Ca2+ exchanger, NCX1, NCX2, and NCX3, in neuronal PC12 cells. *Journal of neurochemistry, 122*(5), 911-922.

Slow, E. J., Graham, R. K., Osmand, A. P., Devon, R. S., Lu, G., Deng, Y., . . . Wetzel, R. (2005). Absence of behavioral abnormalities and neurodegeneration in vivo despite widespread neuronal huntingtin inclusions. *Proceedings of the National Academy of Sciences of the United States of America, 102*(32), 11402-11407.

Sørensen, S. A., Fenger, K., & Olsen, J. H. (1999). Significantly lower incidence of cancer among patients with Huntington disease. *Cancer, 86*(7), 1342-1346.

Spires, T. L., Grote, H. E., Varshney, N. K., Cordery, P. M., van Dellen, A., Blakemore, C., & Hannan, A. J. (2004). Environmental enrichment rescues protein deficits in a mouse model of Huntington's disease, indicating a possible disease mechanism. *The Journal of neuroscience, 24*(9), 2270-2276.

Stack, E. C., Kubilus, J. K., Smith, K., Cormier, K., Del Signore, S. J., Guelin, E., . . . Ferrante, R. J. (2005). Chronology of behavioral symptoms and neuropathological sequela in R6/2 Huntington's disease transgenic mice. *Journal of Comparative Neurology, 490*(4), 354-370.

Steffan, J. S., Kazantsev, A., Spasic-Boskovic, O., Greenwald, M., Zhu, Y.-Z., Gohler, H., . . . Thompson, L. M. (2000). The Huntington's disease protein interacts with p53 and CREB-binding protein and represses transcription. *Proceedings of the National Academy of Sciences, 97*(12), 6763-6768.

Stenger, C., Naves, T., Verdier, M., & Ratinaud, M.-H. (2011). The cell death response to the ROS inducer, cobalt chloride, in neuroblastoma cell lines according to p53 status. *International journal of oncology, 39*(3), 601.

Stine, O. C., Li, S.-H., Pleasant, N., Wagster, M. V., Hedreen, J. C., & Ross, C. A. (1995). Expression of the mutant allele of IT-15 (the HD gene) in striatum and cortex of Huntington's disease patients. *Human molecular genetics, 4*(1), 15-18.

Subasinghe, S., Greenbaum, A. L., & McLean, P. (1985). The insulin-mimetic action of Mn< sup> 2+</sup>: Involvement of cyclic nucleotides and insulin in the regulation of hepatic hexokinase and glucokinase. *Biochemical medicine, 34*(1), 83-92.

Suhr, S. T., Chang, E. A., Rodriguez, R. M., Wang, K., Ross, P. J., Beyhan, Z., . . . Cibelli, J. B. (2009). Telomere dynamics in human cells reprogrammed to pluripotency. *PLoS ONE, 4*(12), e8124. doi: 10.1371/journal.pone.0008124

Suzuki, M., Nagai, Y., Wada, K., & Koike, T. (2012). Calcium leak through ryanodine receptor is involved in neuronal death induced by mutant huntingtin. *Biochemical and biophysical research communications, 429*(1), 18-23.

Suzuki, S., Tanaka, T., Poyurovsky, M. V., Nagano, H., Mayama, T., Ohkubo, S., . . . Suzuki, Y. (2010). Phosphate-activated glutaminase (GLS2), a p53-inducible regulator of glutamine metabolism and reactive oxygen species. *Proceedings of the National Academy of Sciences, 107*(16), 7461-7466.

Takahashi, K., Okita, K., Nakagawa, M., & Yamanaka, S. (2007). Induction of pluripotent stem cells from fibroblast cultures. *Nat Protoc, 2*(12), 3081-3089. doi: 10.1038/nprot.2007.418

Takahashi, K., & Yamanaka, S. (2006). Induction of pluripotent stem cells from mouse embryonic and adult fibroblast cultures by defined factors. *Cell, 126*(4), 663-676. doi: 10.1016/j.cell.2006.07.024

Tang, T.-S., Slow, E., Lupu, V., Stavrovskaya, I. G., Sugimori, M., Llin√°s, R., . . . Bezprozvanny, I. (2005). Disturbed Ca2+ signaling and apoptosis of medium spiny neurons in Huntington's disease. *Proceedings of the National Academy of Sciences of the United States of America, 102*(7), 2602-2607.

Tholey, G., Ledig, M., Mandel, P., Sargentini, L., Frivold, A., Leroy, M., . . . Wedler, F. (1988). Concentrations of physiologically important metal ions in glial cells cultured from chick cerebral cortex. *Neurochemical research, 13*(1), 45-50.

Trettel, F., Rigamonti, D., Hilditch-Maguire, P., Wheeler, V. C., Sharp, A. H., Persichetti, F., . . . MacDonald, M. E. (2000). Dominant phenotypes produced by the HD mutation in STHdhQ111 striatal cells. *Human molecular genetics, 9*(19), 2799-2809.

Trujillo, K. M., Yuan, S.-S. F., Eva, Y.-H. L., & Sung, P. (1998). Nuclease activities in a complex of human recombination and DNA repair factors Rad50, Mre11, and p95. *Journal of Biological Chemistry, 273*(34), 21447-21450.

Tuchman, M., Lichtenstein, G. R., Rajagopal, B., McCann, M. T., Furth, E. E., Bavaria, J., . . . Berry, G. T. (1997). Hepatic glutamine synthetase deficiency in fatal hyperammonemia after lung transplantation. *Annals of internal medicine, 127*(6), 446-449.

Turski, L., Bressler, K., Rettig, K. J., Löschmann, P. A., & Wachtel, H. (1991). Protection of substantia nigra from MPP+ neurotoxicity by N-methyl-D-aspartate antagonists. *Nature, 349*(6308), 414-418. doi: 10.1038/349414a0

Vallier, L., Reynolds, D., & Pedersen, R. A. (2004). Nodal inhibits differentiation of human embryonic stem cells along the neuroectodermal default pathway. *Developmental Biology, 275*(2), 403-421. doi: 10.1016/j.ydbio.2004.08.031

van Dellen, A., Blakemore, C., Deacon, R., York, D., & Hannan, A. J. (2000). Delaying the onset of Huntington's in mice. *Nature, 404*(6779), 721-722.

Vaseva, A. V., Marchenko, N. D., Ji, K., Tsirka, S. E., Holzmann, S., & Moll, U. M. (2012). p53 opens the mitochondrial permeability transition pore to trigger necrosis. *cell, 149*(7), 1536-1548.

Velloso, N. d. A., Dalmolin, G. D., Gomes, G. M., Rubin, M. A., Canas, P. M., Cunha, R. A., & Mello, C. F. (2009). Spermine improves recognition memory deficit in a rodent model of Huntington‚Äôs disease. *Neurobiology of learning and memory, 92*(4), 574-580.

Waclaw, R. R., Wang, B., & Campbell, K. (2004). The homeobox gene Gsh2 is required for retinoid production in the embryonic mouse telencephalon. *Development, 131*(16), 4013-4020. doi: 10.1242/dev.01272

Waghorn, B., Yang, Y., Baba, A., Matsuda, T., Schumacher, A., Yanasak, N., & Hu, T. C. C. (2009). Assessing manganese efflux using SEA0400 and cardiac T1-mapping manganese-enhanced MRI in a murine model. *NMR in Biomedicine, 22*(8), 874-881.

Walker, F. O. (2007). Huntington's disease. *The Lancet, 369*(9557), 218-228.

Walter, T., De Andraca, I., Chadud, P., & Perales, C. G. (1989). Iron deficiency anemia: adverse effects on infant psychomotor development. *Pediatrics, 84*(1), 7-17.

Wang, H.-F., & Liu, F.-C. (2001). Developmental restriction of the LIM homeodomain transcription factor Islet-1 expression to cholinergic neurons in the rat striatum. *Neuroscience, 103*(4), 999-1016.

Wang, S., & Shi, X. (2001). Mechanisms of Cr (VI)-induced p53 activation: the role of phosphorylation, mdm2 and ERK. *Carcinogenesis, 22*(5), 757-762.

Wardman, P., & Candeias, L. P. (1996). Fenton chemistry: an introduction. *Radiation research, 145*(5), 523-531.

Waters, L. S., Minesinger, B. K., Wiltrout, M. E., D'Souza, S., Woodruff, R. V., & Walker, G. C. (2009). Eukaryotic translesion polymerases and their roles and regulation in DNA damage tolerance. *Microbiology and Molecular Biology Reviews, 73*(1), 134-154.

Wedler, F., & Denman, R. (1984). Glutamine synthetase: the major Mn (II) enzyme in mammalian brain. *Current topics in cellular regulation, 24*, 153-169.

Wedler, F. C., Denman, R. B., & Roby, W. G. (1982). Glutamine synthetase from ovine brain is a manganese (II) enzyme. *Biochemistry, 21*(25), 6389-6396.

Wedler, F. C., & Ley, B. W. (1994). Kinetic, ESR, and trapping evidence for in vivo binding of Mn (II) to glutamine synthetase in brain cells. *Neurochemical research, 19*(2), 139-144.

Wexler, N. S. (2004). Venezuelan kindreds reveal that genetic and environmental factors modulate Huntington's disease age of onset. *Proceedings of the National Academy of Sciences of the United States of America, 101*(10), 3498-3503.

Weydt, P., Pineda, V. V., Torrence, A. E., Libby, R. T., Satterfield, T. F., Lazarowski, E. R., . . . Strand, A. D. (2006). Thermoregulatory and metabolic defects in Huntington's disease transgenic mice implicate PGC-1alpha in Huntington's disease neurodegeneration. *Cell metabolism, 4*(5), 349-362.

White, J. K., Auerbach, W., Duyao, M. P., Vonsattel, J.-P., Gusella, J. F., Joyner, A. L., & MacDonald, M. E. (1997). Huntingtin is required for neurogenesis and is not impaired by the Huntington's disease CAG expansion. *Nature genetics, 17*(4), 404-410.

Wild, E. J., & Tabrizi, S. J. (2007). Huntington's disease phenocopy syndromes. *Current opinion in neurology, 20*(6), 681-687.

Williams, B. B., Kwakye, G. F., Wegrzynowicz, M., Li, D., Aschner, M., Erikson, K. M., & Bowman, A. B. (2010). Altered manganese homeostasis and manganese toxicity in a Huntington's disease striatal cell model are not explained by defects in the iron transport system. *Toxicological Sciences, 117*(1), 169-179.

Williams, B. B., Li, D., Wegrzynowicz, M., Vadodaria, B. K., Anderson, J. G., Kwakye, G. F., . . . Bowman, A. B. (2010). Disease-toxicant screen reveals a neuroprotective interaction between Huntington's disease and manganese exposure. *Journal of neurochemistry, 112*(1), 227-237.

Woda, J. M., Calzonetti, T., Hilditch-Maguire, P., Duyao, M. P., Conlon, R. A., & Macdonald, M. E. (2005). Inactivation of the Huntington's disease gene (Hdh) impairs anterior streak formation and early patterning of the mouse embryo. *BMC Dev Biol, 5*, 17. doi: 10.1186/1471-213X-5-17

Xiao, G., Fan, Q., Wang, X., & Zhou, B. (2013). Huntington disease arises from a combinatory toxicity of polyglutamine and copper binding. *Proceedings of the National Academy of Sciences, 110*(37), 14995-15000.

Xiao, L., Gong, L., Yuan, D., Deng, M., Zeng, X., Chen, L., . . . Hu, X. (2010). Protein phosphatase-1 regulates Akt1 signal transduction pathway to control gene expression, cell survival and differentiation. *Cell Death & Differentiation, 17*(9), 1448-1462.

Xu, L., Kappler, C. S., Mani, S. K., Shepherd, N. R., Renaud, L., Snider, P., . . . Menick, D. R. (2009). Chronic administration of KB-R7943 induces up-regulation of cardiac NCX1. *Journal of Biological Chemistry, 284*(40), 27265-27272.

Yu, H., Iyer, R. K., Kern, R. M., Rodriguez, W. I., Grody, W. W., & Cederbaum, S. D. (2001). Expression of arginase isozymes in mouse brain. *Journal of neuroscience research, 66*(3), 406-422.

Zajac, M. S., Pang, T. Y. C., Wong, N., Weinrich, B., Leang, L. S. K., Craig, J. M., . . . Hannan, A. J. (2010). Wheel running and environmental enrichment differentially modify exon-specific BDNF expression in the hippocampus of wild-type and pre-motor symptomatic male and female Huntington's disease mice. *Hippocampus, 20*(5), 621-636. doi: 10.1002/hipo.20658

Zeitlin, S., Liu, J.-P., Chapman, D. L., Papaioannou, V. E., & Efstratiadis, A. (1995). Increased apoptosis and early embryonic lethality in mice nullizygous for the Huntington's disease gene homologue. *Nature genetics, 11*(2), 155-163.

Zeron, M. M., Hansson, O., Chen, N., Wellington, C. L., Leavitt, B. R., Brundin, P., . . . Raymond, L. A. (2002). Increased sensitivity to N-methyl-D-aspartate receptor-mediated excitotoxicity in a mouse model of Huntington's disease. *Neuron, 33*(6), 849-860.

Zhang, H., Li, Q., Graham, R. K., Slow, E., Hayden, M. R., & Bezprozvanny, I. (2008). Full length mutant huntingtin is required for altered Ca2+ signaling and apoptosis of striatal neurons in the YAC mouse model of Huntington's disease. *Neurobiology of Disease, 31*(1), 80-88. doi: 10.1016/j.nbd.2008.03.010

Zhang, N., An, M. C., Montoro, D., & Ellerby, L. M. (2010). Characterization of human Huntington's disease cell model from induced pluripotent stem cells. *PLoS currents, 2*.

Zhang, S., Fu, J., & Zhou, Z. (2004). In vitro effect of manganese chloride exposure on reactive oxygen species generation and respiratory chain complexes activities of mitochondria isolated from rat brain. *Toxicology in vitro, 18*(1), 71-77.

Zhang, X., Huang, C. T., Chen, J., Pankratz, M. T., Xi, J., Li, J., . . . Ayala, M. (2010). Pax6 is a human neuroectoderm cell fate determinant. *Cell stem cell, 7*(1), 90-100.

Zhao, F., Zhang, J.-B., Cai, T.-J., Liu, X.-Q., Liu, M.-C., Ke, T., . . . Luo, W.-J. (2012). Manganese induces p21 expression in PC12 cells at the transcriptional level. *Neuroscience, 215*, 184-195.

Zhou, H., Wu, S., Joo, J. Y., Zhu, S., Han, D. W., Lin, T., . . . Ding, S. (2009). Generation of induced pluripotent stem cells using recombinant proteins. *Cell Stem Cell, 4*(5), 381-384. doi: 10.1016/j.stem.2009.04.005

Zidenberg-Cherr, S., Keen, C. L., Lönnerdal, B., & Hurley, L. S. (1983). Superoxide dismutase activity and lipid peroxidation in the rat: developmental correlations affected by manganese deficiency. *The Journal of nutrition, 113*(12), 2498.

Zuccato, C., & Cattaneo, E. (2007). Role of brain-derived neurotrophic factor in Huntington's disease. *Prog Neurobiol, 81*(5-6), 294-330. doi: 10.1016/j.pneurobio.2007.01.003

Zuccato, C., Tartari, M., Crotti, A., Goffredo, D., Valenza, M., Conti, L., . . . Timmusk, T. (2003). Huntingtin interacts with REST/NRSF to modulate the transcription of NRSE-controlled neuronal genes. *Nature genetics, 35*(1), 76-83.

Zuccato, C., Valenza, M., & Cattaneo, E. (2010). Molecular mechanisms and potential therapeutical targets in Huntington's disease. *Physiological reviews, 90*(3), 905-981.